Contributions to Pursuit-Evasion Game Theory

by

Dave Wilson Oyler

A dissertation submitted in partial fulfillment
of the requirements for the degree of
Doctor of Philosophy
(Aerospace Engineering)
in the University of Michigan
2016

Doctoral Committee:

Associate Professor Anouck Renee Girard, Chair
Professor Anthony M. Bloch
Professor Daniel J. Inman
Professor Pierre Tshimanga Kabamba (Deceased)
Professor Ilya Vladimir Kolmanovsky

©Dave Wilson Oyler

2016

To my family, friends, and mentors.

ACKNOWLEDGMENTS

First and foremost, I would like to thank my advisors, Professors Anouck Girard and Pierre Kabamba, for all of the support they have given me over the course of my graduate career. I value their wisdom and guidance very highly, and their mentoring, which covered a wide variety of topics, not strictly academics, has been instrumental to my personal and professional growth. I would also like to thank Professor Ilya Kolmanovsky for his guidance throughout my graduate career, especially during my final year at UM. I am grateful to Professors Anthony Bloch and Daniel Inman as well for joining my committee and offering valuable and insightful feedback about my research.

I am also very appreciative of the help I have received over the years from my lab mates, especially Ricardo Bencatel, Jonathan Las Fargeas, Moritz Niendorf, Johnhenri Richardson, and Jinwoo Seok. Other colleagues have also played essential parts in this journey, from helping me through critical milestones like the Ph.D. Qualifying Exams, to simply making the office an enjoyable place to work. To list every name would take many pages, but I am sincerely grateful for each and every one of them.

I would also like to acknowledge the United States Air Force and the Boeing Company for funding my research, and the Air Force Research Laboratory for their collaboration. I am also grateful for the support of the University of Michigan, the Rackham Graduate School, and the Department of Aerospace Engineering.

Finally, I would like to thank my amazing family and friends for their steady support and constant encouragement.

TABLE OF CONTENTS

LIST OF FIGURES

LIST OF TABLES

LIST OF ABBREVIATIONS

CC Curve-curve

CS Curve-straight

ESPP Euclidean Shortest Path Problem

HC Homicidal Chauffeur

MPME Multiple Pursuer, Multiple Evader

MPSE Multiple Pursuer, Single Evader

PE Pursuit-Evasion

P3 Prey, Protector, and Predator

SPSE Single Pursuer, Single Evader

SPME Single Pursuer, Multiple Evader

UAV Unmanned Air Vehicle

UGV Unmanned Ground Vehicle

VIP Very Important Player

LIST OF SYMBOLS

a_i distance between C_{i-2} and E_i, where $C_0 = P$

$\mathscr{B}$ set of players in the Blue team

$\mathcal{B}_{AB}$ boundary between the dominance regions of players A and B

$\mathcal{B}_\ell(x_{E0}, y_{E0})$ the ℓ-neighborhood around the point (x_{E0}, y_{E0})

c constant for simplifying expressions for the sensitivity of dominance boundaries to changes in parameters

C optimal capture location

$\hat{C}$ candidate for C

$\mathcal{C}_c$ set of all candidates for C

C_H point where the hole in the reachable set for a Dubins car closes

C_i capture point of the i-th evader

C_j^* optimal capture point of E, considering only P_j

cl$()$ closure of a set

c_ψ bound on rate of heading change

d distance between initial locations of players

$\bar{d}$ mean value of d

d_{c1} distance traveled by E_2 prior to the capture of E_1

$\mathcal{D}_E$ dominance region where E is dominant over all pursuers

$\mathcal{D}_{E/P_i}$ dominance region where E is dominant over a specific pursuer P_i

$\mathcal{D}^i_{E/P_k}$ the portion of $\mathcal{D}_{E/P_k}$ contained in $\mathcal{R}_i$

d_i distance between C_{i-1} and E_i, where $C_0 = P$

$\mathcal{D}^i$ portion of evader's dominance region that is contained in $\mathcal{R}_i$

d_k distance between initial locations of E and P_k

d_{max} maximum distance between the dominance boundaries for pointwise and ℓ-neighborhood capture

d_{min} minimum distance between the dominance boundaries for pointwise and ℓ-neighborhood capture

d_P distance between initial locations of E and P in a P3 game

d_R distance between initial locations of E and R in a P3 game

$\mathcal{DS}\{\zeta_1, \zeta_2/\zeta_3\}$ dispersal surface generated by starting from ζ_1 and passing either ζ_2 or ζ_3

$\mathcal{D}(x_{E0}, y_{E0})$ dominance region for a specified initial evader location

$\mathcal{D}(x_{E0}, y_{E0}, t_B)$ dominance region for a specified initial evader location and time delay

d_2' total distance between P and E_2 at t_{c1}

E position of evader

$\mathscr{E}$ set of all evaders

$\vec{E}$ vector of initial locations for all evaders

E' location where E enters $\mathcal{R}_i$ under optimal play

$E[.]$ expected value of a function

E_i position of player E_i

$E[J]^{ub}$ upper bound for the maxmin $E[J]$

f game dynamics

f_c system dynamics in Cartesian coordinates

f_r risk function

$g = \{g_1, g_2, ..., g_f\}$ sequence of generating points in a player's path to $\mathcal{R}_i$

G running payoff

H Hamiltonian function

(h, k) Cartesian coordinates of center of Apollonius Circle

J payoff

K terminal payoff

k_1, k_2, k_3, k_4 controller gains

ℓ capture radius

m number of pursuers

n number of evaders

$\mathcal{N}$ set of nodes in a fully connected directional graph where each node is a player location

P position of pursuer

$\mathscr{P}$ set of all pursuers

$\vec{p}$ vector of adjoint variables

P' location where P enters $\mathcal{R}_i$ under optimal play

$\mathcal{P}_{\mathcal{D}}$ a mapping from each point in the environment into the probability that a certain player dominates that point

P_i position of player P_i

P'_k location where P_k enters $\mathcal{R}_i$ under optimal play

q number of protectors in a P3 game

$Q(r, \theta)$ optimization constraint, describes $\mathcal{B}_{ER}$

R position of protector

$\mathscr{R}$ set of players in the Red team

$\bar{r}$ mean value of r

r_A radius of Apollonius circle

$\mathcal{R}_c$ candidate region where C might be located

$\mathcal{R}_E$ region in the partitioned plane that contains the evader's initial location

$r_{E,i} = r_{E,i}(\theta, d_i, t_{B,i})$ polar radius at angle θ of a point in $\mathcal{B}_{E_iP}$

$\mathcal{R}_i$ a region in the partitioned plane, bounded by singular surfaces

$r_{Pk} = r_{Pk}(\theta, d_k, t_{B,k})$ polar radius at angle θ of a point in $\mathcal{B}_{EP_k}$

r_R polar radius of a point in $\mathcal{B}_{ER}$

(r_{X_j}, θ_{X_j}) polar coordinates of X_j

(r, θ) polar coordinates of a point on the dominance boundary

(r^*, θ^*) the optimal location for rendezvous in the P3 game of degree

s arbitrary obstacle vertex visible from g_f

$\mathcal{S}$ set containing locations of obstacles

S_1 control surface

S_2 control surface

t time

t_B delay between starting times of players

$\bar{t}_B$ mean value of t_B

$t_{B,k}$ delay between starting times of E and P_k

t_c time that elapses before capture

t_{ci} capture time of the i-th evader

t'_{ci} optimal capture time of E_i for a specific capture order

t^*_{ci} optimal capture time of E_i over all capture orders

$\bar{t}_{ci}$ time between the capture of E_{i-1} and E_i

$t_c[i]$ capture time associated with the i-th element in $\mathcal{C}_c$

t_{cf} final capture time; i.e., capture time of the last evader to captured

t^A_{cf} value of t'_{cf} associated with capture order ζ_A

t^{ub}_{cf} upper bound for t_{cf}

$t^*_{C,j}$ capture time associated with C^*_j

$t_{E'}$ time when E reaches E' under optimal play

t_f terminal time

t_ℓ time required for the evader to travel a distance ℓ

$t_{P'}$ time when P reaches P' under optimal play

$t_{P'_k}$ time when P_k reaches P'_k under optimal play

t_R time when the first R_k achieves rendezvous with E

t_1 time when reachable set for Dubin's car becomes doubly connected

t_2 time when internal boundary of reachable set for Dubin's car is formed strictly by end-points of CC paths

t_3 time when internal hole in reachable set for Dubin's car vanishes

$\vec{u}_B$ vector of inputs controlled by the Blue team

$\vec{u}_B^*$ optimal strategy for the Blue team

$\vec{u}_R$ vector of inputs controlled by the Red team

$\vec{u}_R^*$ optimal strategy for the Red team

u_ψ heading rate input

v velocity

V Value of a game

v_E velocity of evader

v_{Ej} velocity of evader E_j

v_P velocity of pursuer

v_{Pi} velocity of pursuer P_i

$\mathcal{VS}\{\zeta_1, \zeta_2\}$ visibility surface due to the visibility of point ζ_2 from point ζ_1

w probability distribution for the identity of the VIP

w_i probability that E_i is the VIP

w_r weight of risk

w_t weight of terminal time

$\vec{x}$ state vector

$\vec{x}_c$ state vector in Cartesian coordinates

$\hat{x}_c$ estimate of $\vec{x}_c$

$\tilde{x}_c$ error in the estimate of $\vec{x}_c$

$\hat{x}_E$ estimate of x_E

$\tilde{x}_E$ error in the estimate of x_E

(x_E, y_E) Cartesian coordinates of evader's position

$(x_{E,0}, y_{E,0})$ Cartesian coordinates of evader's initial position

$\vec{x}_f$ state vector at the terminal time

(x_f, y_f) final location of a player

(x_i, y_i) initial location of a player

X_j an intersection of the boundary segments of $\mathcal{R}_c$

(x_P, y_P) Cartesian coordinates of pursuer's position

$(x_{P,0}, y_{P,0})$ Cartesian coordinates of pursuer's initial position

$\vec{x}_\pi$ state vector in polar coordinates

$\vec{y}_c$ system outputs in Cartesian coordinates

$\hat{y}_E$ estimate of y_E

$\tilde{y}_E$ error in the estimate of y_E

$\vec{y}_\pi$ system outputs in polar coordinates

$z = [\gamma, d, \theta, t_B]$ Gaussian random vector of parameters that define the dominance boundary

$\bar{z}$ mean of z

z_0 linearization point

α ratio of the initial distance between R and E to the initial distance between P and E

α_ψ difference between β and ψ_P

$\alpha_{\psi,des}$ difference between β and $\psi_{P,des}$

β line of sight angle from pursuer to evader

$\hat{\beta}$ estimate of β

Γ goal set for an evader

γ ratio of player speeds

$\bar{\gamma}$ mean value of γ

γ_{Pj} ratio of speeds between P_j and E

γ_{Rk} ratio of speeds between R_k and E

Δ distance from evader to dominance boundary

δ distance between pursuer and evader

$\hat{\delta}$ estimate of δ

δ_{des} desired value of δ

δ_i distance between E_{i-1} and E_i

ϵ small, positive parameter

ϵ_2 small, positive parameter

ζ set of all potential capture sequences

ζ^* capture order that minimizes the maxmin payoff

ζ_A arbitrary capture order

η total number of players

η_s number of obstacle vertices in $\mathcal{S}$

$\bar{\theta}$ mean value of θ

θ_i^0 direction of zero azimuth for E_i

θ_P angle between E's lines of sight to R and P

λ Lagrange multiplier

λ_i angle between the line from E_i to E_{i-1} and the line from E_i to C_{i-1}

λ_{S1} design parameter, decay rate of S_1

λ_{S2} design parameter, decay rate of S_2

μ sign of the rate of change of δ

$\hat{\mu}$ estimate of μ

$\tilde{\mu}$ error in the estimate of μ

ξ arbitrary point in the plane, used in proofs

ρ minimum turn radius

ρ_E minimum turn radius of evader

ρ_P minimum turn radius of pursuer

σ_i angle between the line from E_{i-1} to E_{i-2} and the line from E_{i-1} to E_i, where $E_0 = P$

σ_r^2 variance of r

Σ_z covariance of z

ϕ independent variable in parametric description of isochrones for Dubin's car

ψ_E heading of evader

$\vec{\psi}_E$ vector of headings for all evaders

$\vec{\psi}_E^*$ vector of evader headings that maximizes the minimum payoff

ψ_{Ei} heading of i-th evader

ψ_{Ei}^* optimal heading of i-th evader

ψ_P heading of pursuer

ψ_P^* optimal pursuer heading

$\psi_{P,des}$ desired value of ψ_P

ω dummy variable for integration

ABSTRACT

Contributions to Pursuit-Evasion Game Theory

by

Dave Wilson Oyler

Chair: Anouck R. Girard

This dissertation studies adversarial conflicts among a group of agents moving in the plane, possibly among obstacles, where some agents are pursuers and others are evaders. The goal of the pursuers is to capture the evaders, where capture requires a pursuer to be either co-located with an evader, or in close proximity. The goal of the evaders is to avoid capture. These scenarios, where different groups compete to accomplish conflicting goals, are referred to as pursuit-evasion games, and the agents are called players.

Games featuring one pursuer and one evader are analyzed using dominance, where a point in the plane is said to be dominated by a player if that player is able to reach the point before the opposing players, regardless of the opposing players' actions. Two generalizations of the Apollonius circle are provided. One solves games with environments containing obstacles, and the other provides an alternative solution method for the Homicidal Chauffeur game. Optimal pursuit and evasion strategies based on dominance are provided.

One benefit of dominance analysis is that it extends to games with many players. Two foundational games are studied; one features multiple pursuers against a single evader, and the other features a single pursuer against multiple evaders. Both are solved using dominance through a reduction to single pursuer, single evader games. Another game featuring competing teams of pursuers is introduced, where an evader cooperates with friendly pursuers to rendezvous before being captured by adversaries.

Next, the assumption of complete and perfect information is relaxed, and uncertainties in player speeds, player positions, obstacle locations, and cost functions are studied. The sensitivity of the dominance boundary to perturbations in parameters is provided, and probabilistic dominance is introduced. The effect of information is studied by comparing solutions of games with perfect information to games with uncertainty. Finally, a pursuit law is developed that requires minimal information and highlights a limitation of dominance regions.

These contributions extend pursuit-evasion game theory to a number of games that have not previously been solved, and in some cases, the solutions presented are more amenable to implementation than previous methods.

CHAPTER 1

Introduction

In recent years, there have been significant investments and improvements in autonomous vehicle technology. Much of this can be attributed to the increased utilization of remotely operated vehicles and the challenges associated with their operation. For example, Unmanned Air Vehicles (UAVs) have played significant roles in recent military operations, and due to the unavoidable time delays and intermittent communication links associated with operating a UAV from halfway around the world across multiple land- and satellite-based communication links, an increasing number of tasks have been automated. This has lead to a fundamental shift in operations from a model based on in-situ piloting, where an aircraft's control surface deflections are input directly, to a model based on specifying waypoints or other high-level tasks. This shift has been especially important for the operations of underwater vehicles and planetary rovers, where time delays and communication bandwidth limitations are even more severe.

However, the utilization of autonomous mobile vehicles has so far been limited mostly to benign environments, where there can be a reasonable expectation that either the high-level task assignments will be completed or the vehicle will be able to enter a safe state to await further instructions. Returning to the example of UAVs, recent military conflicts have had large disparities in the technological capabilities of the opposing forces, and the use of UAVs has been possible primarily due to the possession of complete air superiority by one of the forces. In a hypothetical future conflict between peers, opposing forces could intervene to prohibit the completion of a UAV's task. Worse still, when a task is unable to be completed, standard safe-state behaviors, such as loitering, could leave the UAV in danger of being destroyed. Thus, a lack of air superiority would prohibit the use of many current operations concepts, and it would render a large amount of autonomous and remotely-operated technology inoperable.

Besides hostile environments, similar challenges exist in unpredictable environments. For example, autonomous driving technology has seen vast improvements in recent years, but one challenge in the autonomous driving problem is that the vehicles must operate in the presence of human drivers. Standard rules of the road exist in part to increase the predictability of all drivers, but nevertheless, human drivers are notoriously unpredictable. One approach to solving this problem is to consider the worst-case behavior; i.e., if an autonomous vehicle is tasked with avoiding collisions while holding its lane or passing another vehicle, then a possible design assumption might be that other drivers will actively attempt to prevent or delay the safe completion of this task. For example, when holding its lane, this would entail driving with a safe amount of headway in case a car in front decelerated rapidly without warning. This is known as "defensive driving", and it is a standard practice among human drivers that stems from the assumption that the environment could become adversarial at any moment.

In order to reach the goal of completely autonomous operations in realistic environments, the environments cannot be assumed to always be benign, and adversarial behavior must be considered. This leads to problem formulations known as adversarial games. One such game, which represents both the UAV and autonomous driving scenarios described above, is the problem of pursuit and evasion, where some agents, known as pursuers, attempt to capture or collide with other agents, known as evaders, while the evaders attempt to prevent this capture from occurring.

1.1 Problem Statement

The problem for the pursuers (evaders) can be stated as follows: given models for the environment and the capabilities of all players, find actions that cause (prevent or delay) capture. From this general statement, several interesting questions can be posed:

- How can individuals determine their optimal actions?
- How can heterogeneous teams cooperate to accomplish their goals?
- How do information and uncertainty influence pursuit and evasion?

These questions are broad, and they involve a great deal of complexity, so to reduce the scope, the following constraints are applied:

- The environment is planar.
- All obstacles are line segments or polygons.
- Players travel at constant speeds.
- Player motions may be further constrained, but only by minimum turn radii.
- All players possess knowledge of the environment as well as the positions and capabilities of all other players, but this knowledge may be subject to uncertainty.

1.2 Original Contributions

The primary contribution of this dissertation is the extension of a solution method for Pursuit-Evasion (PE) games. This extension permits analysis of a number of games that have not been solved in the PE literature, including games in the presence of obstacles, many-player games with heterogeneous teams, and games with uncertain parameters, measurements, or cost functions.

This primary contribution can be separated into the following components:

- Methods for determining the optimal actions in Single Pursuer, Single Evader (SPSE) games. These include a solution for games with simple motion in the presence of obstacles, which has not previously been presented in the literature; a solution for the Homicidal Chauffeur (HC) game, which provides an alternative to existing methods and has benefits when analyzing extensions to the HC game, such as HC with additional pursuers or evaders; and a general method for computing solutions to PE games with arbitrary player dynamics.

- Methods for decomposing many-player games into a collection of SPSE games. These include a solution to the Multiple Pursuer, Single Evader (MPSE) game and contributions to the solution of the Single Pursuer, Multiple Evader (SPME) game. Additionally, the solutions to these two games provide the foundation for a solution to the Multiple Pursuer, Multiple Evader (MPME) game.

- The sensitivity of solutions to PE games with respect to perturbations in the available information. Based on this, solutions for PE games in the presence of uncertainty are provided, and studies are performed on the effect of information on the solutions to PE games.

The primary significance of these methods is that they form a foundation for the analysis of other PE games which have not yet been solved in the literature. For example, in the SPSE game, these methods give the solution in the presence of obstacles, which has not been accomplished in the literature. Furthermore, the solution to the SPSE game serves as the foundation for solutions to games with additional players and games with uncertainty.

Another benefit of these contributions is that they can reduce the computational requirements of solving certain PE problems. Also, in some cases, a significant part of the computation can be performed *a priori*, which reduces the amount of computation that must be performed online. Therefore, these methods can be implemented more easily than some other solutions in the existing literature.

1.3 Organization

This dissertation is organized as follows: Chapter 2 provides a survey of the existing pursuit-evasion literature, and it provides a short introduction to classical methods for solving PE games. This material is derived from [79].

Chapter 3 analyzes SPSE games, and it introduces the method of dominance regions. Two classes of player dynamics are analyzed. In the first, both players can turn instantaneously, and the solution is provided for games in the presence of obstacles. In the second, one player can turn instantaneously, and the other has a constrained minimum turn radius. The material in Chapter 3 is based on material presented in [82], [85], and [80].

Chapter 4 studies problems with additional players. The solution to the MPSE game is provided, and a novel PE game known as the P3 game is introduced and solved. The SPME game is also studied. The content of Chapter 4 stems from material in [85] and [80].

Chapters 3 and 4 assume full and perfect information, and in Chapter 5, this assumption is relaxed. A version of the SPME game with an uncertain cost function is introduced and studied. Next, the sensitivity of solutions to perturbations in game parameters and measurements is studied, and the P3 game is reanalyzed with uncertainty in the measurements. Finally, a game with minimal information is studied, which shows a limitation to the methods proposed in this dissertation. This chapter stems from [84], [81], and [83].

CHAPTER 2

Literature Survey

Pursuit-evasion games have a rich history in the aerospace literature related to problems such as aerial battles between fighter aircraft and homing guidance laws for missiles. However, due to technical challenges, there are many interesting questions open in the literature. Recently, with the increasing prevalence of autonomous vehicles, there is renewed interest in the field. This chapter addresses both the historic and renewed interest by highlighting interesting aspects of the various game structures in the literature as well as the existing solution techniques. It also calls attention to current work and open challenges.

2.1 Introduction

PE games model scenarios with multiple agents where some are pursuers and others are evaders. The goal of the pursuers is to capture the evaders, while the evaders attempt to avoid capture. The term "capture" typically refers to a situation where a pursuer and an evader are colocated, or within some prescribed maximum distance, but other termination conditions are also possible and are discussed in Section 2.2.3.

There are many examples of pursuit-evasion conflicts. In the aerospace field, these include aerial battles between fighter aircraft [43], missiles utilizing homing guidance to hit targets [51], and unmanned aircraft performing surveillance of ground targets [28]. There are also many applications outside the realm of aerospace such as biological studies of predator-prey relationships [15], search and rescue operations [40], and linebackers attempting to tackle the ball carrier in a game of football [51].

Pursuit-evasion games have a rich history in the literature. However, due to technical challenges, practical systems often rely on heuristic methods, such as the air combat tactics outlined in [101], or rule-based simulators such as in [19]. Thus, there are many interesting questions open in the literature.

2.1.1 Problem Description and Notation

This section presents a very general formulation for PE games. In Section 2.2, PE games are divided according to game structure, and more complete problem formulations are provided.

PE games are adversarial conflicts between a number of agents consisting of m pursuers and n evaders. Individual pursuers and evaders are called P_i and E_j, respectively, and they comprise the following sets, $\mathscr{P}$ and $\mathscr{E}$:

$$\begin{aligned} \mathscr{P} &= \{P_i : i = 1, ..., m, \}, \\ \mathscr{E} &= \{E_j : j = 1, ..., n\}. \end{aligned} \tag{2.1}$$

For example, [31] considers a game with two pursuers against a single evader, and [18] considers one pursuer and two evaders. Note that PE games with more than two players are not always conflicts between $\mathscr{P}$ and $\mathscr{E}$. In some cases, teams may consist of both pursuers and evaders. Team games are considered in depth in Section 2.2.4. In addition, $\mathscr{P}$ and $\mathscr{E}$ are not even necessarily disjoint. If a player, M_k, satisfies

$$M_k \in \{\mathscr{P} \cap \mathscr{E}\}, \tag{2.2}$$

then M_k is referred to as a mixed player.

The goal is to determine strategies for the players, where a strategy is a mapping from the game space into the admissible control actions, i.e., it is a vector function of the state.

Due to the inherent complexity of PE games, the existing literature typically assumes that motion occurs within a plane (See Section 2.2.1). Agents move within their environment by controlling their speed and heading. Here, pursuers move with heading ψ_{Pi} and speed v_{Pi}, while evaders move with heading ψ_{Ej} and speed v_{Ej}. Except where noted, in this dissertation the speeds are assumed constant. The motion of the agents may be subject to environmental or kinematic constraints, which are considered in Sections 2.2.1 and 2.2.2, respectively.

PE games often terminate when capture occurs; that is, when the distance between the pursuers and evaders becomes either zero or less than a prescribed quantity, ℓ. However, the literature also contains PE games with other termination conditions, such as visibility-based games. These are considered in Section 2.2.3.

As in [48], PE games may have a finite number of outcomes or a continuum. Games with a finite number of outcomes, such as whether or not capture occurs, are referred to as games of kind. Alternatively, there may be a continuum of possible outcomes, such as the time that elapses before capture, or the distance of the evader from a goal when capture occurs, which one team seeks to minimize while the other attempts to maximize. These games are referred to as games of degree, and the quantity that the players seek to maximize or minimize is the payoff. Let J be the payoff, and $\vec{x}$ be the state vector, which contains the locations and possibly the headings of the players, depending on the particular dynamics of the game. Let the dynamics be given by $f(\vec{x}, \vec{u}_B, \vec{u}_R)$, where one team is known as the Blue team and control inputs $\vec{u}_B$ while the other team is known as the Red team and controls $\vec{u}_R$. These inputs may include, among other things, the player's headings, heading rates, or speeds (if not constant). If $\vec{u}_B = \vec{u}_B(\vec{x})$ and $\vec{u}_R = \vec{u}_R(\vec{x})$, then $\vec{u}_B$ and $\vec{u}_R$ are known as strategies. The value of the game, V, is given by:

$$V(\vec{x}) = \min_{\vec{u}_B(\vec{x})} \max_{\vec{u}_R(\vec{x})} J(\vec{x}). \tag{2.3}$$

Games with different payoffs are considered in Section 2.2.3.

Finally, the information available to the players can have a significant effect on PE games. This information may include the state, the structure of the environment, the amount of the environment that can be sensed at a given time, the speed and maneuverability of the opponent, and even whether a given player belongs to $\mathscr{P}$, $\mathscr{E}$, or both. These topics are all discussed in Section 2.2.5.

2.1.2 Scope

This dissertation focuses on PE games in continuous space. There is a body of existing work that focuses on search and pursuit-evasion on graphs, and these works are collected and organized in references [1], [21], and [32].

There have been a number of textbooks written about PE games. Additionally, this work makes use of a number of concepts from differential game theory that are not strictly limited to PE games. For more detailed analysis, and for definitions of terms, the reader is referred to the following textbooks: [5], [48], [33], [51], [44], [114], and [59].

2.1.3 Organization

The remainder of this chapter is organized as follows: In Section 2.2, a variety of game structures are provided along with formal problem statements. Section 2.3 describes a number of solution methods from the literature. Challenges and open problems are described in Section 2.4, and a summary is provided in Section 2.5.

2.2 Game Structure

This section describes some of the versions of PE games in the literature. It considers games with different environments, dynamics, termination conditions, payoffs, team structures, and available information. Formal problem statements and applications are provided for some of the more common games.

2.2.1 Environment

First, consider the environment in which the players move. PE games are typically used to model physical agents moving in space, and the most general environment is therefore three-dimensional. Reference [54] extends the state space to $\mathbb{R}^n$. However, as Section 2.3 describes, many solution methods for PE games suffer from the curse of dimensionality, and for this reason much of the literature considers games in the plane. Extensions of the two dimensional plane have been analyzed, such as games on the surface of a cone [66] and games on a two dimensional manifold [65]. Additionally, [111] uses a method of projections to simplify the game space for higher dimensional games and reduce the effect of the curse of dimensionality.

PE games have also been formulated in bounded environments and environments with obstacles. PE games in the presence of obstacles include Isaac's game of Obstacle Tag [48] [49] and visibility-based games [9]. One version of PE in a bounded environment is known as the Lion and Man Game [30], and a version of this game with a circular obstacle is studied in [53]. There are also examples of PE games in the literature where the environment contains obstacles that do not affect the players symmetrically [85]. This could be the case in a game where an unmanned aerial vehicle (UAV) competes against a ground vehicle. The ground-based vehicle must move around obstacles while the UAV can simply fly over them.

Table 2.1 shows an organized list of references categorized by the type of environment considered.

Environment Type	References
2-Dimensional:	[3] [7] [8] [10] [11] [13] [9] [12] [16] [17] [18] [30] [31] [36] [37] [38] [39] [46] [49] [50] [52] [53] [57] [67] [68] [61] [62] [66] [69] [70] [72] [78] [85] [82] [89] [88] [90] [96] [97] [98] [99] [100] [103] [113]
3-Dimensional:	[19] [26] [27] [41] [42] [47] [52] [101] [105] [108] [111] [115]
n-Dimensional:	[54] [65]
Obstacles:	[7] [8] [10] [11] [13] [9] [12] [38] [48] [49] [52] [53] [54] [78] [85] [82] [98]
Bounded:	[7] [8] [16] [30] [52] [53] [9]

Table 2.1: References Organized By Game Environment.

2.2.2 Player Dynamics

This section describes the way that the players typically move in PE games. Specifically, it considers constraints on the players' turn radii and the speed ratios between the players. Specific games that are treated frequently in the literature are formulated. Table 2.2 categorizes references by player dynamics.

Player Dynamics	References
Simple Motion:	[3] [7] [8] [10] [11] [13] [9] [12] [16] [18] [30] [31] [36] [38] [48] [49] [50] [52] [53] [54] [57] [62] [65] [66] [85] [82] [99]
Homicidal Chauffeur:	[26] [37] [48] [74] [89] [88] [113] [115]
Two Cars:	[26] [37] [48] [52] [67] [69] [70] [72] [100] [111]

Table 2.2: References Organized By Player Dynamics.

2.2.2.1 Simple Motion and Classical Pursuit

First, consider a game where all players move with fixed speeds, and where the players control their headings directly. That is, inertia is not considered, and the players can change direction abruptly, leading to paths that need not be smooth. This is often referred to as simple motion, and much of the literature considers games where all players move according to these rules. Now, consider the rate of change of the range, δ, between a pursuer P_i and an evader E_j, where the line of sight angle from P_i to E_j is β:

$$\dot{\delta} = v_{Ej} \cos(\beta - \psi_{Ej}) - v_{Pi} \cos(\beta - \psi_{Pi}). \tag{2.4}$$

Since v_{Pi} and v_{Ej} are constant, P_i minimizes $\dot{\delta}$ by choosing

$$\psi_{Pi} = \beta.$$

This is often referred to as classical pursuit, pure pursuit, or pursuit-guidance. Similarly, E_j maximizes $\dot{\delta}$ by choosing

$$\psi_{Ej} = \beta.$$

This strategy is referred to as classical evasion, pure evasion, or anti-pursuit evasion. These are the optimal pursuit and evasion strategies for a single pursuer versus a single evader if the payoff is time to capture and both players move with simple motion and have full information [48]. Note that when the evader plays optimally,

$$\dot{\delta} = v_{Ej} - v_{Pi} \cos(\beta - \psi_{Pi}), \tag{2.5}$$

and the range decreases whenever

$$\cos(\beta - \psi_{Pi}) > \frac{v_{Ej}}{v_{Pi}}. \tag{2.6}$$

Clearly, if $v_{Ej} > v_{Pi}$, (2.6) is never satisfied, and capture is impossible. Therefore, in most PE games,

$$\forall i \in 1, ..., m, \forall j \in 1, ..., n, v_{Pi} > v_{Ej}. \tag{2.7}$$

However, while this is usually true, there is existing work that considers evaders that are as fast [53] or faster [50] than their pursuer(s). There is also a special class of games that considers players with equal speeds, and this is described in Section 2.2.2.3.

2.2.2.2 Homicidal Chauffeur

One of the PE games most treated in the literature is the Homicidal Chauffeur (HC) game [48], which considers a single pursuer against a single evader. Both move with fixed speeds, where $v_P > v_E$. P controls the turn rate, $\dot{\psi}_P$, and P's radius of curvature is bounded. That is,

$$-c_\psi \leq \dot{\psi}_P \leq c_\psi \tag{2.8}$$

for a given c_ψ. E, on the other hand, moves with simple motion. Thus, P's advantage in speed is countered by E's advantage in maneuverability. Capture usually occurs when the distance between P and E is less than a given ℓ, and the payoff is typically the time to capture.

2.2.2.3 Game of Two Identical Cars

Another PE formulation is the game of two cars in which both the pursuer and the evader have bounded turn radii [48]. A special case of this is the game of two identical cars, in which the pursuer and evader have the same speed and the same minimum turn radius [69]. That is, for a given c_ψ,

$$\begin{aligned} v_P &= v_E, \\ -c_\psi \leq &\dot{\psi}_P \leq c_\psi, \\ -c_\psi \leq &\dot{\psi}_E \leq c_\psi. \end{aligned} \tag{2.9}$$

This game is particularly interesting to air combat scenarios, and so termination of the game often occurs when the pursuer is in a tail-chase [72]; that is, the game ends when P maneuvers into a position directly behind E, or within some prescribed angle of this position, and also within some prescribed maximum distance. This distance represents a missile's maximum range, so it may be larger than a typical capture ball in other PE games, and it is sometimes infinite [72].

2.2.3 Termination Conditions & Payoffs

As discussed previously, the PE literature contains a variety of termination conditions and payoffs. This section discusses a few of the more common termination conditions, and Table 2.3 shows a list of references organized by these conditions.

Termination	References
Capture:	[7] [8] [27] [37] [41] [61] [66] [70] [72] [46] [113] [115]
Colocation:	[16] [18] [38] [48] [49] [53] [54] [62] [85] [82] [98] [99]
Proximity:	[3] [26] [36] [48] [50] [67] [65] [69] [78] [89] [88] [100] [111]
Target Guarding:	[27] [48] [52] [57] [90] [96] [103] [104]
Visibility:	[10] [11] [13] [9] [12] [38]

Table 2.3: References Organized By Termination Conditions.

2.2.3.1 Capture

As stated previously, one common termination condition is capture. As a slight abuse of notation, let P_i and E_j refer to the positions of the ith pursuer and jth evader, respectively. Then capture typically means either of the following:

- Colocation of the players:

$$\|P_i - E_j\| = 0, \tag{2.10}$$

- Proximity of the players:

$$\|P_i - E_j\| < \ell. \tag{2.11}$$

One common payoff for games that terminate with capture is simply

$$J = t_c, \tag{2.12}$$

where t_c is the time that elapses between the start of the engagement and capture. For games with multiple evaders, the payoff could have a number of forms, such as the capture time of the first evader [99], the capture time of the final evader [62], or the average capture time.

2.2.3.2 Escape or Target Guarding

Suppose that in addition to avoiding capture, E_j desires to reach a goal set, Γ. This goal could be a safe-haven, as in [82], which prevents capture indefinitely if reached by E_j, or it might be a target which P_i seeks to defend from E_j's attack [48] [57]. As a more complicated example, consider a three player game where one mixed player seeks to not only evade a pursuer, but also to reach an adversarial goal state, where Γ is the location of an evader. This game is discussed in Section 2.2.4.2.

The games described above all have more than one potential termination condition. They end when either E_j reaches Γ or when P_i captures E_j. Payoffs for these types of games are typically E_j's distance from Γ when capture occurs.

2.2.3.3 Visibility-based games

Many times in the literature PE games are used to model surveillance scenarios [9]. In these situations capture may not be necessary, and the pursuers often seek only to maintain an unbroken line of sight to the evader [12]. The evaders seek to escape by breaking the line of sight. Payoffs in visibility-based games are often simply the time that elapses before the line of sight is broken, but more complicated payoffs are possible as well. For example, P_i may also attempt to minimize $\|P_i - E_j\|$. Reference [38] analyzes a similar game with two potential termination conditions, and it provides sufficient conditions for a pursuer to achieve capture without loss of visibility.

2.2.4 Team Games

Many PE games consider scenarios with more than two players. This can lead to interesting questions in cooperation and group behavior. For example, [108] applies PE games to a multiple vehicle formation control problem, and [78] considers swarms of UAVs in combat environments. The following sections consider two teams, called Red and Blue and denoted by $\mathscr{R}$ and $\mathscr{B}$, respectively. Table 2.4 provides a list of PE games that feature more than two players.

Team Configuration	References
Multiple Pursuers:	[3] [7] [8] [16] [31] [48] [50] [52], [54] [68] [57] [78] [85] [98] [100] [108]
Multiple Evaders:	[18] [61] [62] [98] [99] [108]
Mixed Teams/Players:	[17] [36] [85] [90] [96] [103] [104]

Table 2.4: References Organized By Team Configuration.

2.2.4.1 Coordinated pursuit or coordinated evasion

The simplest cases involving additional players are those that only account for additional pursuers and evaders, but still maintain the following two conditions

1.
$$\{\mathscr{P} \cap \mathscr{E}\} = \emptyset, \tag{2.13}$$

2.
$$\begin{gathered} \mathscr{R} = \mathscr{P} \;\; and \;\; \mathscr{B} = \mathscr{E} \\ or \\ \mathscr{R} = \mathscr{E} \;\; and \;\; \mathscr{B} = \mathscr{P}. \end{gathered} \tag{2.14}$$

That is, no player is both a pursuer and an evader, and teams consist of strictly pursuers or strictly evaders. For example, [20] considers a group of pursuers, while [62] and [61] consider a team of evaders cooperating to maximize the time required for a single pursuer to capture all evaders.

This formulation can be used to model biological scenarios such as cooperative hunting which has been observed in champanzees [14] [15], and applying it to a game with a single pursuer against a group of evaders with different speeds has been shown to result in herding behaviors [99].

2.2.4.2 Mixed teams

As discussed in Section 2.2.3.2, a single player may be both a pursuer and an evader. This may occur, for example, in military rescue scenarios or in the case of wildlife protecting its offspring. Teams can also be mixed, and may include any combination of pursuers, evaders, and mixed players.

The Lady, the Bandit, and the Bodyguards One version of a PE game with mixed teams in the literature is known as the Lady, the Bandit, and the Bodyguards [96]. This game consists of an evader, E, called the Lady, a pursuer, P, known as the Bodyguard, and a mixed player, M, known as the Bandit. The teams are as follows:

$$\mathscr{B} = \{E, P\}, \quad \mathscr{R} = \{M\}. \tag{2.15}$$

In this game, P pursues M while M pursues E, and the game terminates when either of the two captures occurs. The payoff is typically given by the distance between M and E when P captures M; i.e.,

$$J = \|M - E\|. \tag{2.16}$$

This game has been used to model scenarios involving a homing missile or torpedo (M) attacking a target (E) equipped with a counterweapon (P) that is capable of destroying the incoming threat [17] [90] [103] [104]. It has also been referred to as the Active Target Defense game [36] [34] [35].

Prey, Protector, and Predator Another PE game with mixed teams is known as the Prey, Protector, and Predator (P3) game [85]. Here there are two pursuers, a predator, P, and a protector, R, and one mixed player, the prey, E. The teams are as follows:

$$\mathscr{B} = \{E, R\}, \quad \mathscr{R} = \{P\}. \tag{2.17}$$

Both P and R pursue E, and E attempts to evade P and rendezvous with R. The game terminates either when P captures E or when E and R rendezvous.

2.2.5 Information

Another aspect in which PE games differ is the amount of information available to the players. This information can take a variety of forms including the locations and strategies of other players, the environment in which the players move, and even the number of players and their roles. If a player is able to gain information that their opponent does not have, they may gain a significant advantage in the game, and therefore players often face trade-offs between exploiting known information and exploring to gain new information. These topics can be quite challenging to address, and there are many interesting questions still open in this area.

2.2.5.1 Sensing Limitations

As discussed previously, realistic PE games often take place in complex environments. These games can be further complicated by considering the case where the environment is unknown a priori. Also, in some cases, the players are equipped with sensors that are not able to detect their opponents or team mates at all times. Two common types of sensors in the literature are those based on line of sight [13] and those based on proximity [16]. Consider a game that terminates with capture where the players are equipped with either of these types of sensors. The best strategies for the players to follow when they are unable to sense their opponent's position may not be trivial. For example, the players could act based on the last detected location, they could attempt to predict their opponent's current location, or they could act in a way that increases the likelihood of detecting their opponent in the future at the cost of a potentially decreased payoff.

Other types of sensor limitations have also been studied. For example, [61] considers a game where the pursuer's probable position has uniform distribution within a disk with known center and radius. References [113] and [115] also consider games where player locations may be known imperfectly, and in these works position information is allowed to be jammed by an adversary. There are also examples in the literature of games where the players have access to sensor networks that can improve their sensing capabilities [98].

While much of the PE literature assumes perfect information, this is rare in practice. At the least, measurements are often noisy, but in addition to inaccuracies, the information provided by sensors can vary widely, and a number of techniques and measurements have been utilized for target localization in pursuit and homing scenarios. Some of these measurements provide large amounts of information, including systems that measure the line of sight rate and time to impact for missile guidance [87], and localization methods that utilize multiple acoustic transmitters or multiple receivers [58] [107]. Other measurements have been utilized that provide only line of sight information, including some optical and electromagnetic sensors used in terminal guidance [23] [29]; Very High Frequency (VHF) radio transmitters with directional antennas for tracking wildlife [64] [63]; and directional passive acoustic devices for torpedo guidance [95] and marine animal tracking [75]. Finally, low-cost applications have made use of very limited sensors, including range-only measurements [109] and measurements of the sign of the range-rate [112] [81] [83].

2.2.5.2 Player Traits

Knowledge of the number of players, their roles, and their physical characteristics, such as speed and maximum turn radius, can also have a significant impact on PE games. Many of the tools in the PE literature, such as the construction of dominance regions (Section 2.3.4), require knowledge of the players' speeds. These tools must be modified if that information is unknown. References [113] and [115] consider games where characteristics such as speed and maneuverability are not known perfectly.

Additionally, the roles of pursuer and evader may not be specified. Consider again the game of two identical cars from Section 2.2.2.3 which is often used to model air combat. In a more realistic air combat scenario, both players wish to attack if they have the advantage, or flee if their opponent has the advantage. A natural extension of the game is therefore to classify both players as mixed players. Then, before determining what actions to take, the players should first evaluate the game configuration and determine whether it is more advantageous to pursue or to evade. This problem is often referred to as role determination or the two-target game, and it has been studied extensively in [27] [37] [42] [43] [70] [72] [113].

Combining different forms of missing information can lead to more realistic, but often unmanageable, game formulations. For example, in the problem of role determination in [70], the players have perfect information about their opponent's location, speed, and turning radius. It is often assumed that opponent speed and turning radius are provided by intelligence, but allowing uncertainty in these values could lead to interesting insights.

2.2.5.3 Strategies

When missing information is considered, players may not be able to determine the optimal action to take. They may then resort to a specific strategy, and knowledge of an opponent's strategy can allow it to be exploited. For example, consider the Lady, the Bandit, and the Bodyguards game, as described in 2.2.4.2. Player M usually represents a homing missile or torpedo, and most of the literature assumes that M is the type of weapon in use today. Therefore, previous work typically assumes that M accounts only for its pursuit of E and that M has no knowledge of the existence of P. M therefore employs a potentially suboptimal strategy, and the blue team is able to exploit this predictable behavior to maximize the distance between M and E at the moment of M's capture by P [36].

2.3 Solution Methods

This section describes a number of solution methods that are used in the literature, and Table 2.5 provides a list of references that utilize each solution method.

Solution Method	References
Dynamic Programming:	[10] [13] [12] [18] [48] [65] [66] [69] [88] [100] [108] [113] [115]
Indirect Method:	[26] [31] [36] [39] [53] [61] [70] [90] [96] [103] [111]
Viscosity Solutions:	[4] [24] [25] [60] [106]
Barrier & Reach Sets:	[11] [37] [41] [42] [48] [53] [67] [68] [69] [70] [72] [89] [100] [111] [46]
Dominance Regions:	[7] [8] [85] [82]
Apollonius Circles:	[18] [38] [48] [50] [99]
Partitioning Problems:	[2] [3] [31] [57] [97] [99]
Enforced Strategy:	[3] [16] [17] [19] [27] [36] [39] [42] [47] [62] [98] [99] [103] [104]
Approximations:	[9] [46] [52] [62] [74] [111]
Geometric Methods:	[16] [17] [49] [54] [66] [57] [85] [82] [97]

Table 2.5: References Organized By Solution Method.

2.3.1 Dynamic Programming

One solution method for PE games is as outlined in [48]. It is essentially an application of dynamic programming methods with two competing controls. Thus, if solved, it provides both the value of the game and the optimal strategies for each player. If the optimal strategies $\vec{u}_B^*(\vec{x})$ and $\vec{u}_R^*(\vec{x})$ are unique, or if one is chosen from a set of optimal strategies, then substituting these strategies into the game's dynamics, $f(\vec{x}, \vec{u}_B, \vec{u}_R)$, and integrating provides the optimal paths from a given set of initial conditions to the game's termination.

Consider a payoff of the following form:

$$J(\vec{x}) = \int_{t_0}^{t_f} G(\vec{x})\,\mathrm{d}t + K(\vec{x}(t_f)). \tag{2.18}$$

As discussed in [48], the value of the game satisfies the following equation:

$$\sum_i \frac{\partial V}{\partial x_i} f_i(x, \hat{u}_B, \hat{u}_R) + G(x, \hat{u}_B, \hat{u}_R) = 0, \tag{2.19}$$

where $\hat{u}_B$ and $\hat{u}_R$ are functions of both $\vec{x}$ and $\frac{\partial V}{\partial \vec{x}}$, and they become the optimal strategies $\vec{u}_B^*(\vec{x})$ and $\vec{u}_R^*(\vec{x})$ once $V(\vec{x})$ is known. Reference [48] refers to this as the Main Equation.

Differentiating (2.19) with respect to each x_k leads to the following:

$$\frac{d}{dt}\frac{\partial V}{\partial x_k} = -\left(\sum_i \frac{\partial V}{\partial x_i}\frac{\partial f_i}{\partial x_k} + \frac{\partial G}{\partial x_k}\right), \tag{2.20}$$

and applying $\vec{u}_B^*$ and $\vec{u}_R^*$ to the game dynamics gives:

$$\dot{\vec{x}} = f(\vec{x}, \vec{u}_B^*(\vec{x}), \vec{u}_R^*(\vec{x})). \tag{2.21}$$

If $\vec{x} \in \mathbb{R}^\eta$, then equations (2.20) and (2.21) represent 2η ordinary differential equations in the 2η unknowns $\vec{x}$ and $\frac{\partial V}{\partial \vec{x}}$. These are referred to as the path equations.

When solving games, it is typical to start from the known capture conditions and integrate backward in time. This changes the signs in (2.20) and (2.21) and results in a set of 2η equations known as the retrogressive path equations (RPE) which are Hamilton-Jacobi equations.

Generally, the curse of dimensionality makes numerically solving the RPE a difficult task. For certain fully nonlinear, partial differential equations, including Hamilton-Jacobi equations, a type of solution known as a viscosity solution has been shown to both exist and be unique under a variety of hypotheses [24] [25] [60]. These viscosity solutions have also been shown to not require convexity [4]. Reference [106] studies the Dirichlet problem for first-order Hamilton-Jacobi equations and makes use of viscosity sub- and supersolutions to show the existence of the value for a class of PE differential games.

2.3.2 Indirect Method

Consider an extension of the Pontryagin Maximum Principle (PMP) [94] that applies to differential games, including PE games [91]. The Hamiltonian, H, is given by

$$H = -G + \vec{p}f, \tag{2.22}$$

where $\vec{p}$ is a vector of adjoint variables satisfying

$$\dot{\vec{p}} = -\frac{\partial H}{\partial \vec{x}}. \tag{2.23}$$

A necessary condition for the trajectory $\bar{x}(t)$ with inputs $\bar{u}_B(\bar{x})$ and $\bar{u}_R(\bar{x})$ to be a minmax solution is that

$$H(\bar{x}(t), \bar{u}_B(\bar{x}), \bar{u}_R(\bar{x}), \vec{p}(t)) = \min_{u_B} \max_{u_R} H(\vec{x}(t), u_B(\vec{x}), u_R(\vec{x}), \vec{p}(t)), \tag{2.24}$$

i.e., $\bar{u}_B, \bar{u}_R$ is a saddle point of the Hamiltonian. The first-order necessary conditions are

$$\frac{\partial H}{\partial u_B} = \frac{\partial H}{\partial u_R} = 0, \tag{2.25}$$

and the second-order conditions are

$$\frac{\partial^2 H}{\partial u_B^2} > 0, \quad \frac{\partial^2 H}{\partial u_R^2} < 0. \tag{2.26}$$

In some cases, specific properties of games can lead to simplifications in the solution. For example, it is often the case that the Hamiltonian is separable in the two player's controls, and therefore, in some cases the controls and optimal trajectories can be determined through optimal control techniques such as quadratic programming. For example, [10] and [11] make use of this separability to solve a visibility-based PE game in the presence of a circular obstacle.

2.3.3 Singular Surfaces

As discussed in [48] and [59], it is often the case that the solutions of differential games exhibit different behaviors in different regions of the game space. The boundaries between these regions are known as singular surfaces. Thus, solving these games consists of two stages, known as the solution in the small and the solution in the large. The solution in the small refers to the smooth parts of the solution between singular surfaces, and it is the result of solving the equations in Section 2.3.1. The solution in the large involves decomposing the game space into i regions, R_i, such that within each R_i the solution is smooth, i.e., $\forall i, \forall \vec{x} \in R_i, V(\vec{x}) \in C^1$.

Finding the solution in the large involves the determination of singular surfaces which can take a variety of forms. Here, the focus is on two forms, dispersal surfaces and the barrier in games of kind. Other types of singular surfaces exist, and [89] discusses their construction for games with HC dynamics. For additional information on singular surfaces, the reader is referred to [48] and [59].

2.3.3.1 Dispersal Surfaces

One type of singular surface is known as a dispersal surface, which is a surface in the game space in which the optimal paths move away from the surface on both sides. For example, consider a player deciding which direction of travel is shortest to move around an obstacle. The surface for which both paths are equally short is a dispersal surface, and locations that are close together, but separated by the dispersal surface have significantly different outcomes. A similar choice is required in PE games on a surface of revolution, such as the surface of a cylinder, for which the geodesic curve between two points may not be unique.

Another example of a dispersal surface occurs in PE games with HC dynamics. Consider a scenario where the evader is directly behind the pursuer and sufficiently far away. The pursuer should turn as sharply as possible, but the optimal choice of direction is not unique. Similarly, reference [102] considers games with a different type of choice, where the game can be terminated on multiple target sets, and it provides a decomposition of the game space that allows switching between strategies for these different target sets.

2.3.3.2 The Barrier in Games of Kind

In games of kind, the objective is to identify which initial conditions lead to capture and which conditions lead to escape. These are referred to as the capture and escape sets, respectively. The problem is to find the barrier between these two sets. Note that these sets can be empty. For example, if P is faster than E and at least as maneuverable, P can always travel to E's starting point and follow the same path to capture. Thus, the escape set would be empty for that particular game.

One way to calculate the barrier that is common in the literature is to determine the min-max controls by constructing the Hamiltonian, then to apply those controls to the terminal set and calculate the reach set backward in time, where a reach set is the set of all initial states from which a path exists that takes the initial state to the final state. For example, this method is used in [9] and [69].

These techniques have also been applied to linear dynamic games in [46]. There, the two aircraft collision avoidance problem is considered, and backward reachable sets are used to determine a polytopic approximation to the set of points for which aircraft 2 can collide with aircraft 1, no matter how hard aircraft 1 tries to prevent the collision. Reference [100] considers a similar collision avoidance problem with two noncooperative pursuers and one evader.

2.3.4 Dominance Regions

An alternative solution method that has been utilized in the literature makes use of dominance regions, where a point is said to be dominated by a player if they are able to reach that point before their opponent, regardless of the opponent's actions. Dominance regions provide the complete solution to capture games with full information, but they have not been described in the literature for all types of capture games. This section describes the dominance regions for planar games with no obstacles where all players move with simple motion.

2.3.4.1 Apollonius Circles

Consider a single pursuer, single evader game in the plane with no obstacles and full information. Reference [48] shows that the dominance regions are divided by an Apollonius circle, which is given by:

$$\left(\gamma^2 - 1\right) r^2 + \left(2d\cos(\theta)\right) r - d^2 = 0, \tag{2.27}$$

where (r, θ) are polar coordinates with origin at the evader's initial location and the direction of zero azimuth along the line of sight to the pursuer; $\gamma = v_P/v_E$ is the speed ratio, and d is the initial distance between the players. If the payoff is time to capture, then if both players act optimally, capture will occur at C, the point on the dominance boundary with the highest payoff for E. The optimal strategies therefore dictate that both players travel to C in minimum time, which leads to heading angles that agree with the previous analysis in Section 2.2.2. The value of the game is the minimum time required for the players to reach C.

Apollonius Circles can also be used in more complicated games. For example, [48] describes the game of the two cutters and the fugitive ship, in which two pursuers cooperate to capture a single evader. In this case, two Apollonius Circles are needed, and the intersection of the two circles is E's dominance region. As before, capture occurs at the point on the dominance boundary with the highest payoff for E, and all players travel there in minimum time.

Reference [50] considers multiple slow pursuers against a fast evader. Apollonius circles are used to determine the number of pursuers required to guarantee capture as well as a strategy that the pursuers can follow.

Reference [38] considers PE in an unknown environment with visibility constraints, and it uses Apollonius circles to identify regions in the game space where capture occurs before loss of visibility. Since visibility constraints are included, the analysis considers only the portion of the standard Apollonius circle that can be reached by both players along straight-line paths, but it does not consider the overall structure of the dominance region or how the dominance regions change due to the presence of the obstacle.

2.3.4.2 Partitioning Problems and Voronoi Diagrams

Many cooperative PE strategies rely on knowing which player can reach a given point first. For example, [7] and [8] study a cops and robbers game with polygonal obstacles, where a cops and robbers game is a game where the players take turns moving, and they show that three pursuers are always sufficient and sometimes necessary to capture an evader. The strategy involves partitioning the environment such that the locations of the pursuers confine the evader to a polygon. The pursuers are then able to decrease the size of the polygon with each move, and eventually they capture the evader.

Reference [3] considers relay pursuit of a single maneuvering target by a team of pursuers where only the closest pursuer actively pursues the target. This problem is equivalent to partitioning the space into dominance regions among the entire team of pursuers, and it can be accomplished by analyzing the pairwise dominance regions for all potential pairs of pursuers. One simplification that allows the dominance regions for large numbers of players to be determined more easily is to assume that all players move at the same speeds.

In this case, the speed ratios are all equal to 1, and for each pairwise dominance boundary, the first term in (2.27) goes to zero, causing the Apollonius Circle to degenerate into the line given by

$$r = \frac{d}{2\cos(\theta)}, \tag{2.28}$$

which is the perpendicular bisector of the line segment connecting the locations of the players. Partitions of the plane into dominance regions with this method are known as Voronoi Diagrams, and they are treated often in the literature (see Table 2.5).

The concept of Voronoi Diagrams has also been extended to cases where the players are affected by currents [2]. Reference [97] extends Voronoi Diagrams to scenarios where the players move at different speeds, but it focuses on crystal growth, and therefore paths are not allowed to pass through the dominance regions of any other competitor. Instead crystals can only wrap around others as they grow. This differs from dominance in PE games, because dominance in PE games does not prevent a player from traveling through a point where their opponent dominates, it simply means that they can't reach that particular point before their opponent does.

Reference [99] features a heterogeneous group of evaders with different speeds and limited sensing radii against a single, fast predator. A weighted Voronoi diagram is used to inform the evasion strategies, and group herding behaviors are shown to be the result of each evader attempting to minimize the set of potential pursuer positions for which that evader has a shorter capture time than all other evaders.

2.3.5 Enforcement of Pursuit/Evasion Strategies

Due to the difficulties of solving PE games analytically, it is common to consider a single player and assume a strategy for the opponent. This technique can simplify the problem by reducing the analysis from a minmax problem to a simpler one-sided optimization problem. Additionally, one drawback to using a PE game formulation is that it is inherently conservative. That is, the opponent is assumed to take the worst-case actions, and if this is not true in the actual scenario, then it can be possible to achieve better performance.

For example, in [39] [51], proportional navigation is shown to be the optimal guidance law for a pursuer with linear autopilot dynamics in a differential game with a time varying cost functional. Thus, in the literature, evaders often assume proportional navigation strategies for their pursuer. This leads to a simplification of the problem from a minmax problem to a one-sided optimal control problem, and [39] uses this method to show that the well known evasion strategy referred to as jinking is optimal when used against proportional navigation.

As another example, as described in Section 2.2.2.1, classical pursuit and classical evasion are optimal in single-pursuer, single-evader games with simple motion and perfect information. These strategies have also been observed in nature [56] [116]. For this reason, the literature often enforces these strategies on one or more players, even in scenarios that do not hold to the assumptions of SPSE and perfect information. For example, [36] considers a cooperative defense strategy against an attacking missile utilizing classical pursuit, and the missile's known strategy is able to be exploited due to its predictability. Similarly, [99] shows that in a game with a single pursuer and multiple evaders, strategies based on pure pursuit and evasion can lead to herding behavior.

2.3.6 Other Approaches

Reference [92] studies PE games governed by linear differential equations where the terminal set is a linear manifold. Conditions are provided that ensure the existence of a set of initial conditions for which capture can be achieved, and conditions are also provided for initial conditions where capture can be avoided indefinitely. Reference [93] also studies linear PE games, and it provides two methods for solving the pursuit problem using constructions of convex sets.

Alternative mathematical formulations have been proposed to solve PE games. For example, in [42], a bicricterion game formulation is used which provides open-loop guidance maneuvers. One benefit of this approach is that the solution need not be a saddle point, and therefore the existence of the solution is more easily proved. In [37] and [41], an approach utilizing Lyapunov functions is used to determine the winning regions for each player. An approach based on online model predictive control has been used in [27], and other methods such as genetic algorithms, machine learning [105], and reinforcement learning with level-k games [86] have been applied to learn effective strategies in PE scenarios. Discretization and sampling-based algorithms have also been utilized to provide fast numerical computations in PE scenarios [52] [74] [26].

Due to the complexity of PE problems, the practical solution for pilots in air combat has been the application of a number of heuristics that attempt to maneuver the pilot into an advantageous position. These heuristics are described in detail in [101], and a rule-based simulator using many of the same maneuvers is described in [19]. The literature has shown some of these maneuvers to be optimal under certain conditions [47], but many are still simply based on pilot experience. Reference [71] describes some of the challenges of developing a fully autonomous air combat guidance strategy as well as the challenge of convincing pilots that differential game theory can provide maneuver logic that is better than the pilot's intuition.

2.4 Challenges & Open Problems

There are many open problems in the field of PE games, ranging from questions that require extensions of existing techniques to those that have not even been answered in the simplest cases.

For example, [9] shows the existence of a value function, as well as an offline scheme to compute it, for a visibility-based target tracking game with a single circular obstacle. However, the existence of a value function and the optimal strategies for that game in the case of general polygonal environments are stated as open problems.

As discussed in Section 2.2.1, much of the existing literature focuses on systems with few dimensions, such as a single pursuer and a single evader in a two dimensional environment. Higher order problems involving complicated environments, constrained dynamics, or additional players are challenging with existing techniques.

Games with limited information provide many interesting open questions, and these types of games often represent the most interesting and realistic scenarios. However, they are also typically difficult to analyze. For example, uncertainty in an opponent's location prevents the use of some existing techniques. PE games in uncertain environments present similar challenges to existing techniques. These types of problems have practical significance, because in order to implement PE strategies and algorithms on mobile robots, the limitations of these robots must be accounted for. For example, the localization and mapping problem is addressed often within the mobile robotics community, and a combined problem involving PE while mapping and exploring an environment would have many applications.

Another interesting question regarding information involves the representation of uncertainty in the information available to the players. For example, a player can gain significant advantages if they are able to recognize and capitalize on situations where their opponent plays suboptimally due to a lack of information. However, utilizing this type of strategy can be detrimental if the opponent employs deception to mask the availability of important information. This type of problem framework is typically unmanageable, because it leads to arguments involving infinite regression where player A's strategy depends upon what A believes player B knows, what A suspects B believes about A's knowledge, and so on. Since game theory assumes a worst-case opponent, typical solutions simply assume a worst-case information pattern. However, the ability to represent uncertainty in information, even for simplified examples, could lead to interesting insights.

2.5 Summary

PE games have a rich history in the literature, and they have many practical applications both within and outside the aerospace field. They can be used to model aerial battles between fighter aircraft, surveillance problems for mobile robots, autonomous driving with collision avoidance, and other interesting scenarios. Interest in the field of PE has grown in recent years due to the increasing prevalence of mobile robots as well as improvements in their capabilities. A number of solution techniques and heuristics have been discussed in the literature, but many questions are still open. Improvements to existing techniques and advances on these open challenges can lead to significant benefits, including improved security and surveillance capabilities and better disaster response techniques.

CHAPTER 3

Single-Pursuer, Single-Evader Games

This chapter studies planar Single Pursuer, Single Evader (SPSE) games where the players move with fixed speeds. The goal of the pursuer is to capture the evader, and the goal of the evader is to avoid capture, where capture means pointwise capture, unless otherwise specified. Specifically, this chapter further develops the method of dominance regions that was introduced in Chapter 2. Recall that a point in the plane is said to be dominated by one of the players if that player is able to reach the point before the opposing player, regardless of the opposing player's actions, and a dominance region is the set of all points dominated by a particular player.

The primary contributions of this chapter are two generalizations of the Apollonius circle dominance boundary. Theorem 3.2.5 and Remark 3.2.6 provide the dominance boundary for PE games with simple motion in the presence of obstacles. Remark 3.3.1 provides the dominance boundary for PE games that feature simple motion against a Dubins car, and it provides an alternative method for analyzing the Homicidal Chauffeur and Suicidal Pedestrian games. As another contribution, this chapter shows that an analysis of dominance provides complete solutions to many PE games, including not only games of kind, but games of degree as well. For example, optimal pursuit and evasion strategies are provided for the PE game of degree with time to capture as the payoff.

Besides solving SPSE games, one important benefit of this chapter's contributions is that they simplify the analysis of games with additional players. Thus, even though the

HC problem has been solved previously, the alternative method of analysis provided in this chapter forms an important foundation for the analysis of MPME games in Chapter 4. Likewise, these contributions serve as a foundation for the analysis of games with uncertainty in Chapter 5.

3.0.1 Problem Statement

The problems addressed in this chapter can be stated as follows:

P3.1 **Dominance Regions:** Given two players, a pursuer, P, with constant speed v_P and minimum turn radius ρ_P, and an evader, E, with constant speed v_E and minimum turn radius ρ_E, moving in a plane with full and perfect information (i.e., each player exactly knows v_P, ρ_P, v_E, and ρ_E, as well as the locations of both players at all times), find the locus of points, $\mathcal{B}_{PE}$, such that $\mathcal{B}_{PE}$ separates the region of the plane dominated by P from the region dominated by E.

P3.2 **Pursuit and Evasion Strategies:** Given the scenario described in P3.1, and additionally given $\mathcal{B}_{PE}$, find the optimal pursuit and evasion strategies for the game of degree with time to capture as the payoff.

Note that the solution to P3.1 is $\mathcal{B}_{PE}$, the boundary between the two players' dominance regions, and as Sections 3.2.3, 3.2.4, and 3.3.2 show, the construction of $\mathcal{B}_{PE}$ does not take the roles of pursuer and evader into account, but instead views both players simply as mobile agents. However, the construction of $\mathcal{B}_{PE}$ provides all of the information required to solve P3.2 once the roles are specified. This is discussed in Sections 3.1.2, 3.2.6, and 3.3.4.

3.0.2 Organization

This chapter is organized as follows: Section 3.1 provides preliminary information from the literature, including a description of the Apollonius circle and its use in PE games.

Section 3.2 considers PE with simple motion (i.e., $\rho_P = \rho_E = 0$) in the presence of obstacles, and Section 3.3 considers PE where one of the players is a Dubins car (i.e., either $\rho_P \neq 0$ or $\rho_E \neq 0$). Note that Section 3.2 provides two methods for constructing the dominance regions, and the method in Section 3.2.3 is general and not limited to simple motion dynamics. Finally, Section 3.4 provides a summary of the chapter's results.

3.1 Preliminaries

3.1.1 Classical Pursuit/Evasion

Consider the SPSE game with simple motion, which can be stated as follows: Given a pursuer, P, at position (x_P, y_P) with fixed speed v_P and heading input ψ_P, and an evader, E, at position (x_E, y_E) with fixed speed v_E and heading input ψ_E, and subject to the following dynamics:

$$\begin{aligned}\dot{x}_P &= v_P \cos\psi_P, \\ \dot{y}_P &= v_P \sin\psi_P, \\ \dot{x}_E &= v_E \cos\psi_E, \\ \dot{y}_E &= v_E \sin\psi_E,\end{aligned} \tag{3.1}$$

and given as payoff the capture time, t_c, when the pursuer is colocated with the evader; find the inputs ψ_P^* and ψ_E^* such that ψ_P^* and ψ_E^* maximize the minimum t_c or, equivalently, minimize the maximum t_c.

The solution to this problem can be determined by defining β as the line of sight angle from P to E, and then considering the change in the range, δ, between the players with respect to time as a function of their headings:

$$\dot{\delta} = v_E \cos(\beta - \psi_E) - v_P \cos(\beta - \psi_P). \tag{3.2}$$

From (3.2), P minimizes $\dot{\delta}$ by choosing $\psi_P = \beta$, and E maximizes $\dot{\delta}$ by choosing $\psi_E = \beta$.

These strategies maximize the minimum time to capture, or, equivalently, minimize the maximum time to capture. They are typically referred to as classical pursuit and classical evasion, and they lead to behaviors where P travels directly toward E along the line of sight and E flees directly away from P in the same direction.

3.1.2 Apollonius Circles

The Apollonius circle is the set of all points for which the ratio of distances to two fixed points is constant. In a Cartesian coordinate system with arbitrary origin, where $P = (x_P, y_P)$ and $E = (x_E, y_E)$ are the fixed points, and γ is the ratio of the distance from P to the distance from E, the center of the Apollonius circle, (h, k), is:

$$(h, k) = \left(\frac{x_P - \gamma^2 x_E}{1 - \gamma^2}, \frac{y_P - \gamma^2 y_E}{1 - \gamma^2} \right), \tag{3.3}$$

and the radius, r_A, is:

$$r_A = \frac{\gamma}{1 - \gamma^2} \sqrt{(x_P - x_E)^2 + (y_P - y_E)^2}. \tag{3.4}$$

Note that in the context of this dissertation, the fixed points represent the locations of the pursuer and evader, and the Apollonius circle gives the points where P and E can meet if both follow straight-line paths. Hence, γ represents not only the ratio of distances traveled by P and E in a common time, t, but also the ratio of their constant speeds:

$$\gamma = \frac{v_P t}{v_E t} = \frac{v_P}{v_E}. \tag{3.5}$$

An alternative expression, which will be utilized in later sections, gives the Apollonius circle in polar coordinates (r, θ). Take the following implicit description of the Apollonius circle:

$$(x - h)^2 + (y - k)^2 - r_A^2 = 0, \tag{3.6}$$

and substitute $r\cos\theta = x$ and $r\sin\theta = y$:

$$(r\cos\theta - h)^2 + (r\sin\theta - k)^2 - r_A^2 = 0. \tag{3.7}$$

Expand and rearrange to arrive at:

$$r^2 - 2r(h\cos\theta + k\sin\theta) + (h^2 + k^2 - r_A^2) = 0. \tag{3.8}$$

A version of this equation which will be useful in later sections places the origin at the location of the evader and the direction of zero azimuth along the line of sight to the pursuer, with d defined as the initial distance between the players. Thus, $x_E = y_E = y_P = 0$ and $d := x_P$. This gives the following:

$$h = \frac{d}{1-\gamma^2}, \qquad k = 0, \qquad r_A = \frac{\gamma d}{1-\gamma^2}. \tag{3.9}$$

Substitute these values for h, k, and r_A into (3.8), then multiply the resulting equation by $(\gamma^2 - 1)$ to arrive at:

$$\left(\gamma^2 - 1\right) r^2 + \left(2d\cos(\theta)\right) r - d^2 = 0. \tag{3.10}$$

As discussed in [48] [51], the Apollonius circle can be applied to solve a variety of PE games, including both P3.1 and P3.2.

Theorem 3.1.1 *For a SPSE game where both players move with simple motion in a plane containing no obstacles, the dominance regions of the PE game are separated by an Apollonius circle.*

Theorem 3.1.1 provides solutions to games of kind, for which there are a finite number of possible outcomes; e.g., the question of whether or not E can reach a safe haven before being captured. Additionally, the dominance regions provide the solution to the more general game of kind which asks simply whether or not P can capture E at all, given enough time. If E's dominance region is bounded, which is always the case if $v_P > v_E$, then P dominates this game of kind, and given the optimal strategy, P will always be able to capture E. This type of strategy that guarantees victory for one player is called a dominant strategy. In this case, since $v_P > v_E$, and since P is as maneuverable as E, one dominant strategy is that P simply travels to E's initial location and then follows the same path as E until capture occurs. However, the notion of dominance regions is not specific to the dynamics of simple motion, which this example considers, and knowledge of the dominance regions can be used to construct dominant strategies in other cases as well. Additionally, the usefulness of dominance regions is not limited to games of kind. The information they provide is sufficient to solve games of degree as well, which have a continuum of outcomes; e.g., the question of how long it takes for P to capture E.

Theorem 3.1.2 *In a SPSE game of degree with no obstacles where the payoff is the time to capture, which P seeks to minimize and E seeks to maximize, the optimal strategies are such that capture occurs at the point, C, on the Apollonius circle that is farthest from E's initial position, and optimal play dictates that P and E both travel to C in minimum time [48].*

Note that when no obstacles are present, P, E, and C are co-linear. Thus, the strategies that result from this construction are equivalent to classical pursuit and classical evasion. If P and E both play optimally, then they travel straight to the capture point, and the Apollonius circle at any intermediate point is tangent to the initial circle at C. If either player deviates from their optimal strategy and travels laterally, then the optimal capture point changes, and the resulting path for the other player curves.

3.2 Simple Motion

This section considers PE games where both players move with simple motion, and it presents two methods for constructing the dominance regions. The first involves finding

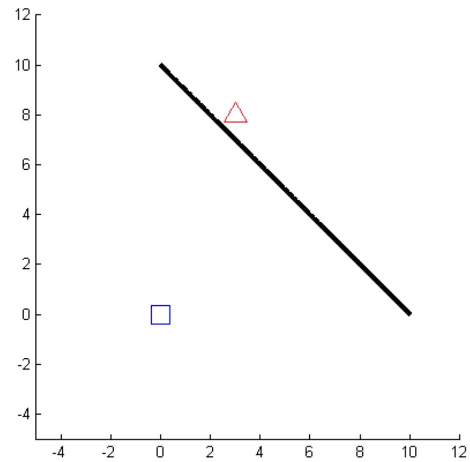

Figure 3.1: Example scenario: SPSE with simple motion.

the intersection of bundles of isochrones, where an isochrone is a level curve for the value function of a time-optimal control problem. This method is general, and is not limited to simple motion dynamics. The second method is based on the first, but utilizes the equations of motion to provide the dominance regions in closed form. Hence, it is limited to PE with simple motion. This method involves identifying singular surfaces that divide the plane into regions, and then determining closed form expressions for the portion of the dominance boundary that lies in each region.

3.2.1 Motivating Example

Consider the SPSE game in Figure 3.1, in which the environment contains a line segment obstacle. Here, the $\square$ represents the evader and the $\triangle$ represents the pursuer. Unless otherwise specified, the pursuer is twice as fast as the evader. This scenario is used throughout Section 3.2 to illustrate a number of concepts. For this example, previous methods are unable to answer the following questions:

Q3.1 What are the dominance regions?

Q3.2 Which player benefits from the the obstacle and which player is hindered by it?

Q3.3 How can the game be analyzed if the obstacle affects the players asymmetrically?

Q3.4 What are the optimal pursuit and evasion strategies in the presence of the obstacle?

The remainder of Section 3.2 starts from a reduced version of this example with only one player. Then, it slowly adds complexity and addresses each question in turn.

3.2.2 Time-Optimal Paths & Isochrones

This subsection addresses a foundational version of the motivating example that consists of a single player moving in the presence of the obstacle. Consider the following time-optimal control problem: Given an agent moving with simple motion and speed v, initial and final locations, (x_i, y_i) and (x_f, y_f), and a set of known obstacles, $\mathcal{S}$, find a path that connects (x_i, y_i) to (x_f, y_f) without intersecting $\mathcal{S}$ such that the time required for the agent to reach (x_f, y_f) is minimized.

Here, the agent moves with constant speed, and therefore time-optimal paths correspond to paths with the smallest Euclidean distance. These paths can be determined using [73] and [45]. For this work, we are interested in level curves for the value function of this time-optimal control problem, and these level curves are referred to as isochrones.

The following theorems are useful for future developments, and their proofs involve the propagation of a simulated wavefront in the plane [73].

Theorem 3.2.1 *In the absence of obstacles, the time-optimal paths are straight lines, and the isochrones are concentric circles centered at the agent's initial location.*

Theorem 3.2.2 *In the presence of a set of polygonal obstacles, the time-optimal paths are broken lines, breaking at obstacle vertices, and the isochrones form arcs of concentric circles centered at generating points, where a generating point is either an obstacle vertex or the agent's initial location.*

Theorem 3.2.3 *The curves that separate the plane into regions with unique generating points are either line segments or arcs of hyperbola.*

The preceding theorems are illustrated in Figure 3.2a, which shows a bundle of isochrones of different durations for the evader in the motivating example. The thick line is the obstacle, the thin lines are isochrones, and the dotted lines are the curves that separate the regions with different generating points. In region 1, the time-optimal paths are unaffected by the obstacle, and the isochrones form concentric circles centered at the evader's initial location. For destinations in regions 2 and 3, the time-optimal paths break at the obstacle's end points, and the isochrones form concentric circles centered at the end points. Regions 2 and 3 are separated by an arc of hyperbola where each point on the arc can be reached in equal time by traveling around the obstacle in either direction.

Figure 3.2b shows the isochrones for the pursuer, and the isochrones are plotted for the same time durations as in Figure 3.2a. Note that the pursuer is faster than the evader, so the isochrones in Figure 3.2b are spaced farther apart.

3.2.3 Dominance Boundary as an Intersection of Isochrone Bundles

This subsection provides the dominance regions in SPSE games with obstacles. The method presented involves finding the intersection of bundles of isochrones, and this method is shown to agree with Theorem 3.1.1 when no obstacles are present. The method is then used to construct the dominance regions for a PE game with an obstacle, which the previous literature is unable to do.

3.2.3.1 Intersection of Isochrone Bundles

Section 3.2.2 describes how isochrones can be constructed for each player for a specified time duration. A bundle of isochrones, i.e., a set of curves parameterized by the time duration, t, is then formed for each player, as in Figures 3.2a and 3.2b, where the two

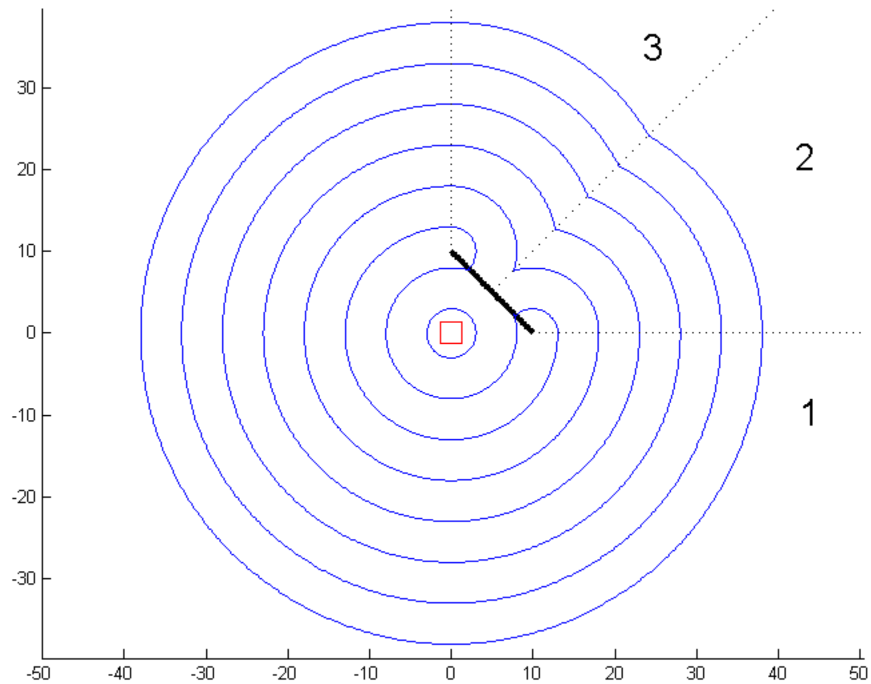

(a) Evader

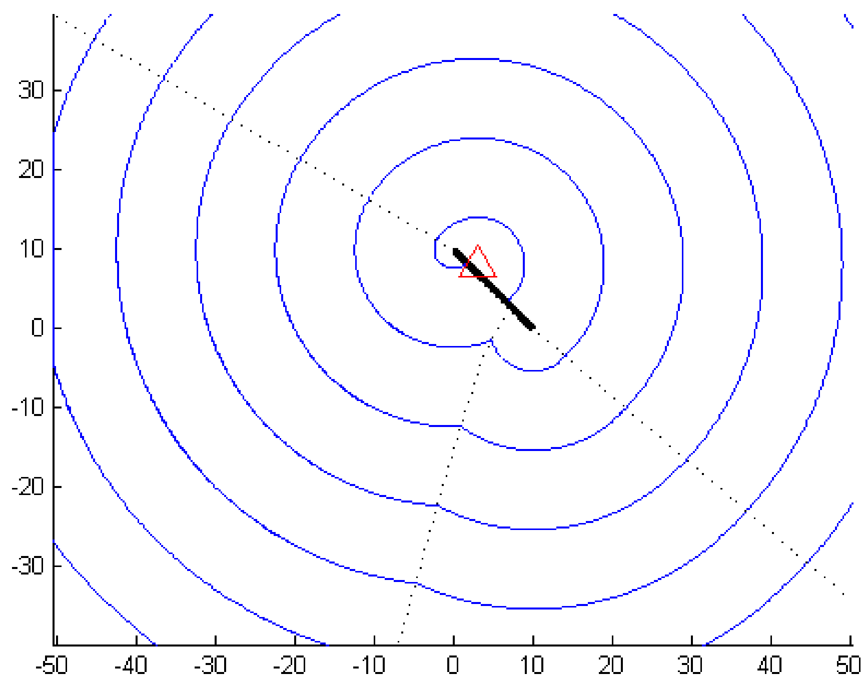

(b) Pursuer

Figure 3.2: Bundles of isochrones.

bundles are parameterized by a common variable, t. Elimination of this common parameter leads to the region of points over all time where the players can meet if both follow time-optimal paths.

Theorem 3.2.4 *In the PE game with obstacles, the plane is exhaustively divided into three disjoint regions:*

1) A region where a player strictly dominates,

2) A region where the other player strictly dominates,

3) A region where neither player dominates.

Moreover, the third region is obtained by intersecting bundles of isochrones.

Proof: Consider an arbitrary point in the plane. For that point, solve the two time-optimal control problems of moving from the initial locations of the two players to the arbitrary point. Only two outcomes are possible: either one transfer time is strictly smaller than the other, or the two transfer times are equal. In the first alternative, the arbitrary point is in the interior of one of the two dominance regions. In the second alternative, the arbitrary point is at the interface between the two dominance regions. However, that case is characterized by the equality of the transfer time; therefore, the point belongs to the intersection of the bundles of isochrones. □

As an example, consider the PE game with no obstacles in a Cartesian coordinate system with origin at the evader's initial location. If the pursuer's initial location is $(x_{P,0}, y_{P,0})$, then for a given time, t, the isochrones for each player are given by:

$$x_E^2 + y_E^2 = v_E^2 t^2, \tag{3.11a}$$

$$(x_P - x_{P,0})^2 + (y_P - y_{P,0})^2 = v_P^2 t^2. \tag{3.11b}$$

Divide (3.11a) by v_E^2 and (3.11b) by v_P^2, then apply transitivity of equality to eliminate the common parameter, t. Also, since the intersections of the isochrones are the points where $x_E = x_P$ and $y_E = y_P$, drop the subscripts to yield:

$$\frac{x^2 + y^2}{v_E^2} = \frac{(x - x_{P,0})^2 + (y - y_{P,0})^2}{v_P^2}. \tag{3.12}$$

Substitute $x_{P,0} = d$, $y_{P,0} = 0$, and $\gamma = v_P/v_E$:

$$(\gamma^2 - 1)(x^2 + y^2) + 2dx - d^2 = 0. \tag{3.13}$$

Finally, convert from Cartesian coordinates to polar coordinates by substituting $x^2+y^2 = r^2$ and $x = r\cos(\theta)$ to arrive at:

$$(\gamma^2 - 1)r^2 + (2d\cos(\theta))r - d^2 = 0, \tag{3.14}$$

which agrees with (3.10).

3.2.3.2 Two Player PE with a Line Segment Obstacle

Figure 3.3 shows this method for a PE game in the presence of a line segment obstacle. In Figure 3.3a, the bundles of isochrones from Figures 3.2a and 3.2b are shown, and each intersection of isochrones of the same duration is marked by a $*$. In Figure 3.3b, the isochrone bundles are removed for clarity, and a much larger number of intersections are plotted to form the boundary between the two dominance regions. In both figures, the circle is the Apollonius circle that would determine dominance if the obstacle was not present, and it is included to show how the dominance boundary changes due to the presence of the obstacle. The effects of obstacles are discussed in greater detail in Section 3.2.4.3.

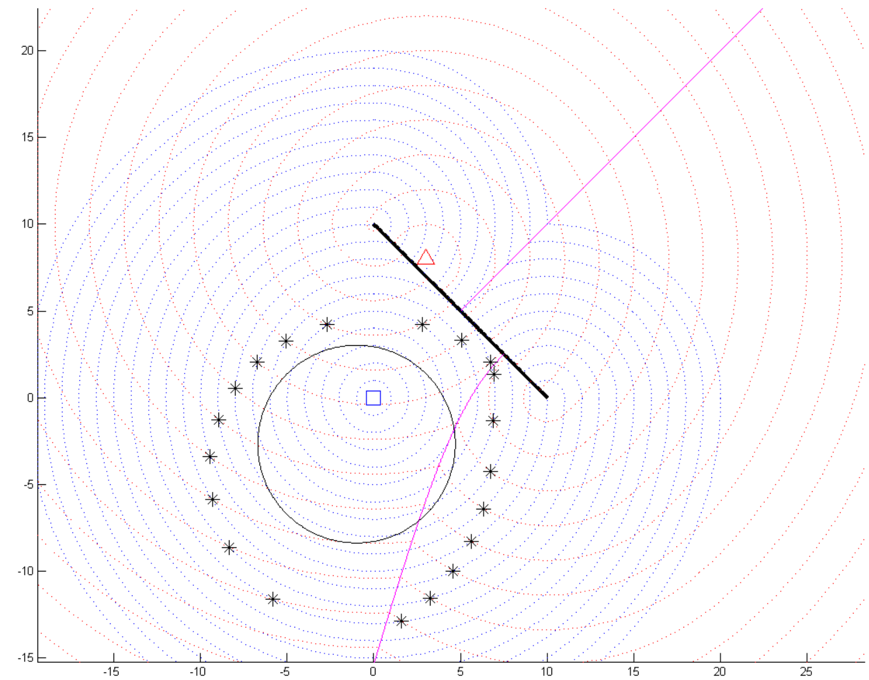

(a) Intersection of isochrone bundles

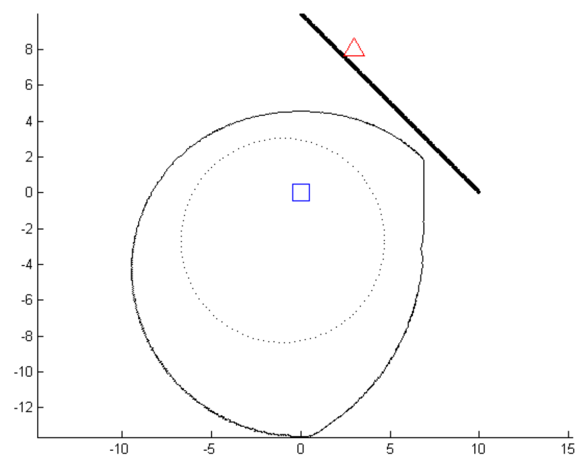

(b) Dominance Regions

Figure 3.3: Dominance regions formed by isochrone intersections.

3.2.4 Dominance Boundary in Closed Form

The dominance boundary in Figure 3.3b is piecewise smooth with two distinct cusps. As described in [48], this occurs in the solutions of many differential games. Following [48], in this section, the dominance boundaries are constructed analytically by determining singular surfaces and the solution in the small, where singular surfaces are curves that divide the plane into regions where the solution behaves differently in each region, and the solution "in the small" refers to the smooth part of the solution that occurs between singular surfaces. The solution in the small is presented in Section 3.2.4.1.

The solution need not be smooth when it crosses a singular surface, and in Section 3.2.4.2, the cusps in Figure 3.3b are shown to occur at singular surfaces. The solution in its entirety is referred to as the solution "in the large", and it is obtained by identifying the singular surfaces and piecing together solutions in the small in regions delineated by singular surfaces. This is described in Section 3.2.4.2.

3.2.4.1 Solution in the Small

As stated in Theorem 3.2.2, in the presence of obstacles, the isochrones always form arcs of concentric circles centered at known points. Therefore, when considering the intersections of isochrone bundles, the solution in the small is as follows:

Theorem 3.2.5 *Each portion of the dominance boundary satisfies the following condition for a specific value of t_B and d:*

$$\left(\gamma^2 - 1\right) r^2 + 2\left(d\cos\theta - \gamma^2 v_A t_B\right) r + \left(\gamma^2 v_A^2 t_B^2 - d^2\right) = 0. \tag{3.15}$$

Proof: From Theorem 3.2.2, time-optimal paths are made up of a number of straight line segments. Consider two players moving along the final segments of their time-optimal paths to a candidate capture point. In general, the players begin their final segments at different times, so let A be the first player to begin its final segment, and for simplicity

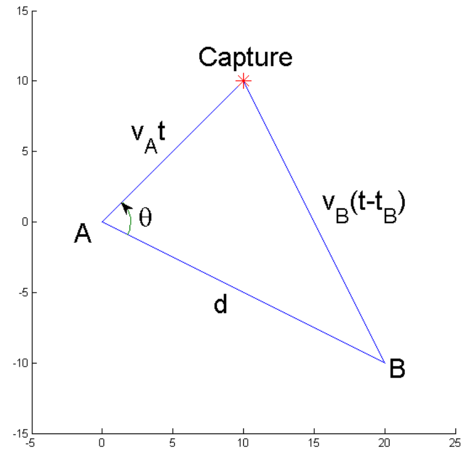

Figure 3.4: Geometry of final segments of time-optimal paths.

assume that A departs on this segment at $t = 0$. Let B be the other player, and let t_B be the time that elapses before B departs on its final segment.

The locus of intersections of the isochrone bundles can be determined from Figure 3.4, where d is the distance between the starting points of the final segments. From the law of cosines:

$$v_B^2(t - t_B)^2 = v_A^2 t^2 + d^2 - 2v_A t d \cos(\theta). \tag{3.16}$$

Rearrange (3.16) and let $\gamma = v_B/v_A$ to obtain

$$(\gamma^2 - 1)t^2 + 2\left(\frac{d}{v_A}\cos(\theta) - \gamma^2 t_B\right)t + \left(\gamma^2 t_B^2 - \frac{d^2}{v_A^2}\right) = 0. \tag{3.17}$$

Define $r = v_A t$, substitute $t = r/v_A$ into (3.17), and multiply the resulting equation by v_A^2 to obtain

$$\left(\gamma^2 - 1\right) r^2 + 2\left(d\cos\theta - \gamma^2 v_A t_B\right) r + \left(\gamma^2 v_A^2 t_B^2 - d^2\right) = 0. \tag{3.18}$$

This quadratic equation is easily solved for r, and it defines, in polar form, the locus of points where A and B can meet at the end of the final segments of their paths, with the origin at the start of A's final segment and the direction of zero azimuth along the line of sight from the origin to B's position at $t = t_B$. □

Note that when $t_B = 0$ in (3.15), the quadratic form of the standard Apollonius circle given by (3.10) is recovered.

Depending on the values of t_B and d, (3.15) can take the following three forms:

1) A limaçon: when $t_B \neq 0$ and $d \neq 0$;

2) An Apollonius circle: when $t_B = 0$ and $d \neq 0$;

3) A circle centered at an obstacle vertex: when $t_B \neq 0$ and $d = 0$.

Note that the fourth case, when $t_B = d = 0$ at an obstacle vertex, is ignored because capture occurs when the players reach that location.

Consider the third form of the solution which applies to regions where both players travel past the same obstacle vertex at different times. Note that if A is faster than B, then A dominates the entire region. Therefore, isochrones only intersect in this type of region if $v_B > v_A$. Since both players' isochrones are concentric circles centered at the same location, the resulting locus of intersections is also a circle centered at the same vertex. The radius can be computed from (3.15) with $d = 0$:

$$\left(\gamma^2 - 1\right) r^2 - 2\gamma^2 v_A t_B \, r + \gamma^2 v_A^2 t_B^2 = 0. \tag{3.19}$$

This equation has two solutions for r:

$$r_1 = \frac{\gamma v_A t_B}{\gamma - 1}, \quad r_2 = \frac{\gamma v_A t_B}{\gamma + 1}. \tag{3.20}$$

However, since $v_B > v_A$, $\gamma > 1$, and therefore $r_1, r_2 > 0$. Here, r_2 corresponds to a suboptimal path for A where A turns around and heads back toward the obstacle vertex at the moment that B reaches the vertex. Therefore, for time-optimal paths, the isochrones intersect along the circle with radius r_1.

3.2.4.2 Solution in the Large

In this section, the solution in the large is constructed by identifying the singular surfaces in two player PE games and then assembling the portions of the solutions in the small that lie in regions delineated by these surfaces. The dominance boundary is continuous, but it need not be smooth, and this section explains why cusps often occur at the singular surfaces, as noted previously.

The singular surfaces in the following remark can be categorized using the taxonomy of [48]. A dispersal surface is a curve for which time-optimal paths move away from the surface on both sides, and in this context, it separates two regions of the plane and represents a choice for one of the players about which direction to travel around an obstacle. A surface of type (p, u, p) is one where time-optimal paths that are sufficiently close to the surface are parallel to it on both sides, and where time-optimal paths are allowed to coincide with the surface. These surfaces represent a difference of behavior in the time-optimal paths of nearby points, where on one side of the surface the time-optimal paths require a turn at an obstacle, while on the other side no turn is required. For the remainder of this work, the surfaces of type (p, u, p) are referred to as visibility surfaces because they occur when an obstacle blocks the visibility from a generating point. The term "generating point" is used in the context of Theorem 3.2.2.

Remark 3.2.6 *The curves described in Theorem 3.2.3, which separate the plane into regions with unique generating points, are the singular surfaces for the two-player PE game in the plane in the presence of obstacles. These singular surfaces consist of:*

1) Visibility surfaces, which are portions of straight lines emanating from a generating obstacle vertex and extending away from another generating point parallel to the line of sight;

2) Dispersal surfaces, which are arcs of hyperbola.

For example, consider again the reduced version of the motivating example from Section 3.2.3.2. Figure 3.5a shows this scenario with the singular surfaces depicted with dotted lines and the dominance regions determined by assembling the solutions in the small for each region. For this scenario, the visibility surfaces separate regions that can be reached by both players with straight-line paths (those labeled with “1” in the figure) from regions where one of the players must travel around the obstacle (those labeled with “2” in the figure). If a player’s destination is a point located near one of these surfaces, then paths that are sufficiently close to the surface on either side are parallel to the surface. The only difference is that on one side of the surface the time-optimal path is straight, while on the other side of the surface the time-optimal path requires a slight bend at the obstacle vertex. For clarity, let the visibility surface denoted $\mathcal{VS}\{\zeta_1, \zeta_2\}$ be the surface generated due to the visibility of point ζ_2 from point ζ_1; i.e., it is the surface with endpoint ζ_2 that extends away from ζ_1.

The dispersal surfaces in Figure 3.5a are the arcs of hyperbola that separate two regions that are both labeled with “2”. If a player’s destination is a point located near a dispersal surface, then that player is faced with a decision about which way to travel around the obstacle. Points that are very close together but on opposite sides of the dispersal surface have significantly different time-optimal paths. Again, for notation, let the dispersal surface $\mathcal{DS}\{\zeta_1, \zeta_2/\zeta_3\}$ refer to a surface that is generated by starting from point ζ_1 and traveling past either point ζ_2 or point ζ_3 (where the two paths have the same distance).

The following points are noteworthy:

- The cusps in the dominance boundary occur where the dominance boundary intersects the dispersal surface, and they are the result of the difference in behavior for points that are close together, but on opposite sides of the dispersal surface.

- The singular surfaces are the same as the curves described in Theorem 3.2.3 for a single agent in the presence of obstacles, but they take on additional significance in the context of the PE game.

- The dominance boundary in Figure 3.5a, which is formed by assembling the solutions in the small between singular surfaces, agrees with the result obtained by intersecting isochrone bundles in Figure 3.3.

3.2.4.3 Effect of Obstacles on PE Games

Figure 3.5 shows two example scenarios. For both scenarios, the pursuer is twice as fast as the evader, the pursuer's starting location is given by $\triangle$, and the evader's starting location is given by $\square$. The thick line represents the obstacle, and the dotted lines are the singular surfaces. Regions labeled with "1" can be reached by both players with straight line paths, regions labeled with "2" require one player to travel around the obstacle, and regions labeled with "3" require both players to travel around the obstacle. The thin curve represents the boundary between dominance regions. For comparison, the dashed circle is the Apollonius circle that defines dominance in the absence of the obstacle.

As Figure 3.5 shows, in some cases the dominance region in the presence of the obstacle is contained in the original Apollonius circle, while in other cases it encompasses the Apollonius circle. This shows that the obstacle can be either a benefit or a hindrance to both players, depending on the initial player locations. In Figure 3.5b, the faster pursuer benefits from the obstacle, while in Figure 3.5a the slower evader benefits.

3.2.5 Obstacles With Greater Complexity

The motivating example includes a line segment obstacle which affects both players symmetrically, but the theorems and methods provided in previous sections are not limited to obstacles with these properties. This section provides dominance regions for two types of more complicated obstacles. The first scenario involves polygonal obstacles, and the second involves an obstacle that has asymmetric effects on the players. The key results of this subsection are that isochrones still determine dominance, and that Theorem 3.2.5 and Remark 3.2.6 still hold.

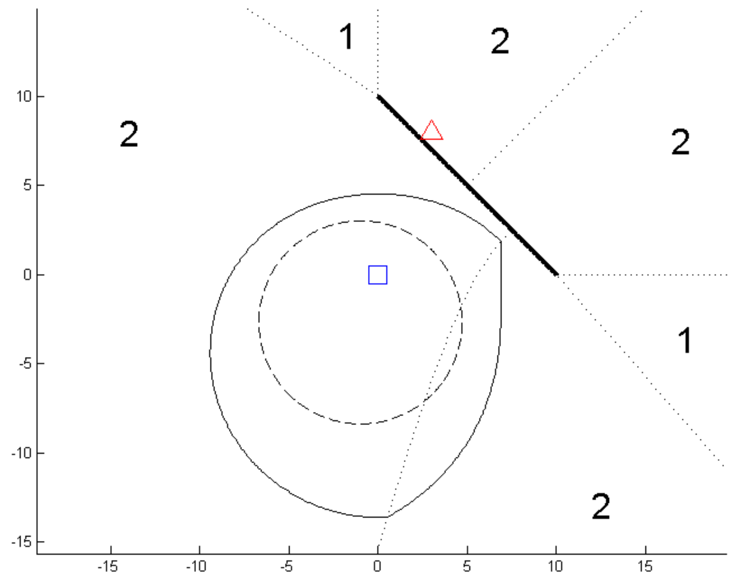

(a) Evader benefits from obstacle

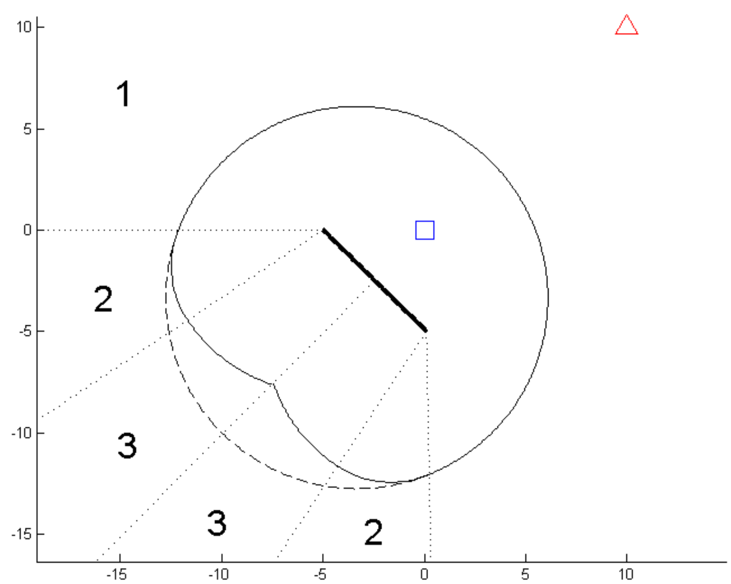

(b) Pursuer benefits from obstacle

Figure 3.5: Effect of obstacles on dominance regions.

3.2.5.1 Polygonal Obstacles

When more complex obstacles are introduced, the solution method remains unchanged. The number of singular surfaces increases due to the increased number of generating points, but the singular surfaces are still determined by Remark 3.2.6, and they can be constructed using [73] and [45]. Similarly, the isochrones are still arcs of concentric circles, and therefore the solution in the small from Section 3.2.4.1 holds. Figure 3.6 shows how the version of the motivating example used in Figures 3.3 and 3.5a changes when a third vertex is added to make the obstacle triangular.

The dashed lines represent the singular surfaces, and the faint dotted lines show the previously determined dominance boundary and dispersal surface from the motivating example where the obstacle consists of only the line segment between vertices 1 and 2.

In this case, the dispersal surface generated by the □ consists of portions of two hyperbolas, labeled “a” and “b”. Points on curve “b” can be reached in equal time by traveling past either vertex 1 or 3. Points on curve “a” can be reached in equal time by traveling past vertex 1 or past both vertices 3 and 2. As expected, these hyperbolas intersect at the singular surface extending upward from vertex 2.

3.2.5.2 Obstacles with Asymmetric Effects

Consider a scenario where the pursuer is an Unmanned Air Vehicle (UAV) and the evader is an Unmanned Ground Vehicle (UGV). Obstacles on the ground, such as streetside curbs or bushes, inhibit the motion of the UGV, but they do not affect the UAV.

Obstacles that have asymmetric effects on the players of a PE game can be analyzed using the techniques described previously. The isochrones are still arcs of concentric circles, and therefore the solution in the small from Section 3.2.4.1 holds. In fact, in this scenario the analysis is simpler because only one player generates singular surfaces, and the number of singular surfaces therefore decreases.

Figure 3.7 considers the motivating example with alternate starting locations. The

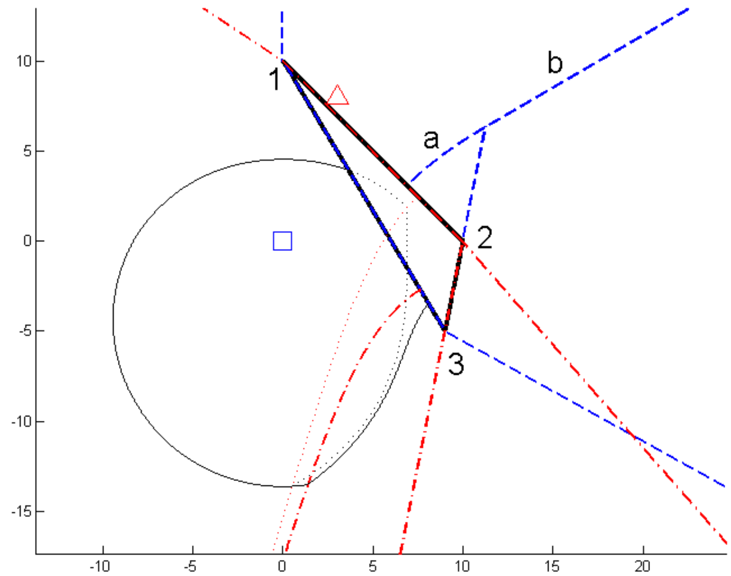

Figure 3.6: Polygonal obstacle.

dashed lines show the 6 singular surfaces, and the dominance boundaries are shown for all four possible scenarios. These scenarios include the case when neither player is affected by the obstacle, when both are affected by the obstacle, and when only one player is affected by the obstacle.

In the region of points that both players can reach with straight-line paths, all four dominance boundaries coincide, and the dominance boundary forms a portion of an Apollonius circle. The remainder of the Apollonius circle is shown by the faint dotted line which gives the dominance boundary when neither player is affected by the obstacle. The other three dominance boundaries diverge from the Apollonius circle when the dominance boundary crosses a singular surface. The boundary labeled "a" represents the scenario where only the $\square$ is affected by the obstacle. Since the $\triangle$ is unaffected, surface "1" is not a singular surface, and the dominance region agrees with the Apollonius circle until it reaches singular surface "2". As expected, since the $\square$ is the only player affected by the obstacle, this dominance region is the worst-case scenario for the $\square$, and it is the smallest of the four

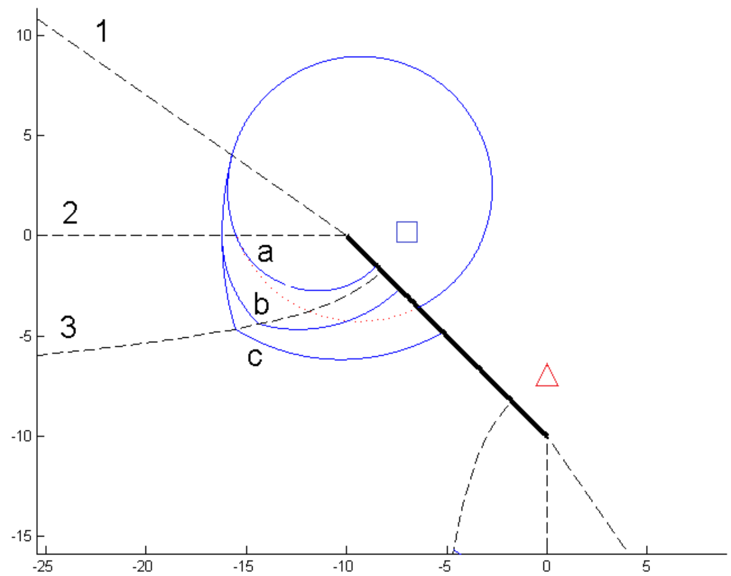

Figure 3.7: Asymmetric PE game.

potential dominance regions.

When only the △ is affected by the obstacle, surface “1” is a singular surface, and the dominance boundary departs from the Apollonius circle when it crosses that surface. However, surface “2” is no longer a singular surface, so the dominance boundary does not deviate again until reaching the hyperbolic dispersal surface, “3”, and this scenario leads to the dominance boundary labeled “c”. Since the △ is the only player affected by the obstacle, this scenario is the best-case scenario for the □, and it leads to the largest dominance region for the □.

Finally, when both players are affected symmetrically by the obstacle, all six singular surfaces affect the solution, and the resulting dominance boundary is curve “b”. As expected, this is an intermediate case in terms of the size of the dominance regions.

3.2.6 Games of Degree & Optimal Strategies

As in Section 3.1.2, construction of the dominance boundary provides the complete solution to not only games of kind, but games of degree as well. If the payoff is the time to capture, then the solution is identical to Theorem 3.1.2; i.e., the optimal capture point, C, that maximizes the minimum time to capture, is the point on the dominance boundary with the longest minimum time path from P's initial location. The optimal strategies are such that both P and E travel to C in minimum time, though in this case P, E, and C are not necessarily co-linear, and the minimum time paths are not necessarily single line segments.

Theorem 3.2.7 *Let $\mathcal{R}_i$ be an arbitrary region in the partitioned plane. The following are the only possibilities within $\mathcal{R}_i$ for the location of the optimal capture point, C:*

1) *A point (r, θ) satisfying all three of the following: Equation* (3.15)*, $(r, \theta) \in \mathcal{R}_i$, and $\partial r / \partial \theta = 0$ along* (3.15)*. These conditions only hold for:*

   (a) $\theta = \{0, \pi\}$*,*

   (b) Any θ if $d = 0$;

2) *An intersection of* (3.15) *with either a singular surface or an obstacle;*

3) *An intersection between obstacle edges and/or singular surfaces.*

Furthermore, possibilities 2 and 3 are only valid if no point satisfies possibility 1.

Proof: Let $\mathcal{R}_i$ be an arbitrary region in the partitioned plane; hence, it may only be bounded by obstacles and/or singular surfaces. Let $\mathcal{D}^i \subset \mathcal{R}_i$ be the portion of E's dominance region that is contained in $\mathcal{R}_i$, and let P' and E' be the locations where P and E enter $\mathcal{R}_i$ under optimal play.

By definition, if $C \in \mathcal{D}^i$, then it must be the point in $\mathcal{D}^i$ that maximizes P's minimum travel time. Let ξ be an arbitrary point in the interior of $\mathcal{D}^i$. Then, since ξ is in the interior of $\mathcal{D}^i$, P can always travel for an additional length of time $\mathrm{d}t$ in the direction from P' to ξ

without leaving $\mathcal{D}^i$. Therefore, C may only occur on the boundary of $\mathcal{D}^i$, which consists strictly of obstacle edges, singular surfaces, and curves satisfying (3.15).

Let $\bar{\mathcal{B}}$ be an arbitrary boundary segment of $\mathcal{D}^i$ that does not satisfy (3.15); i.e., it is either an edge of a polygonal obstacle or a singular surface. By Remark 3.2.6, it is therefore either a portion of a line or a portion of a hyperbola with P' or E' as a focus. Let $\mathcal{B}$ be the complete line or hyperbola containing $\bar{\mathcal{B}}$, and for simplicity let H' represent either P' or E', depending on which is applicable for $\mathcal{B}$. Define a reference frame with origin H', and let the polar representation of $\mathcal{B}$ be $r_{\mathcal{B}}(\theta_{\mathcal{B}})$, where for a hyperbolic boundary, the direction of zero azimuth is toward the hyperbola's vertex, and for a linear boundary, the direction of zero azimuth is the direction of the perpendicular intersector. Finally, let $\hat{\theta}_{\mathcal{B}}$ be the smallest positive angle for which $r_{\mathcal{B}}(\hat{\theta}_{\mathcal{B}})$ is undefined (i.e., the line $\theta_{\mathcal{B}} = \hat{\theta}_{\mathcal{B}}$ is either parallel to a linear $\mathcal{B}$ or parallel to the asymptote of a hyperbolic $\mathcal{B}$). Then $\mathcal{B}$ is entirely contained in $(-\hat{\theta}_{\mathcal{B}}, \hat{\theta}_{\mathcal{B}})$, and the distance from H' to $\mathcal{B}$ is a convex function of $\theta_{\mathcal{B}}$ over the interval $(-\hat{\theta}_{\mathcal{B}}, \hat{\theta}_{\mathcal{B}})$. Therefore the only possible maxima in $\bar{\mathcal{B}}$ are at its end points.

Finally, consider curves in (r, θ) satisfying (3.15), and let $\mathcal{D}_\theta \subset [0, 2\pi)$ be the domain of values for θ over which $(r, \theta) \in \mathcal{R}_i$. Maxima of $r(\theta)$ must either occur at the boundary of $\mathcal{D}_\theta$ or at a critical point within $\mathcal{D}_\theta$. Consider (3.15) again:

$$\left(\gamma^2 - 1\right) r^2 + 2\left(d\cos\theta - \gamma^2 v_A t_B\right) r + \left(\gamma^2 v_A^2 t_B^2 - d^2\right) = 0. \tag{3.21}$$

Differentiate with respect to θ:

$$2\left(\gamma^2 - 1\right) r \frac{\partial r}{\partial \theta} - 2dr\sin\theta + 2\left(d\cos\theta - \gamma^2 v_A t_B\right) \frac{\partial r}{\partial \theta} = 0, \tag{3.22}$$

Solve for $\partial r/\partial\theta$:

$$\frac{\partial r}{\partial \theta} = \frac{dr\sin\theta}{(\gamma^2 - 1)r + d\cos\theta - \gamma^2 v_A t_B}. \tag{3.23}$$

Setting (3.23) equal to zero provides a necessary condition for θ to be a maximizer of $r(\theta)$ for θ not on the boundary of $\mathcal{D}_\theta$, and there are three situations where this can occur. One is the degenerate case $r \equiv 0$.The second case, $d = 0$, is discussed in Section 3.2.4.1. Since the dominance boundary forms an arc of a circle when $d = 0$, all locations on that portion of the dominance boundary have the same capture time. The final case is:

$$\sin\theta = 0 \quad \Rightarrow \quad \theta = \{0, \pi\}. \tag{3.24}$$

Note that $\theta = \{0, \pi\}$ represents movement of the evader both toward and away from the pursuer, and therefore one is a minimizer of $r(\theta)$ while the other is a maximizer of $r(\theta)$, depending on the particular $\mathcal{R}_i$.

Equation (3.15) is periodic in θ with period 2π, and thus over the restricted domain $[0, 2\pi)$, either $(r(\pi), \pi)$ or $(r(0), 0)$ is the global maximizer. Therefore, if the maximizer is in $\mathcal{R}_i$, no other point in $\mathcal{D}^i$ needs to be evaluated. The only other possibilities for maximizers on curves satisfying (3.15) require $(r(\pi), \pi) \notin \mathcal{R}_i$ or $(r(0), 0) \notin \mathcal{R}_i$ (depending on which is the maximizer), and they occur at the boundaries of the interval $\mathcal{D}_\theta$, where the dominance boundary intersects an obstacle or singular surface. $\square$

Note that in the absence of obstacles, $\mathcal{R}_i$ is unbounded, $\mathcal{D}_\theta = [0, 2\pi)$, and hence C occurs where $\theta = \pi$, which agrees with the classical evasion strategy.

As before, if C is located on a curve satisfying (3.15), and if both players act optimally, then at any intermediate point in the game, the dominance boundary is tangent to the initial boundary at C. This is illustrated in Figure 3.8a, which shows a PE game with the same parameters as Figures 3.3 and 3.5a. The pursuer's initial location is given by the $\triangle$, and the evader's initial location is given by the $\square$. The minimum time paths are shown, and as expected, C remains in the same location as both players travel along these time-optimal paths to reach it. The dominance boundary is plotted for the initial time and three intermediate points in time, and as expected, all are tangent to the initial boundary at C.

Figure 3.8b shows the same conditions as Figure 3.8a, except that in this case only the evader follows the optimal strategy. As before, the pursuer and evader begin at the points labeled P and E, respectively, leading to the initial dominance boundary marked DB with optimal capture point C. Here, the pursuer acts suboptimally and travels around the obstacle in the wrong direction. This causes E's path to curve as the minmax capture point moves, and E gains advantage due to P's suboptimal play. The locations of P and E at a later time are given by P' and E', and the dominance boundary at that time is marked DB' with capture point C'. Note that capture at C' occurs at a later time than the original minmax capture at C.

As Theorem 3.2.7 states, the point C is not always on a curve satisfying (3.15). For example, Figure 3.9 shows a scenario with two line segment obstacles, depicted with thick lines. The thin curves represent the dominance boundary, and dashed lines represent singular surfaces. For clarity, the figure only shows the singular surfaces that bound the regions containing portions of the dominance boundary. In this scenario, C is located at the intersection of a dispersal surface and an obstacle. When C is not on a curve satisfying (3.15), it does not remain in the same location throughout the game. As the pursuer moves, the dispersal surface changes, and therefore C moves with it.

Finally, note that if the optimal capture occurs in a region where $d = 0$, which occurs when both players pass the same obstacle vertex, then the evader has a choice of C, with all possibilities leading to the same minmax capture time. However, at the moment when the evader passes the vertex and chooses a direction to travel, the point C becomes fixed.

3.2.7 Notes for Fast Implementation

Consider the Euclidean Shortest Path Problem (ESPP) in an environment with many obstacles. Shortest paths can be computed, as discussed in [73] and [45], and the ESPP can be decomposed into the construction of a visibility graph and a search problem using that

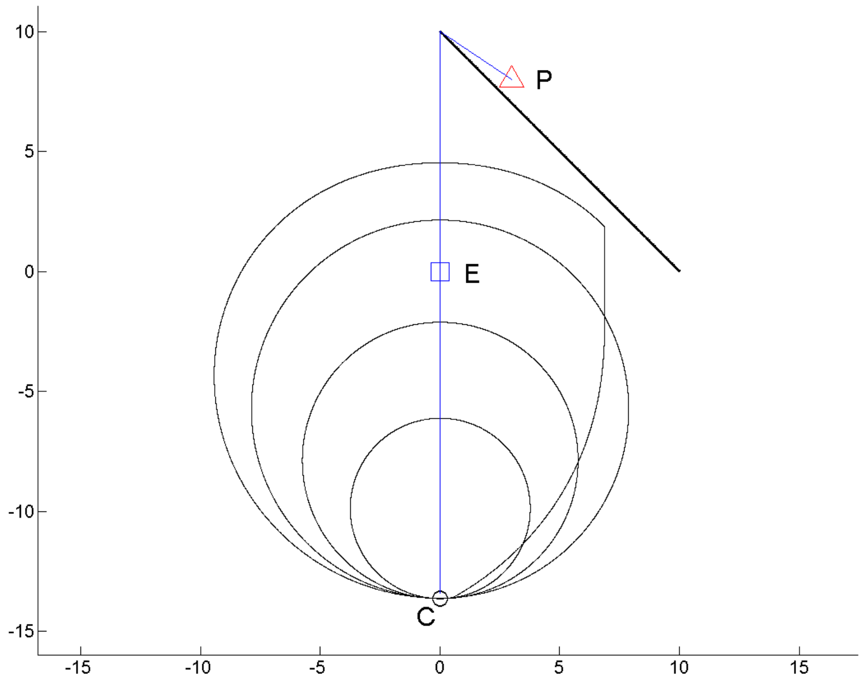

(a) Optimal play

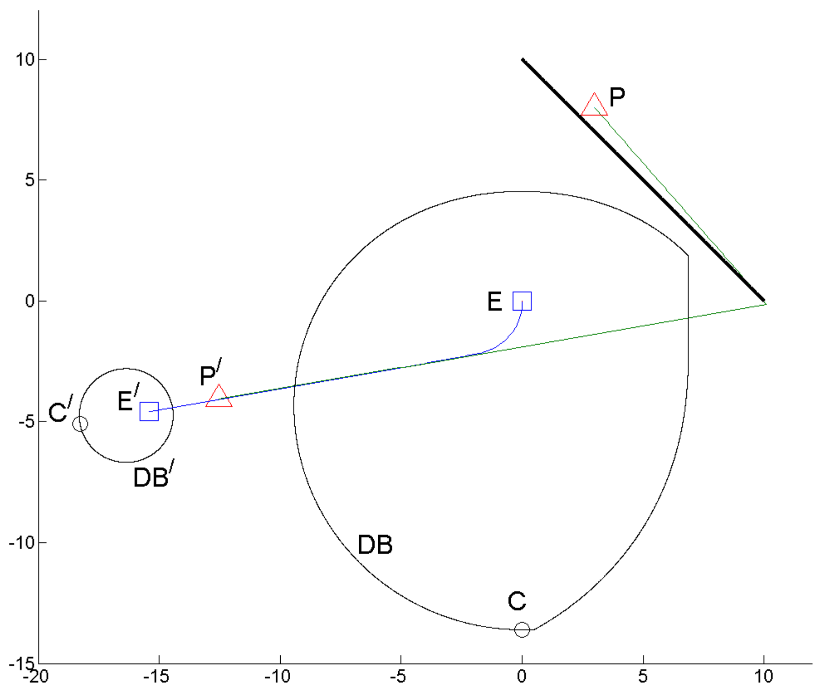

(b) Suboptimal pursuit

Figure 3.8: Dominance regions during the game.

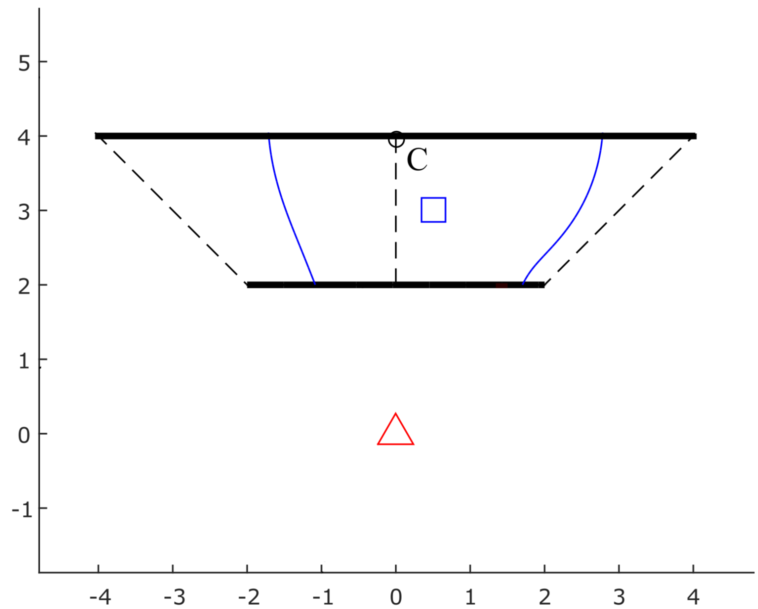

Figure 3.9: Capture point at intersection of singular surface and obstacle.

graph [77]. A nice feature of this approach is that the visibility graph can be constructed *a priori*. In a similar way, the PE game can be reduced to the following subproblems, and many of the required computations can be completed *a priori*:

1) The Euclidean shortest path problem,

2) The construction of singular surfaces,

3) The determination of the optimal capture point.

Like the visibility graph in subproblem 1, much of subproblem 2 can be constructed *a priori* because many of the singular surfaces depend only upon the locations of the obstacles. Then, during the game, a small number of surfaces are added based on the locations of the players. This is discussed in Section 3.2.7.1. Also, Theorem 3.2.7 simplifies the determination of the optimal capture point, and Section 3.2.7.2 makes use of the theorem to provide an algorithm to quickly determine the location of C. Once C is known, optimal pursuit and evasion reduce to the ESPP from an initial location to C. Furthermore, since both players can calculate their opponent's optimal path as well as their own, the game only requires further computations if the opponent plays suboptimally. Hence, this framework can potentially reduce the online computations required to implement optimal pursuit or evasion in practice.

3.2.7.1 Partitioning of the Environment

Many of the region boundaries can be determined *a priori*, and only a small number of updates need to be made at runtime. As noted in Section 3.2.2, the partitioning of the plane can be done in a computationally efficient way that grows as $\mathcal{O}(\eta_s \log \eta_s)$, where η_s is the number of obstacle vertices. In some cases, recomputing the surfaces might be preferable over storing and retrieving them. This section illustrates the decomposed approach, and the tradeoffs between computation and memory are left as future work. Additionally, it is unnecessary to consider all singular surfaces when determining the optimal capture point. This is considered in more detail in Section 3.2.7.2, but here all surfaces are considered in order to illustrate concepts.

Consider the environment shown in Figure 3.10, where obstacle ABD has the same dimensions as the obstacle in Figure 3.6. The visibility surfaces correspond to edges of the visibility graph that are extended until they intersect obstacles, and since the visibility graph is constructed as part of the ESPP, the visibility surfaces can be constructed simultaneously with very little additional computation. For example, the visibility graph is shown in 3.11a, and the visibility surfaces are added in 3.11b.

The hyperbolic dispersal surfaces correspond to specific sequences of generating points, and therefore, many of them can be computed *a priori* as well. Figure 3.12 shows some of the precomputable dispersal surfaces with their associated generating point sequences.

The only surfaces that must be computed at runtime include those generated by the locations of the players. Figure 3.13 shows the additional surfaces required if the players are placed in the same locations relative to obstacle ABD as they were previously in

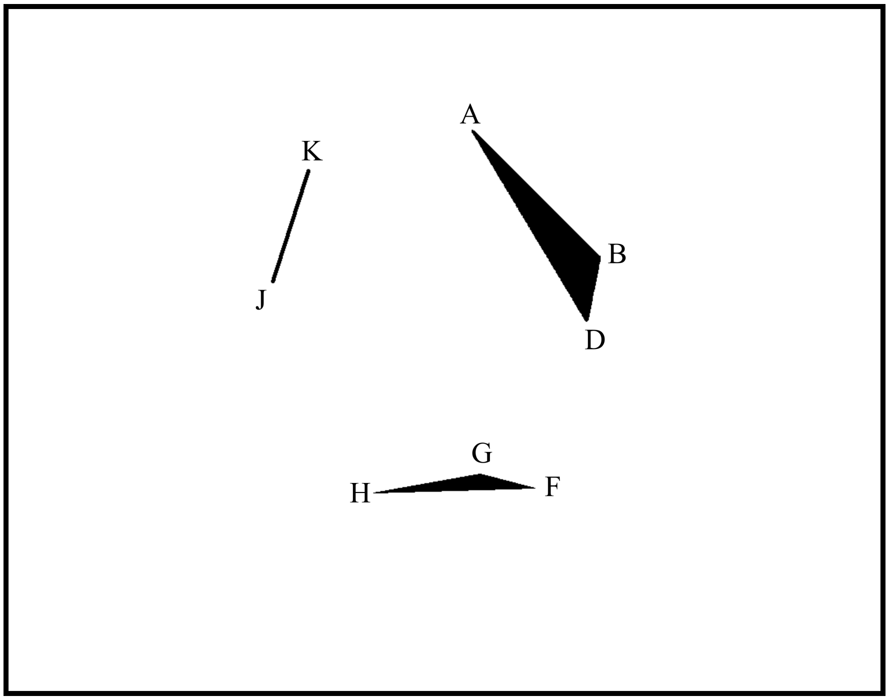

Figure 3.10: Example Environment

Figure 3.6. The runtime surfaces include those from Figure 3.6 as well as six additional surfaces due to the two additional obstacles. These include the visibility surfaces $\mathcal{VS}\{E,\cdot\}$ and $\mathcal{VS}\{P,\cdot\}$ as well as the dispersal surfaces $\mathcal{DS}\{E, A/D\}$, $\mathcal{DS}\{E, A/(D,B)\}$, and $\mathcal{DS}\{P, A/(B,D)\}$. Again, the additional visibility surfaces coincide with edges that must be added to the visibility graph for the ESPP, so the additional computation for PE is minimal. Also note that the number of additional surfaces depends on the number of obstacles visible from the player's locations. Therefore, no surfaces are added due the pursuer's position except the three from Figure 3.6, because neither obstacle JK nor obstacle FGH is visible from P.

3.2.7.2 Fast computation of the optimal capture point

To reduce unnecessary calculations when locating C, note that it is unnecessary to consider all regions. The dominance regions are continuous, and it is therefore sufficient to begin with the region containing the evader and move outward to neighboring regions until the

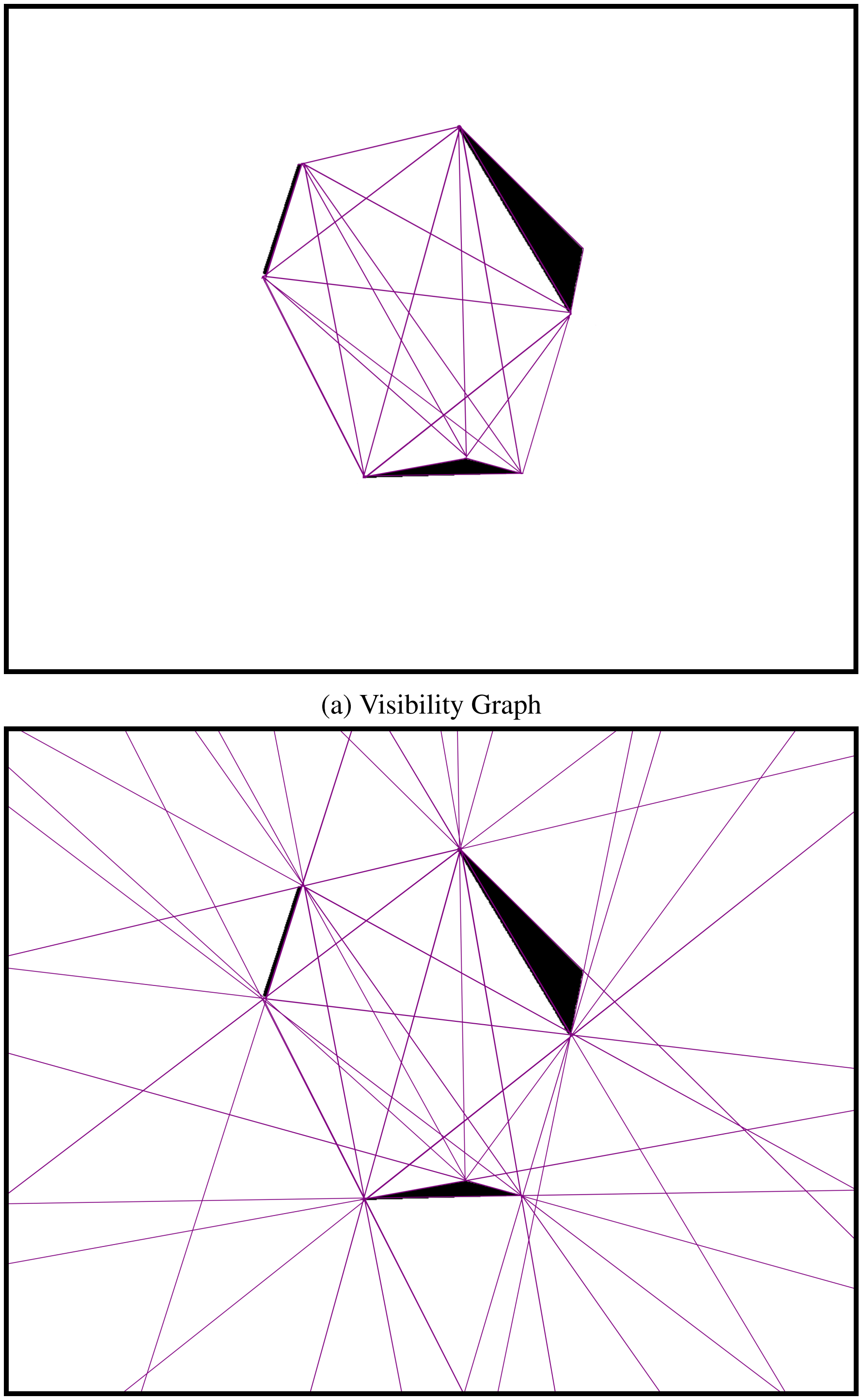

(a) Visibility Graph

(b) Visibility graph with singular surfaces added.

Figure 3.11: Relationship between singular surfaces and visibility graph.

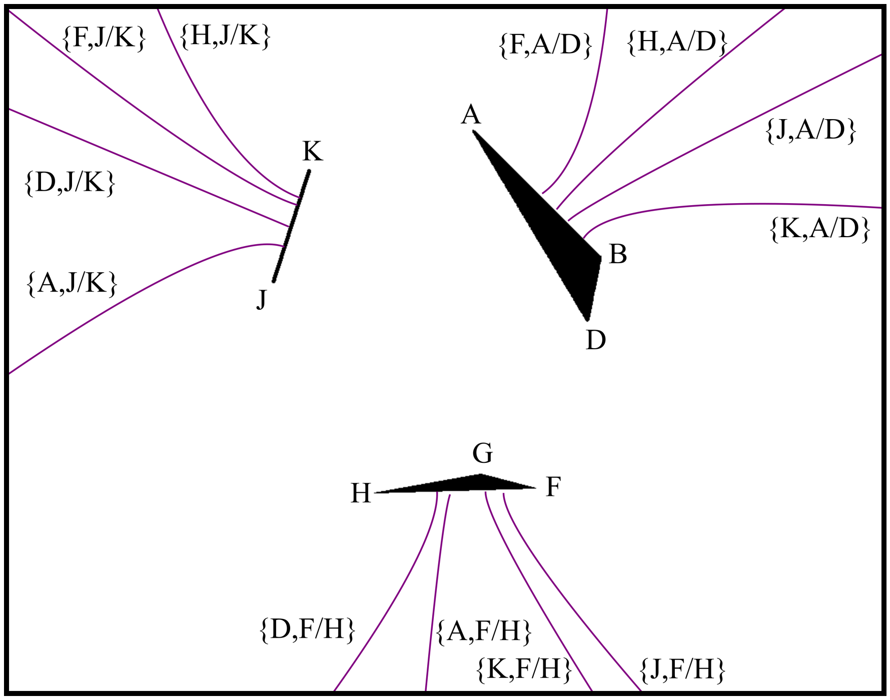

Figure 3.12: Hyperbolic Singular Surfaces

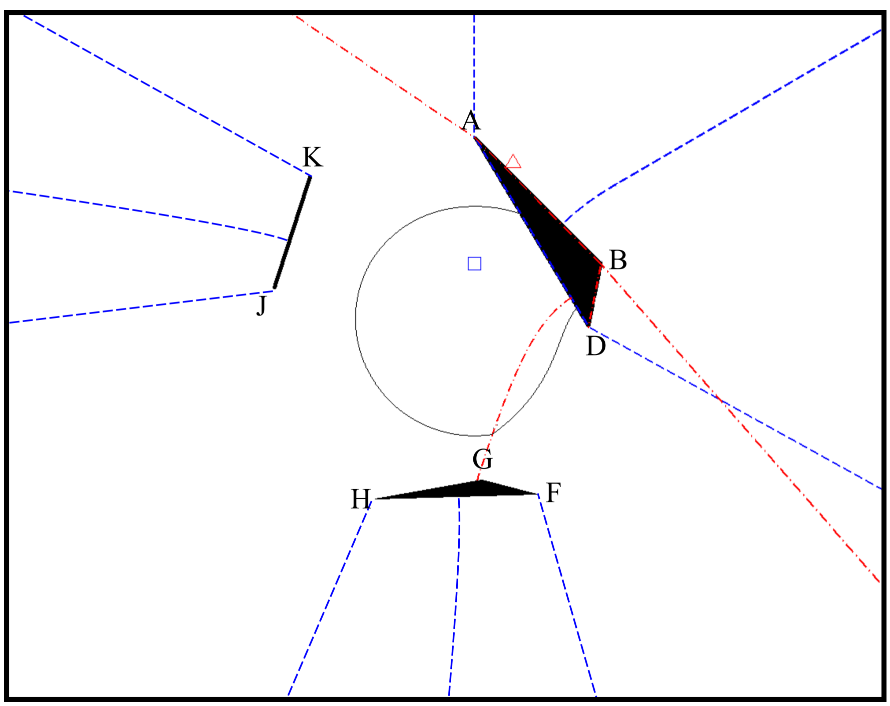

Figure 3.13: Singular surfaces added at runtime

evader's dominance region (and therefore the dominance boundary) is known in its entirety. Furthermore, for the same reason, it is unnecessary to consider all singular surfaces. The relevant surfaces can be determined by solving ESPPs and noting the generating points traversed by the players. Let $g = \{g_1, g_2, ..., g_f\}$ be the sequence of generating points in a player's path to an arbitrary region, and let s be an arbitrary obstacle vertex visible from g_f. The relevant region boundaries are as follows:

1) Obstacle edges,
2) $\mathcal{VS}\{g_f, s\}, \forall s$,
3) $\mathcal{VS}\{g_{f-1}, g_f\}$,
4) Dispersal surfaces associated with any subsequence of g.

For example, consider the region containing the evader in Figure 3.14. To determine the generating points traversed by the players, solve the ESPP from each player's initial location to the evader. The potential region boundaries are shown in Figure 3.14, and are determined as follows: The generating point sequence for the evader consists solely of E, so the only relevant boundaries due to the evader are the six visibility surfaces $\mathcal{VS}\{E, \cdot\}$. The generating point sequence for the pursuer is $\{P, A\}$, so the relevant boundaries due to the pursuer are the six visibility surfaces $\mathcal{VS}\{A, \cdot\}$, the visibility surface $\mathcal{VS}\{P, A\}$, and the dispersal surface $\mathcal{DS}\{P, A/(B, D)\}$.

The optimal capture point can then be calculated with Algorithm 1, where $\mathcal{R}_E$ is the region containing the evader and $\mathcal{R}_c$ is a candidate capture region which P and E enter at locations P' and E', respectively, and at times $t_{P'}$ and $t_{E'}$, respectively. Also, $\hat{C}$ is a candidate for C, $\mathcal{C}_c$ is a set of all valid candidates discovered, and $t_c[i]$ is the capture time associated with the i-th element in $\mathcal{C}_c$. Finally, let X_j be an intersection of the boundary segments of $\mathcal{R}_c$ with coordinates (r_{X_j}, θ_{X_j}).

For each candidate capture region, Algorithm 1 first computes d and t_B, which are necessary to define $r(\theta)$ with (3.15). Then, it checks whether any $\hat{C}$ that can be a global

```
Add $\mathcal{R}_E$ to list of candidate regions;
while not at end of list of candidate regions do
    determine $P'$, $E'$, $t_{P'}$ and $t_{E'}$ for next $R_c$ (by solving ESPPs);
    $d = ||P' - E'||$;
    if $t_{P'} \geq t_{E'}$ then
        $t_B = t_{P'} - t_{E'}$;
        $\hat{C} = (r(\pi), \pi)$;
    else
        $t_B = t_{E'} - t_{P'}$;
        $\hat{C} = (r(0), 0)$;
    end
    if $\hat{C} \in \mathcal{R}_c$ then
        add $\hat{C}$ to set $\mathcal{C}_c$;
    else if $d$=0 then
        Set $\hat{C}$ to any $(r, \theta) \in \mathcal{R}_c$ satisfying (3.15);
        add $\hat{C}$ to set $\mathcal{C}_c$;
    else
        foreach $X_j \in \mathcal{R}_c$ do
            if $r_{X_j} < r(\theta_{X_j})$ then
                add $X_j$ to set $\mathcal{C}_c$;
            end
        end
    end
    foreach $X_j \in \mathcal{R}_c$ do
        if $r_{X_j} < r(\theta_{X_j})$ then
            add neighboring region to list of candidate regions;
    end
end
$i^* = \arg\min_i t_c[i]$;
$C = \mathcal{C}_c[i^*]$;
```

Algorithm 1: Computing the optimal capture point.

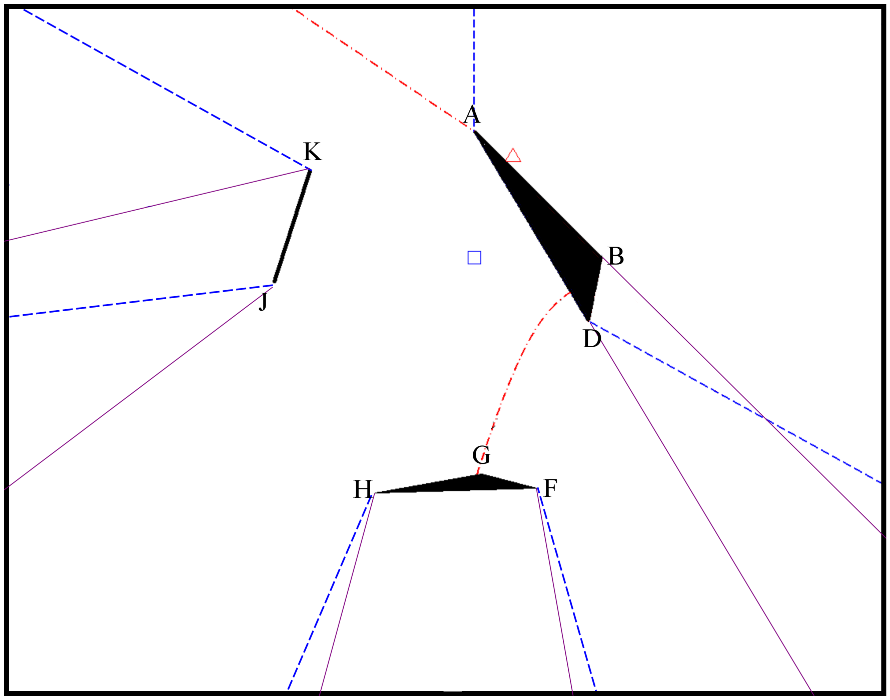

Figure 3.14: Relevant singular surfaces for region containing evader.

maximizer of (3.15) is contained in $\mathcal{R}_c$, and if not, the boundary intersections in the interior of the dominance region are added as candidate capture points. Finally, if the dominance region extends into any adjoining region, that region is added to the list of regions to be evaluated. After all regions containing a portion of the dominance boundary have been evaluated, C is the $\hat{C}$ with the largest associated capture time.

3.3 Simple Motion vs. Dubins Car

This section considers SPSE games where one player moves with simple motion (i.e., $\rho = 0$) and the other player is a Dubins car (i.e., $\rho \neq 0$), and it follows the same development as the SPSE game with simple motion in Section 3.2. Note that the results of this section apply to both the Homicidal Chauffeur (HC) problem (i.e., $\rho_E = 0,\ \rho_P \neq 0$) and the Suicidal Pedestrian problem (i.e., $\rho_E \neq 0,\ \rho_P = 0$). However, in order to simplify notation, the notation in this section is consistent with the HC problem.

3.3.1 Isochrones

Consider the following time-optimal control problem: Given an agent moving in the plane with speed v, minimum turn radius ρ, and initial and final locations (x_i, y_i) and (x_f, y_f), find a path that connects (x_i, y_i) to (x_f, y_f) and satisfies the minimum turn radius ρ such that the time required for the agent to reach (x_f, y_f) is minimized.

Again, the agents move with constant speeds, and therefore time-optimal paths correspond to paths with the smallest Euclidean distance. For this work, we are interested in level sets for the value function of this time-optimal control problem, and the boundaries of these level sets are referred to as isochrones. Alternatively, isochrones form the boundary of the set of points that are reachable by a player at a given time.

3.3.1.1 Dubins Car Isochrones

First, consider a pursuer with minimum turn radius ρ and speed v_P. If the final heading is free, as is the case here, then the optimal paths that end on the boundary of the reachable set are one of two types [22]:

1) Curve-straight (CS): a curved segment with minimum turn radius followed by a straight segment,

2) Curve-curve (CC): two curves in opposite directions, both with minimum radius.

Note that the only other possibilities, a single straight segment or a single curved segment, are special cases of the two types described previously.

For a reference frame with origin at the location of the pursuer and y-axis along the pursuer's velocity vector, the isochrones are given by the following parametric equations [22]:

Curve-Straight For CS paths, the isochrones are:

$$x(\phi, t) = \rho\,(1 - \cos\phi) + (v_P t - \rho\phi)\sin\phi, \tag{3.25a}$$

$$y(\phi, t) = \rho\sin\phi + (v_P t - \rho\phi)\cos\phi, \tag{3.25b}$$

where $0 < \phi < v_P t/\rho$.

Curve-Curve For CC paths, the isochrones are:

$$x(\phi, t) = \rho\left[2\cos\phi - 1 - \cos\left(2\phi - \frac{v_P t}{\rho}\right)\right], \tag{3.26a}$$

$$y(\phi, t) = \rho\left[2\sin\phi - \sin\left(2\phi - \frac{v_P t}{\rho}\right)\right]. \tag{3.26b}$$

Note that the pursuer's reachable set is not simply connected for all t. In particular, it becomes doubly connected at time t_1 [22]:

$$t_1 = \frac{\rho}{v_P}\left(\frac{3\pi}{2} + 1\right). \tag{3.27}$$

The internal boundary that forms at time t_1 is comprised of endpoints of both CS and CC paths. This remains the case until time t_2 [22]:

$$t_2 = \frac{2\pi\rho}{v_P}. \tag{3.28}$$

After time t_2, the internal boundary is comprised solely of endpoints of CC paths. Finally, the internal hole shrinks as t increases until time t_3, when it vanishes [22]:

$$t_3 = \frac{\rho}{v_P}\left(2\pi + \cos^{-1}\frac{23}{27}\right). \tag{3.29}$$

The doubly connected nature of the pursuer's reachable set is revisited in Section 3.3.4.

3.3.1.2 Simple Motion Isochrones

Finally, consider an evader starting from initial location (x_{E0}, y_{E0}) with speed v_E and $\rho_E = 0$. As in Section 3.2, the optimal paths are straight lines, and the isochrones are concentric circles centered at (x_{E0}, y_{E0}), as given in (3.11). To simplify future analysis, consider a case where the evader starts at a different time than the pursuer, and let the delay in the evader's start be t_B. Note that in the game the players begin at the same time, but including t_B simplifies the analysis of evader strategies with turns in Section 3.3.3. Therefore, the isochrones are:

$$(x - x_{E0})^2 + (y - y_{E0})^2 = (v_E(t - t_B))^2. \tag{3.30}$$

3.3.2 Isochrone Intersections

Equations (3.25), (3.26), and (3.30) provide bundles of isochrones, i.e., sets of curves parameterized by the common time duration, t. Elimination of this common parameter leads to the set of points over all time where the players can meet if they follow time-optimal paths.

3.3.2.1 Intersection with Curve-Straight Paths

Consider the intersection of the evader's isochrones with the CS portion of the pursuer's isochrones. First, eliminate x and y by substituting (3.25) into (3.30). Then expand and rearrange the resulting equation to arrive at the following quadratic equation for t:

$$\begin{aligned} 0 = &\frac{1}{2}[v_P^2 - v_e^2]\, t^2 \\ &+ \left[v_P\left((\rho - x_{e0})\sin\phi - y_{e0}\cos\phi - \rho\phi\right) + v_e^2 t_B\right]\ t \\ &+ \Bigg[\rho(-\rho\phi + x_{e0}\phi - y_{e0})\sin\phi + \frac{1}{2}\rho^2\phi^2 + \rho^2 - \rho x_{e0} \\ &+ \rho(-\rho + x_{e0} + y_{e0}\phi)\cos\phi + \frac{1}{2}\left(x_{e0}^2 + y_{e0}^2 - v_e^2 t_B^2\right)\Bigg]. \end{aligned} \tag{3.31}$$

Equation (3.31) can be easily solved for $t(\phi)$. Finally, substitute $t(\phi)$ into (3.25) to arrive at $x(\phi)$ and $y(\phi)$.

3.3.2.2 Curve-Curve

Following the same procedure, eliminate x and y by substituting (3.26) into (3.30), and rearrange the resulting equation to arrive at one of the following:

$$\begin{aligned}
0 &= (v_e^2)t^2 - (2v_e^2 t_B)t \\
&+ 2\rho\Big[y_{e0}\cos(2\phi) - (\rho + x_{e0})\sin(2\phi) + 2\rho\sin(\phi)\Big]\sin(\frac{v_P t}{\rho}) \\
&- 2\rho\Big[(\rho + x_{e0})\cos(2\phi) + y_{e0}\sin(2\phi) - 2\rho\cos(\phi)\Big]\cos(\frac{v_P t}{\rho}) \\
&+ \Big[4\rho y_{e0}\sin(\phi) + 4\rho(\rho + x_{e0})\cos(\phi) - (\rho + x_{e0})^2 - y_{e0}^2 + v_e^2 t_B^2 - 5\rho^2\Big],
\end{aligned} \tag{3.32a}$$

$$\begin{aligned}
0 = &\Big[-2\rho(\rho + x_{e0})\sin(\frac{v_P t}{\rho}) - 2\rho y_{e0}\cos(\frac{v_P t}{\rho})\Big]\sin(2\phi) \\
&+ \Big[2\rho y_{e0}\sin(\frac{v_P t}{\rho}) - 2\rho(\rho + x_{e0})\cos(\frac{v_P t}{\rho})\Big]\cos(2\phi) \\
&+ \Big[4\rho^2\sin(\frac{v_P t}{\rho}) + 4\rho y_{e0}\Big]\sin(\phi) \\
&+ \Big[4\rho^2 cos(\frac{v_P t}{\rho}) + 4\rho(\rho + x_{e0})\Big]\cos(\phi) \\
&+ \Big[v_e^2 t^2 - 2v_e^2 t_B t - (\rho + x_{e0})^2 - y_{e0}^2 + v_e^2 t_B^2 - 5\rho^2\Big].
\end{aligned} \tag{3.32b}$$

Note that CC paths only need to be analyzed for $t <= t_3$, because at $t = t_3$, the hole in the pursuer's reachable set closes, and after t_3, the pursuer's isochrones are made up of strictly CS paths. With experience, pairs of t and ϕ can be found relatively easily using, for example, the Newton-Raphson method with initial guesses based on a small number of subsets of initial conditions. For example,

1) evader positions in front of the pursuer and close by;

2) evader positions beside the pursuer and close by;

3) evader positions behind the pursuer and close by.

For evader positions far from the pursuer, only CS paths intersect the evader's isochrones, and no initial guess is needed. Additionally, this section proposes open-loop methods, but if these open loop methods are used to iteratively recalculate actions, the solutions at the previous step can be used to warm-start the next calculations. This is an area for future work, but its cost has not been prohibitive thus far. Once pairs of t and ϕ have been identified, they can be substituted into (3.26) as before.

3.3.2.3 Examples

This section provides a few examples of isochrone intersections, including an example that verifies this approach by letting $\rho \to 0$, which reproduces the standard Apollonius circle.

First, consider the limit $\rho \to 0$. Equation (3.26) vanishes, and (3.25) becomes:

$$x(\phi, t) = v_P t \sin\phi, \tag{3.33a}$$

$$y(\phi, t) = v_P t \cos\phi. \tag{3.33b}$$

Equation (3.31) reduces to:

$$\frac{1}{2}(v_P^2 - v_E^2)t^2 + \left[v_P\left(-x_{E0}\sin\phi - y_{E0}\cos\phi\right) + v_E^2 t_B\right]t + \frac{1}{2}\left[x_{E0}^2 + y_{E0}^2 - v_E^2 t_B^2\right] = 0. \tag{3.34}$$

Let $t_B = 0$:

$$\frac{1}{2}(v_P^2 - v_E^2)t^2 + v_P\left(-x_{E0}\sin\phi - y_{E0}\cos\phi\right)t + \frac{1}{2}\left(x_{E0}^2 + y_{E0}^2\right) = 0. \tag{3.35}$$

Therefore, from the quadratic formula,

$$t = \frac{v_P\left(x_{E0}\sin\phi + y_{E0}\cos\phi\right)}{(v_P^2 - v_E^2)} \pm \frac{\sqrt{v_P^2\left(x_{E0}\sin\phi + y_{E0}\cos\phi\right)^2 - (v_P^2 - v_E^2)(x_{E0}^2 + y_{E0}^2)}}{(v_P^2 - v_E^2)}. \tag{3.36}$$

$$t(\phi) = \frac{v_P}{v_P^2 - v_E^2}\Bigg[x_{E0}\sin\phi + y_{E0}\cos\phi \\ \pm\sqrt{(x_{E0}\sin\phi + y_{E0}\cos\phi)^2 - \frac{v_P^2 - v_E^2}{v_P^2}(x_{E0}^2 + y_{E0}^2)}\Bigg]. \quad (3.37)$$

Substituting (3.37) into (3.33) and substituting γ for v_P/v_E gives:

$$x(\phi) = \frac{\gamma^2}{\gamma^2 - 1}\sin\phi\Bigg[x_{E0}\sin\phi + y_{E0}\cos\phi \\ \pm\sqrt{(x_{E0}\sin\phi + y_{E0}\cos\phi)^2 - (1-\gamma^{-2})(x_{E0}^2 + y_{E0}^2)}\Bigg], \quad (3.38a)$$

$$y(\phi) = \frac{\gamma^2}{\gamma^2 - 1}\cos\phi\Bigg[x_{E0}\sin\phi + y_{E0}\cos\phi \\ \pm\sqrt{(x_{E0}\sin\phi + y_{E0}\cos\phi)^2 - (1-\gamma^{-2})(x_{E0}^2 + y_{E0}^2)}\Bigg]. \quad (3.38b)$$

For simplicity, let $x_{E0} = 0$ and $y_{E0} > 0$:

$$x(\phi) = \frac{\gamma^2}{\gamma^2 - 1}\sin\phi\left[y_{E0}\cos\phi \pm \sqrt{y_{E0}^2\cos^2\phi - (1-\gamma^{-2})y_{E0}^2}\right], \quad (3.39a)$$

$$y(\phi) = \frac{\gamma^2}{\gamma^2 - 1}\cos\phi\left[y_{E0}\cos\phi \pm \sqrt{y_{E0}^2\cos^2\phi - (1-\gamma^{-2})y_{E0}^2}\right]. \quad (3.39b)$$

Note that $y_{E0} > 0$ is a common factor, and $\cos^2\phi - 1 = -\sin^2\phi$, so simplifying and rearranging terms gives:

$$x(\phi) = \frac{\gamma^2}{\gamma^2 - 1}y_{E0}\sin\phi\left[\cos\phi \pm \sqrt{-\sin^2\phi + \gamma^{-2})}\right], \quad (3.40a)$$

$$y(\phi) = \frac{\gamma^2}{\gamma^2 - 1}y_{E0}\cos\phi\left[\cos\phi \pm \sqrt{-\sin^2\phi + \gamma^{-2})}\right]. \quad (3.40b)$$

Equation (3.40a) gives the result in Cartesian coordinates (x, y). Transforming to polar coordinates yields the folowing:

$$
\begin{aligned}
r^2(\phi) &= x^2(\phi) + y^2(\phi), \\
&= \left(\frac{\gamma^2}{\gamma^2-1}y_{E0}\right)^2 (\sin^2\phi + \cos^2\phi)\left(\cos\phi \pm \sqrt{-\sin^2\phi + \gamma^{-2})}\right)^2, \\
&= \left(\frac{\gamma^2}{\gamma^2-1}y_{E0}\right)^2 \left(\cos\phi \pm \sqrt{-\sin^2\phi + \gamma^{-2})}\right)^2.
\end{aligned}
\tag{3.41}
$$

Thus,

$$
r(\phi) = \pm\frac{\gamma^2}{\gamma^2-1}y_{E0}\left(\cos\phi \pm \sqrt{-\sin^2\phi + \gamma^{-2})}\right). \tag{3.42}
$$

To see that this agrees with the Apollonius circle, solve (3.8) for $r(\theta)$:

$$
r(\theta) = h\cos\theta + k\sin\theta \pm \sqrt{(h\cos\theta + k\sin\theta)^2 - h^2 - k^2 + r_A^2}. \tag{3.43}
$$

Place the origin at the location of the pursuer with the direction of zero azimuth along the x axis. As before, consider an evader at $x_{E0} = 0$, $y_{E0} > 0$. Then, $x_P = y_P = y_E = 0$, and:

$$
h = 0, \qquad k = \frac{-\gamma^2 y_{E0}}{1-\gamma^2}, \qquad r_A = \frac{\gamma y_{E0}}{1-\gamma^2}. \tag{3.44}
$$

Substitute these values for h, k, and r_A into (3.43) and simplify:

$$
\begin{aligned}
r(\theta) &= \frac{-\gamma^2}{1-\gamma^2}y_{E0}\sin\theta \pm \sqrt{\frac{\gamma^4 y_{E0}^2}{(1-\gamma^2)^2}\sin^2\theta - \frac{\gamma^4 y_{E0}^2}{(1-\gamma^2)^2} + \frac{\gamma^2 y_{E0}^2}{(1-\gamma^2)^2}}, \\
&= \frac{\gamma^2}{\gamma^2-1}y_{E0}\sin\theta \pm \left|\frac{\gamma^2}{\gamma^2-1}y_{E0}\right| \sqrt{\sin^2\theta - 1 + \gamma^{-2}}, \\
&= \frac{\gamma^2}{\gamma^2-1}y_{E0}\left[\sin\theta \pm \sqrt{-\cos^2\theta + \gamma^{-2}}\right].
\end{aligned}
\tag{3.45}
$$

Finally, apply the coordinate transformation $\theta = \phi + \pi/2$ to arrive at (3.42).

Figure 3.15a shows a scenario with $\rho = 3$ and $\gamma = 2$ where the evader begins directly in front of the pursuer. Again, the evader begins at the □, and the pursuer begins at the △ with its heading aligned with the vertical axis. The solid curves show the isochrone intersections, and the dotted circles show the tightest turn that the pursuer can achieve.

Note that the isochrone intersections do not form a single, continuous curve. Instead, three curves are formed, corresponding to three types of capture. The curve labeled "1" occurs between P and E, and it represents possible meeting locations if E moves toward P. The curve labeled "2" corresponds to cases where the evader moves away from the pursuer, and the pursuer catches up from behind. Finally, curve "3" forms a continuous curve that surrounds the evader. Note that this illustrates why HC formulations typically define capture by proximity instead of colocation, because as the pursuer approaches the evader, the evader can escape by moving to the side immediately prior to capture. This is discussed in greater detail in Section 3.3.3.2.

Figure 3.15b shows another example, where the evader begins to the side of the pursuer. Note that in both Figures 3.15a and 3.15b, the isochrone intersections are piecewise smooth with distinct cusps. These cusps occur where the dominance boundary intersects singular surfaces which form directly in front of and behind the pursuer as well as along the minimum achievable turn. Thus, they occur at points where the pursuer's behavior changes, either by switching from an initial turn to the left to an initial turn to the right, or by switching from a CS path to a CC path. This is similar to previous discussions for games with simple motion in the presence of obstacles, where cusps also occur at singular surfaces and indicate a change in behavior, such as a change in the optimal direction for a player to move around an obstacle [82] [85].

3.3.3 Dominance Regions

The evader's dominance region consists of all points that it can reach before any possible collocation with the pursuer, but Figure 3.15a illustrates a few important aspects of the HC problem that differ from games where the pursuers move with simple motion.

As discussed in [85], the boundary of the dominance regions is equivalent to the intersections of the isochrones for games with simple motion. In the HC problem, extra care

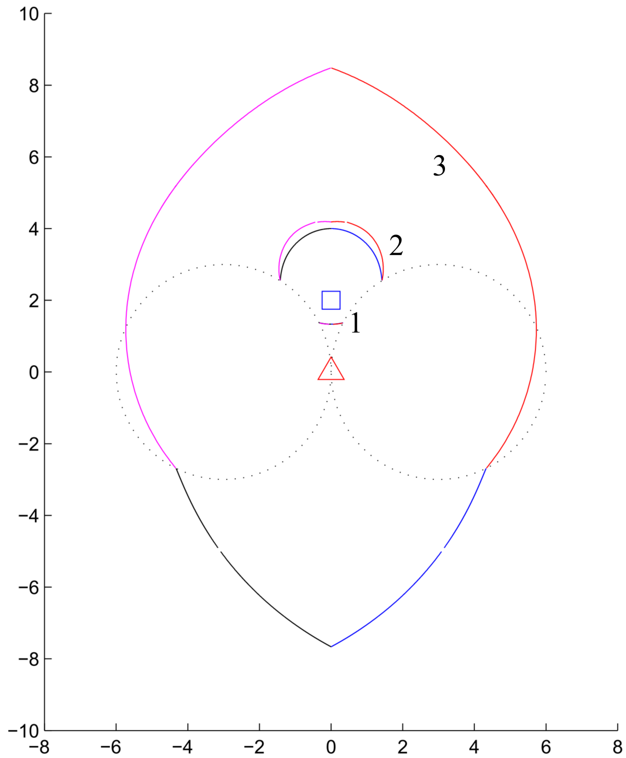

(a) E in front of P

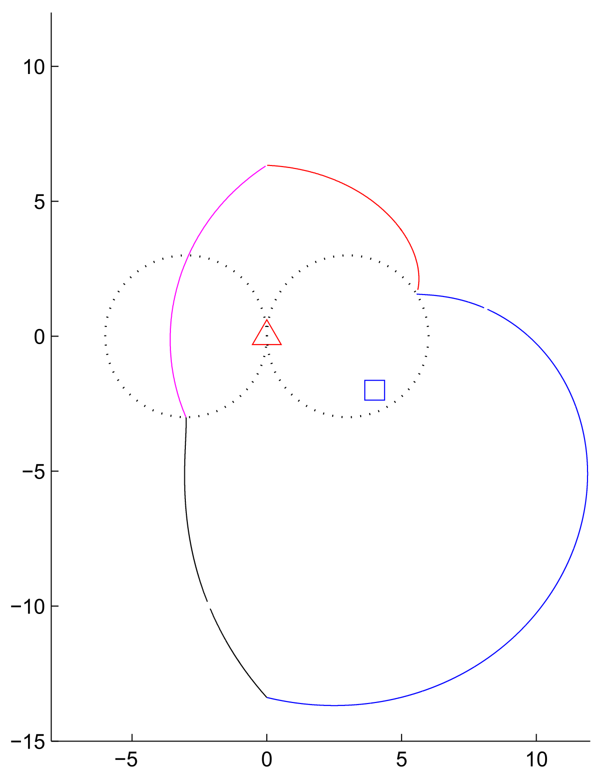

(b) E to the side and rear of P

Figure 3.15: Isochrone Intersections.

must be taken because points that are in the pursuer's reachable set at time τ_1 are not necessarily in the pursuer's reachable set at time τ_2 for $\tau_2 > \tau_1$. This is particularly the case for small τ_1. Thus, even if E cannot reach a particular location ξ without getting captured prior to $t = \tau_1$, E might be able to reach ξ for $t > \tau_2$, and therefore, ξ might be dominated by E, even though P can initially reach ξ before E. For example, consider the isochrone intersections on curve "1" in Figure 3.15a. If E moves to the side and avoids the initial pass by P, then E can return to points on curve "1" without being captured, regardless of the actions of P.

Nevertheless, the following holds:

Remark 3.3.1 *The boundary of the dominance regions in the HC problem is completely defined by* (3.31)*,* (3.25)*,* (3.32)*, and* (3.26)*. However, multiple instances of these equations may be required, each with different values for the constants* $\{x_{E0}, y_{E0}, t_B\}$.

Section 3.3.2 gives the intersections of the isochrones which are all points where the players can meet if traveling along minimum-time paths, but they are not all potential capture locations. Figure 3.16 illustrates this idea using the same scenario as Figure 3.15a. The points on the dashed outer curve between points A and B are isochrone intersections, but they are not potential capture points. If the evader moves away from the pursuer, then capture happens along the solid inner curve between points C and D. Similarly, the evader would be captured along the solid inner curve FG before reaching the dashed outer curve HI.

The solid curves in Figure 3.16 show the portions of the isochrone intersections that the evader can reach with straight line paths before any potential capture (i.e., the curves AH, BI, CD, and FG). The region of the plane that is known to be in the evader's dominance region is then made up of the wedges EHA, ECD, EBI, and EGF. The rest of the intersection points from Figure 3.15a are shown with dotted lines, and they represent an outer bound on the evader's dominance region. The straight dotted lines AC, DB, GI, and FH demarcate the subset of the dominance region that is known after intersecting the isochrone bundles

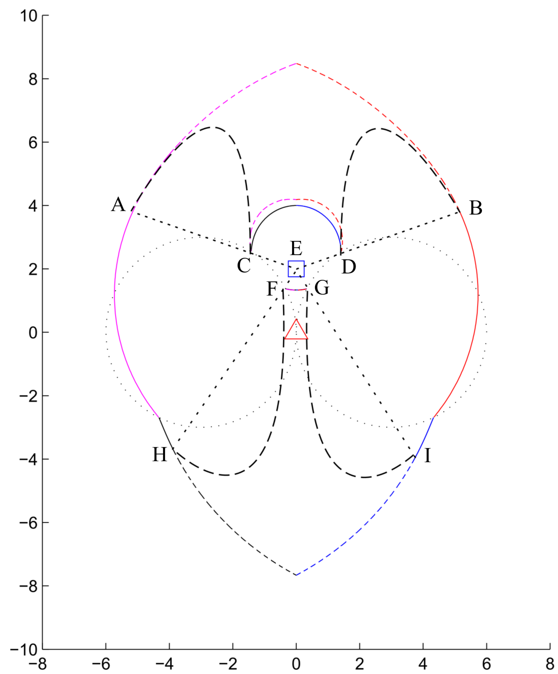

Figure 3.16: From isochrone intersections to dominance regions.

with $t_B = 0$. These lines represent an inner bound for the dominance region. Finally, the dashed curves AC, DB, GI, and FH represent the portion of the dominance boundary which is yet to be determined.

Note that the isochrone intersections with $t_B = 0$ provide an outer bound on E's dominance region. This is because the isochrones with $t_B = 0$ represent minimum-time paths from E's initial position, and the reachable set for paths with turns must be a subset of the reachable set for straight-line paths. Also note that for many initial conditions, such as the scenario in Figure 3.15b, the intersection of isochrone bundles with $t_B = 0$ is equivalent to the dominance boundary, and no additional steps are required.

3.3.3.1 Evasion with Turns

The dominance boundary represents the set of all points at which the pursuer and evader can meet if both follow paths that are time-optimal in the space of all paths where the evader can prevent capture no matter what the pursuer does. Thus, in Figure 3.16, the inner curves CD and FG are equivalent to an obstacle that the evader must avoid on its way to the dominance boundary. Note that the hypothetical obstacle the evader must avoid is not necessarily equivalent to curve CD, but can instead be viewed as a straight line segment connecting C to D. As previously discussed, it is well-known in the literature that the shortest Euclidean path between two points in the presence of polygonal obstacles is a broken line that breaks at the obstacle vertices [73]. Therefore, to determine the remaining portion of the dominance region, consider paths for the evader that first travel from (x_{E0}, y_{E0}) to a point infinitesimally close to C, D, F, or G, but still within the known subset of the evader's dominance region, and then turn and travel into the portion of the plane for which dominance has not yet been determined. These paths represent an evasion strategy where the evader "sidesteps" the pursuer to prevent an early capture.

These turning evasion paths are simple to implement due to the time delay that was built into the equations in Sections 3.3.1 and 3.3.2. The point where the evader turns becomes (x'_{E0}, y'_{E0}), and the time when the turn occurs is t_B. The evader's isochrones are still arcs of concentric circles, although they are now centered at the location of the turn, and therefore the analysis from Section 3.3.2 holds without any changes.

Note that the reachable set of points for turning paths is always contained within the reachable set for straight-line paths, and the isochrones for the turning paths are always tangent to the original isochrones along the direction that the evader was traveling prior to the turn. Therefore, the dominance boundary transitions smoothly across the boundary between regions of straight-line paths and turning paths.

Points C, D, F, and G are the solutions of the system of equations given by (3.30) along with the location of the pursuer along its minimum radius turn. For a clockwise turn, the location is given by:

$$x = \rho - \rho\cos(v_P t/\rho), \tag{3.46a}$$

$$y = \rho \sin(v_P t/\rho), \tag{3.46b}$$

and for a counter-clockwise turn, the location is given by:

$$x = -\rho + \rho \cos(v_P t/\rho), \tag{3.47a}$$

$$y = \rho \sin(v_P t/\rho). \tag{3.47b}$$

This development considers the case of a clockwise turn, but the development is equivalent for the other case. Substitute (3.46) into (3.30):

$$(\rho - \rho \cos(v_P t/\rho) - x_{E0})^2 + (\rho \sin(v_P t/\rho) - y_{E0})^2 = (v_E(t - t_B)^2. \tag{3.48}$$

Rearrange (3.48) to arrive at:

$$\begin{aligned} 0 = {} & 2\rho(x_{E0} - \rho)\cos(\frac{v_P t}{\rho}) - 2\rho y_{E0} \sin(\frac{v_P t}{\rho}) - v_E^2 t^2 \\ & + (2v_E^2 t_B)t + \left(-v_E^2 t_B^2 + (x_{E0} - \rho)^2 + y_{E0}^2 + \rho^2\right). \end{aligned} \tag{3.49}$$

Note that the cusps in the outer curve of the isochrone intersections also occur as solutions to this system of equations, so their locations can also be computed using (3.49).

Figure 3.17 shows the dominance regions for the scenario used in Figures 3.15a and 3.16 after turns have been applied at points C, D, F, and G. The isochrone intersections shown in Figure 3.15a are included for comparison, and as expected, the dominance region is contained within it. The change can be seen at the top of the figure, where a small area has been lost. A very small area is also lost at the bottom of the figure. Note that curves CD and FG from Figure 3.16 are not part of the dominance boundary, because after dodging an early capture, the evader is able to return to areas outside those curves, regardless of the pursuer's actions.

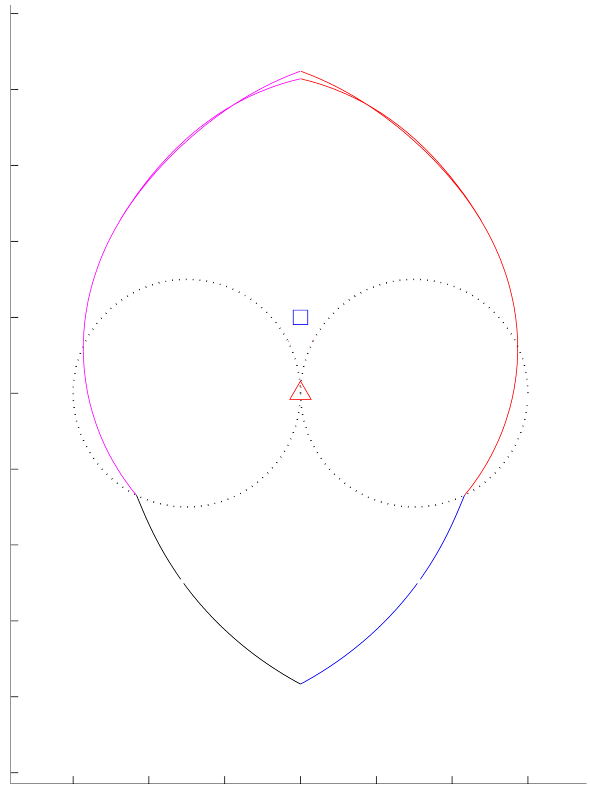

Figure 3.17: Dominance region with evader turns.

3.3.3.2 Capture Radius

Because the evader can always move to the side immediately prior to point capture, typical formulations of the HC game use proximity instead of colocation as the capture condition. Let ℓ be the capture radius. The evader's dominance region is then the set of points that the evader can reach without coming within an ℓ-neighborhood of the pursuer. This section proposes three different ways to incorporate this feature. The first is exact, and the other two are approximate.

In general, instead of constructing the dominance regions for only the point (x_{E0}, y_{E0}), the methods developed in Sections 3.3.2 and 3.3.3 can be used to map a domain of initial evader locations into a set of dominance regions, and the aggregate dominance region is then the intersection over the entire set. For example, if $\partial\mathcal{B}_\ell(x_{E0}, y_{E0})$ represents the boundary of the ℓ-neighborhood around the point (x_{E0}, y_{E0}), then the dominance region, $\mathcal{D}$, is determined by mapping the domain $\{\bar{x}_{E0}, \bar{y}_{E0} : (\bar{x}_{E0}, \bar{y}_{E0}) \in \partial\mathcal{B}_\ell(x_{E0}, y_{E0})\}$ into multiple dominance regions with different initial evader locations, $\mathcal{D}(\bar{x}_{E0}, \bar{y}_{E0})$, and then taking the intersection:

$$\mathcal{D} = \bigcap_{(\bar{x}_{E0},\bar{y}_{E0})} \mathcal{D}(\bar{x}_{E0}, \bar{y}_{E0}). \tag{3.50}$$

The dominance region can also be approximated in the following two ways:

1) Construct a single dominance region, $\mathcal{D}(x_{E0}, y_{E0})$, and then contract it by a distance d_{max} at each point, where d_{max} is given by:

$$d_{max} = \frac{v_E \ell}{v_P - v_E}. \tag{3.51}$$

Note that inflating the evader to a disk of radius d_{max} is an equivalent, but simpler way to accomplish this.

This method is conservative, because the evader can often get closer to the point-capture dominance boundary than d_{max} before capture, depending on the relative headings of the pursuer and evader when they meet at that point on the dominance boundary. The true distance from the point-capture dominance boundary at which the evader would be caught ranges from d_{min} to d_{max}, where:

$$d_{min} = \frac{v_E \ell}{v_P + v_E}. \tag{3.52}$$

2) Make use of t_B. The evader travels a distance of ℓ in time $t_\ell = \ell / v_E$. The dominance region for (x_{E0}, y_{E0}) with $t_B = t_\ell$, denoted $\mathcal{D}(x_{E0}, y_{E0}, t_\ell)$, gives the possible locations where the pursuer enters the capture region from behind the evader, and $\mathcal{D}(x_{E0}, y_{E0}, -t_\ell)$ gives the locations where the pursuer enters the capture region from in front of the evader. The isochrones for $t_B = t_\ell$ and $t_B = -t_\ell$ envelope the isochrones of the entire capture ball, so:

$$\Big(\mathcal{D}(x_{E0}, y_{E0}, t_\ell) \cap \mathcal{D}(x_{E0}, y_{E0}, -t_\ell)\Big) \subset \mathcal{D}. \tag{3.53}$$

3.3.4 Optimal Strategies

As in the case of simple motion, the optimal evasion strategy follows from the dominance regions. If the payoff is the time to capture, which the evader seeks to maximize and the pursuer to minimize, then the maxmin capture point is one of the following:

1) the point on the boundary of the evader's dominance region with the longest capture-avoiding, time-optimal path from the evader's initial location;

2) the point where the hole in the pursuer's reachable set closes at $t = t_3$; i.e., the point within the evader's dominance region that remains outside the pursuer's reachable set for the longest time.

The first alternative is equivalent to the maxmin capture point in PE games where all players move with simple motion. The second alternative exists because the pursuer's reachable set is not simply connected at all times, and if the hole in the pursuer's reachable set is in the interior of the evader's dominance region, then the evader can reach that point without being captured, and capture remains impossible until the hole in the pursuer's reach set becomes too small to contain an ℓ-neighborhood around the evader, which occurs near time $t = t_3$. Note that this is similar to the scenario in Figure 3.9, except that here the hole comes about as a natural consequence of P's dynamics, and no obstacles are required.

The optimal evasion strategy then consists of determining the maxmin capture point and traveling to that point. Note that again, this is an open-loop policy, and as the players move, if the pursuers do not take the optimal actions, then the capture point slides, and the evader's path curves. Also, as was the case for Figure 3.9, if C is located in the hole in the pursuer's reachable set, then it will move at some point during the game.

3.3.4.1 Optimal Point-Capture Location

Similarly to Theorem 3.2.7, the optimal location for point-capture can be determined by examining a small number of candidate locations, and thus it can be computed quickly.

This can be used as an approximation to the optimal strategy for proximity capture.

Theorem 3.3.2 *For a PE game featuring simple motion against a Dubins car, the optimal point-capture location, C, must satisfy one of the following conditions:*

1) *C occurs at an intersection between the dominance boundary and a singular surface;*

2) *C coincides with the location where the hole in P's reachable set closes at $t = t_3$;*

3) *For CS pursuit paths, the parameter ϕ satisfies:*

$$(\rho - x_{E0})\cos\phi + y_{E0}\sin\phi - \rho = 0; \tag{3.54}$$

4) *For CC pursuit paths, the parameters $\{t, \phi\}$ satisfy:*

$$\begin{aligned} &\Big[\rho\sin\phi - (\rho + x_{E0})\sin(2\phi) + y_{E0}\cos(2\phi)\Big]\cos\left(\frac{v_P t}{\rho}\right) \\ &+ \Big[-\rho\cos\phi + (\rho + x_{E0})\cos(2\phi) + y_{E0}\sin(2\phi)\Big]\sin\left(\frac{v_P t}{\rho}\right) \\ &+ (\rho + x_{E0})\sin\phi - y_{E0}\cos\phi = 0. \end{aligned} \tag{3.55}$$

Proof: As previously discussed, the dominance boundary may be made up of multiple instances of isochrone intersections. Consider an arbitrary instance with its associated straight line segment evasion paths and with initial evader location $E' = (x_{E0}, y_{E0})$.

Let ξ be an arbitrary point in the interior of $\mathcal{D}$. Then, since ξ is in the interior of $\mathcal{D}$, E can always travel for an additional length of time $\mathrm{d}t$ in the direction from E' to ξ without leaving $\mathcal{D}$. Therefore, ξ cannot maximize E's travel time, and it may only be the optimal capture point if it maximizes P's travel time. The only way for a point to be in the interior of $\mathcal{D}$ and also maximize P's travel time is for that point to coincide with the location where the hole in P's reachable set closes. This is condition 2 in the theorem.

Let Δ be the distance from E' to a point (x, y) on the dominance boundary, where Δ is given by:

$$\Delta = \sqrt{(x - x_{E0})^2 + (y - y_{E0})^2} = v_E(t - t_B). \tag{3.56}$$

The dominance boundary is piecewise smooth and parameterized by ϕ. For each smooth portion of the dominance boundary, the maximum Δ must either occur at a critical point where $\partial\Delta/\partial\phi = 0$ or at the interface between two smooth segments. These interfaces occur at the singular surfaces, which gives condition 1 in the theorem, and these singular surfaces occur directly in front of and behind the pursuer, or along the pursuer's minimum radius turn.

The only remaining possibilities are critical points where

$$\frac{\partial\Delta}{\partial\phi} = \frac{\partial}{\partial\phi}\left[v_E(t - t_B)\right] = v_E\frac{\partial t}{\partial\phi} = 0, \qquad \Rightarrow \frac{\partial t}{\partial\phi} = 0. \tag{3.57}$$

First consider CS paths. The isochrones are given by (3.25) and (3.30). Take the partial derivative of each equation with respect to ϕ and combine like terms:

$$\frac{\partial x}{\partial\phi} = v_P \sin\phi\frac{\partial t}{\partial\phi} + (v_P t - \rho\phi)\cos\phi, \tag{3.58a}$$

$$\frac{\partial y}{\partial\phi} = v_P \cos\phi\frac{\partial t}{\partial\phi} - (v_P t - \rho\phi)\sin\phi, \tag{3.58b}$$

$$2(x - x_{E0})\frac{\partial x}{\partial\phi} + 2(y - y_{E0})\frac{\partial y}{\partial\phi} = 2v_E^2(t - t_B)\frac{\partial t}{\partial\phi}. \tag{3.58c}$$

Substitute (3.58a) and (3.58b) into (3.58c), and substitute $\partial t/\partial\phi = 0$:

$$2(x - x_{E0})(v_P t - \rho\phi)\cos\phi - 2(y - y_{E0})(v_P t - \rho\phi)\sin\phi = 0. \tag{3.59}$$

Rearrange using common factors:

$$2(v_P t - \rho\phi)\Big[(x - x_{E0})\cos\phi - (y - y_{E0})\sin\phi\Big] = 0. \tag{3.60}$$

Thus, there are two opportunities for the capture point on CS paths. The first is the condition:

$$v_P t - \rho\phi = 0, \tag{3.61}$$

but this gives points on the pursuer's minimum radius turn, which is a singular surface, and hence, this duplicates points already considered. The only other critical points satisfy

$$(x - x_{E0})\cos\phi - (y - y_{E0})\sin\phi = 0. \tag{3.62}$$

Substitute (3.25) into (3.62):

$$\Big(\rho(1-\cos\phi)+(v_P t-\rho\phi)\sin\phi-x_{E0}\Big)\cos\phi-\Big(\rho\sin\phi+(v_P t-\rho\phi)\cos\phi-y_{E0}\Big)\sin\phi = 0. \tag{3.63}$$

Expand and simplify:

$$\rho\cos\phi - \rho\cos^2\phi - x_{E0}\cos\phi - \rho\sin^2\phi + y_{E0}\sin\phi = 0. \tag{3.64}$$

Substitute $\sin^2\phi + \cos^2\phi = 1$ and gather like terms to arrive at

$$(\rho - x_{E0})\cos\phi + y_{E0}\sin\phi - \rho = 0, \tag{3.65}$$

which is condition 3 in the theorem.

Next, consider CC paths and follow the same procedure. The isochrones are given by (3.26) and (3.30). Take the partial derivative of each equation with respect to ϕ:

$$\frac{\partial x}{\partial\phi} = \rho\left[-2\sin\phi + \sin\left(2\phi - \frac{v_P t}{\rho}\right)\left(2 - \frac{v_P}{\rho}\frac{\partial t}{\partial\phi}\right)\right], \tag{3.66a}$$

$$\frac{\partial y}{\partial\phi} = \rho\left[2\cos\phi - \cos\left(2\phi - \frac{v_P t}{\rho}\right)\left(2 - \frac{v_P}{\rho}\frac{\partial t}{\partial\phi}\right)\right], \tag{3.66b}$$

$$2(x - x_{E0})\frac{\partial x}{\partial \phi} + 2(y - y_{E0})\frac{\partial y}{\partial \phi} = 2v_E^2(t - t_B)\frac{\partial t}{\partial \phi}. \tag{3.66c}$$

Substitute (3.66a) and (3.66b) into (3.66c), and substitute $\partial t/\partial \phi = 0$:

$$4\rho(x - x_{E0})\left(-\sin\phi + \sin\left(2\phi - \frac{v_P t}{\rho}\right)\right) + 4\rho(y - y_{E0})\left(\cos\phi - \cos\left(2\phi - \frac{v_P t}{\rho}\right)\right) = 0. \tag{3.67}$$

Since $\rho \neq 0$, divide (3.67) by 4ρ and substitute (3.26) into the resulting equation:

$$\begin{aligned}&\left(\rho\left[2\cos\phi - 1 - \cos\left(2\phi - \frac{v_P t}{\rho}\right)\right] - x_{E0}\right)\left(-\sin\phi + \sin\left(2\phi - \frac{v_P t}{\rho}\right)\right)\\ &+\left(\rho\left[2\sin\phi - \sin\left(2\phi - \frac{v_P t}{\rho}\right)\right] - y_{E0}\right)\left(\cos\phi - \cos\left(2\phi - \frac{v_P t}{\rho}\right)\right) = 0.\end{aligned} \tag{3.68}$$

Expand and simplify to obtain:

$$\begin{aligned}&(\rho\cos\phi - (\rho + x_{E0}))\sin\left(2\phi - \frac{v_P t}{\rho}\right) - (\rho\sin\phi - y_{E0})\cos\left(2\phi - \frac{v_P t}{\rho}\right)\\ &+ (\rho + x_{E0})\sin\phi - y_{E0}\cos\phi = 0.\end{aligned} \tag{3.69}$$

Note that:

$$\begin{aligned}\sin\left(2\phi - \frac{v_P t}{\rho}\right) &= \sin(2\phi)\cos\left(\frac{v_P t}{\rho}\right) - \cos(2\phi)\sin\left(\frac{v_P t}{\rho}\right)\\ &= 2\sin\phi\cos\phi\cos\left(\frac{v_P t}{\rho}\right) - \cos^2\phi\sin\left(\frac{v_P t}{\rho}\right) + \sin^2\phi\sin\left(\frac{v_P t}{\rho}\right),\end{aligned} \tag{3.70a}$$

$$\begin{aligned}\cos\left(2\phi - \frac{v_P t}{\rho}\right) &= \cos(2\phi)\cos\left(\frac{v_P t}{\rho}\right) + \sin(2\phi)\sin\left(\frac{v_P t}{\rho}\right)\\ &= \cos^2\phi\cos\left(\frac{v_P t}{\rho}\right) - \sin^2\phi\cos\left(\frac{v_P t}{\rho}\right) + 2\sin\phi\cos\phi\sin\left(\frac{v_P t}{\rho}\right).\end{aligned} \tag{3.70b}$$

Using (3.70) together with $\sin^2\phi + \cos^2\phi = 1$,

$$\begin{aligned}&\rho\cos\phi\sin\left(2\phi - \frac{v_P t}{\rho}\right) - \rho\sin\phi\cos\left(2\phi - \frac{v_P t}{\rho}\right)\\ &\qquad = \rho\sin\phi\cos\left(\frac{v_P t}{\rho}\right) - \rho\cos\phi\sin\left(\frac{v_P t}{\rho}\right).\end{aligned} \tag{3.71}$$

Substituting (3.70) and (3.71) into (3.69) and rearranging the resulting equation gives:

$$\begin{aligned}
&\Big[\rho \sin\phi - (\rho + x_{E0})\sin(2\phi) + y_{E0}\cos(2\phi)\Big]\cos\left(\frac{v_P t}{\rho}\right) \\
&+ \Big[-\rho\cos\phi + (\rho + x_{E0})\cos(2\phi) + y_{E0}\sin(2\phi)\Big]\sin\left(\frac{v_P t}{\rho}\right) \\
&+ (\rho + x_{E0})\sin\phi - y_{E0}\cos\phi = 0,
\end{aligned} \tag{3.72}$$

which is condition 4 in the theorem. □

Remark 3.3.3 collects and summarizes the results from previous sections and theorems, and it notes all of the equations required to determine the candidate capture points. Once all candidates have been determined, C is the candidate with the maximum capture time.

Remark 3.3.3 *The candidate capture points can be calculated as follows:*

1) *Singular surfaces: Solve* (3.46) *for* t*, then use* (3.49).

2) *Hole in* P*'s reachable set: Find* $t = t_3$ *from* (3.29) *and substitute into* (3.26). *Use* $x = 0$ *to calculate* ϕ*, then use* ϕ *to calculate* y*. Note that this can be computed a priori.*

3) *CS paths: Solve* (3.54) *for* ϕ*, then use* (3.31) *to get* t*, then use* (3.25).

4) *CC paths: Solve* (3.32) *and* (3.55) *for* ϕ *and* t*, then use* (3.26).

3.4 Summary

This chapter considers games between a single pursuer and a single evader, and it develops methods for solving SPSE games that are based on the concept of dominance regions. Two generalizations of the Apollonius circle are provided. The first applies to games where both players move with simple motion, and it enables the study of games with polygonal obstacles. The second applies to games where one player moves with simple motion and the other is a Dubins car. In both cases, it is shown that construction of the dominance regions provides the necessary information for the players to implement their optimal pursuit and evasion strategies, respectively.

CHAPTER 4

Multiple-Pursuer and Multiple-Evader Games

This chapter considers PE games with additional pursuers and evaders. The primary focuses of this chapter are the Multiple Pursuer, Single Evader (MPSE) game, and the Single Pursuer, Multiple Evader (SPME) game. The primary contributions of this chapter are Theorem 4.1.1, which gives the dominance region of a single evader against multiple pursuers, and Algorithm 3 with (4.34), which give the maxmin capture times and locations for a single pursuer against multiple evaders with a specified capture order. Solutions to more complex games build upon these contributions.

This chapter utilizes the results of Chapter 3 by analyzing the MPSE and SPME games through the lens of dominance. Specifically, the MPSE and SPME games are shown to be decomposable into a set of SPSE games. In addition, this chapter adds to the foundation for Chapter 5, which considers the effects of uncertainty. Games that are analyzed with full and perfect information in this chapter are reconsidered as examples for games with uncertain information in Chapter 5 in order to show the influence of information on PE games.

Section 4.1 considers the MPSE game, and it introduces the Prey, Protector, and Predator (P3) game, which is also utilized as an example for games with parametric and measurement uncertainty in Chapter 5. Similarly, Section 4.2 considers the SPME game, which is further utilized in Chapter 5 as an example of a game with an uncertain cost function. Section 4.3 discusses games with both multiple pursuers and multiple evaders (MPME), as well as the benefits of analyzing many-player games through dominance.

4.1 Multiple Pursuers, Single Evader

One benefit of analyzing PE games through dominance is that it allows additional pursuers to be incorporated easily. For example, consider a game with a single evader and m pursuers, called $P_1, P_2, ..., P_m$. Let the region where E is dominant over P_i be the set $\mathcal{D}_{E/P_i}$, and let the boundary of $\mathcal{D}_{E/P_i}$ be the set $\mathcal{B}_{EP_i}$. The evader's dominance region against all pursuers, $\mathcal{D}_E$, can be constructed as follows:

Theorem 4.1.1 *For a MPSE game with m pursuers, the evader's dominance region is:*

$$\mathcal{D}_E = \bigcap_{i=1}^{m} \mathcal{D}_{E/P_i}. \tag{4.1}$$

Proof: Consider an arbitrary point $\xi \in \bigcap_{i=1}^{m} \mathcal{D}_{E/Pi}$. Since $\forall i,\ \xi \in \mathcal{D}_{E/Pi}$, E can reach ξ before being captured by any P_i, and therefore $\xi \in \mathcal{D}_E$. Next, consider $\xi \notin \mathrm{cl}(\bigcap_{i=1}^{m} \mathcal{D}_{E/Pi})$. Then $\exists k$ such that $\xi \notin \mathcal{D}_{E/Pk}$, and thus P_k can capture E prior to E reaching ξ. Therefore, $\xi \notin \mathcal{D}_E$. Finally, consider $\xi \in \partial(\bigcap_{i=1}^{m} \mathcal{D}_{E/P_i})$. Then $\exists k$ such that $\xi \in \partial\mathcal{D}_{E/Pk}$, and P_k can capture E at ξ (but no earlier). Thus, $\xi \in \partial\mathcal{D}_E$. $\square$

4.1.1 Simple Motion

For MPSE games where all players move with simple motion and the payoff is the time to capture, all of the analysis from the SPSE game holds, and the only change is that Theorem 3.2.7 must be amended as follows to account for the additional pursuers:

Theorem 4.1.2 *Let $\mathcal{R}_i$ be an arbitrary region in the partitioned plane, bounded only by obstacles and singular surfaces. The following are the only possibilities within $\mathcal{R}_i$ for the location of the optimal capture point, C:*

1) Any possibility given in Theorem 3.2.7.

2) An intersection between two instances of (3.15).

Proof: The proof of Theorem 4.1.2 follows immediately from Theorem 4.1.1 and the proof of Theorem 3.2.7. The only difference for the MPSE game is that endpoints of dominance boundary segments satisfying (3.15) can be created by not only intersections with obstacles and singular surfaces, but also by intersections with other instances of (3.15) that arise as a result of the additional pursuers. □

Corollary 4.1.3 *For the arbitrary region $\mathcal{R}_i$ and an arbitrary pursuer, P_j, if C_j^* is the global maximizer of the jth instance of* (3.15) *with associated capture time $t_{C,j}^*$, then:*

$$C = C_j^* \quad \Rightarrow \quad \forall k,\ t_{C,j}^* \leq t_{C,k}^*. \tag{4.2}$$

Proof Suppose the contrary; i.e., suppose that $C = C_j^*$, but there exists a pursuer, k, such $t_{C,j}^* > t_{C,k}^*$. Since $t_{C,k}^*$ is the global maximum capture time in $\mathcal{D}_{E/P_k}^i$, this implies that $C_j^* \notin \mathcal{D}_{E/P_k}^i$. However, this contradicts $C = C_j^*$, because the definition of C and Theorem 4.1.1 require that $\forall k,\ C \in \mathcal{D}_{E/P_k}$. □

From Corollary 4.1.3, it is unnecessary to verify that $\forall k,\ C_k^* \in \mathcal{D}_{E/P_k}^i$. It is sufficient to check only the C_k^* with minimum associated $t_{C,k}^*$. Furthermore, the global minimum and maximum capture times for two pursuers can be compared to determine the existence of intersections between instances of (3.15). Therefore, the determination of C for MPSE games can be determined using Algorithm 2.

Add $\mathcal{R}_E$ to list of candidate regions;
while *not at end of list of candidate regions* **do**
> **foreach** *pursuer,* k **do**
>> determine P_k', E', $t_{P_k'}$ and $t_{E'}$ for R_c (by solving ESPPs);
>> $d_k = ||P_k' - E'||$;
>> **if** $t_{P_k'} \geq t_{E'}$ **then**
>>> $t_{B,k} = t_{P_k'} - t_{E'}$;
>>> $C_k^* = (r_{Pk}(\pi), \pi)$;
>>
>> **else**
>>> $t_{B,k} = t_{E'} - t_{P_k'}$;
>>> $C_k^* = (r_{Pk}(0), 0)$;
>>
>> **end**
>
> **end**
> $k^* = \arg\min_k t_{c,k}^*$;
> $\hat{C} = C_{k^*}^*$;
> **if** $\hat{C} \in \mathcal{R}_c$ **then**
>> add $\hat{C}$ to set $\mathcal{C}_c$;
>
> **else if** $d_{k^*} = 0$ **then**
>> Set $\hat{C}$ to any $(r, \theta) \in \mathcal{R}_c$ satisfying the k^*-th instance of (3.15);
>> add $\hat{C}$ to set $\mathcal{C}_c$;
>
> **else**
>> **foreach** $X_j \in \mathcal{R}_c$ **do**
>>> **if** $\forall k,\ r_{X_j} < r_{Pk}(\theta_{X_j})$ **then**
>>>> add X_j to set $\mathcal{C}_c$;
>>>
>>> **end**
>>
>> **end**
>
> **end**
> **foreach** $X_j \in \mathcal{R}_c$ **do**
>> **if** $\forall k,\ r_{X_j} < r_{Pk}(\theta_{X_j})$ **then**
>>> add neighboring region to list of candidate regions;
>
> **end**

end
$i^* = \arg\min_i t_c[i]$;
$C = \mathcal{C}_c[i^*]$;

Algorithm 2: Computing the optimal capture point in MPSE games

4.1.2 Simple Motion vs. Dubins Car

Additional pursuers affect the HC game in the same way as they affect games where all players move with simple motion. However, one additional issue must be considered. As discussed in Section 3.3.3.1, constructing the dominance regions in SPSE games requires the consideration of turns by the evader. In the MPSE game, each turn must be considered against all pursuers. The procedure to construct the evader's dominance region is as follows:

1) Construct the isochrone intersections for the evader with $t_B = 0$ against each pursuer individually.

2) Determine the intersection of the subsets of the pairwise dominance regions generated by straight-line paths for the evader.

3) Determine a turn location and time as in Section 3.3.3.1.

4) Determine the intersection of each pairwise dominance region after the turn.

5) Repeat Steps 3 and 4 until the entire dominance boundary is known.

Once the dominance region has been constructed, the optimal evasion strategy is the same as in Section 3.3.4, with the additional consideration that for capture points located in the hole of a pursuer's reachable set, the point must be outside the reachable sets of all pursuers to be valid. Hence, for an arbitrary hole closure point, C_H, shortest path problems must be solved from each pursuer's initial position to C_H, and C is only colocated with C_H if the minimum time for any pursuer to reach C_H is greater than the maximum capture time on the boundary of E's dominance region.

As in games with simple motion, the possibilities for candidate capture points in MPSE HC games must be amended to include the possibility that C occurs at an intersection of dominance boundaries for more than one pursuer.

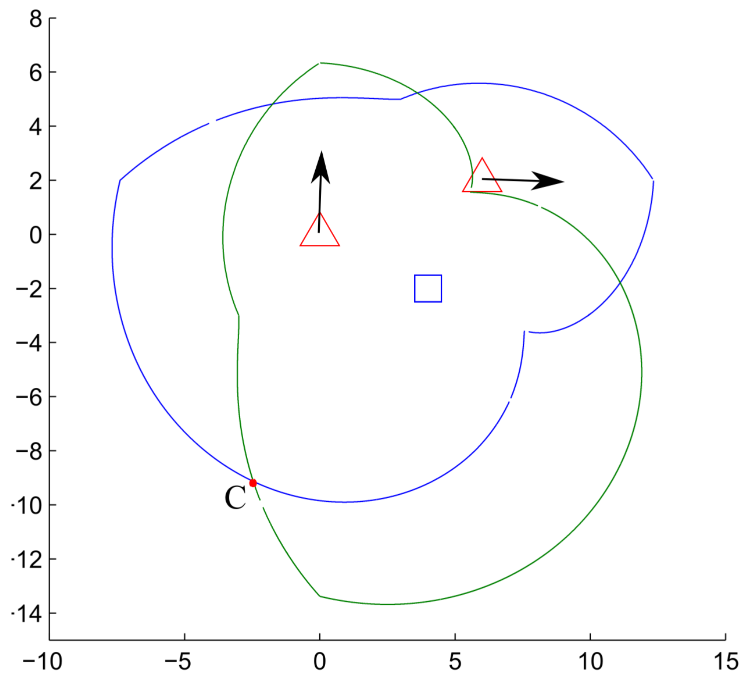

Figure 4.1: Two Pursuer Game

Theorem 4.1.4 *In MPSE HC games, the following are the only possibilities for the location of the optimal capture point, C:*

1) Any possibility given in Theorem 3.3.2.

2) An intersection between pairwise dominance boundaries.

Proof: The proof is identical to the proof of Theorem 4.1.2. □

Figure 4.1 shows an example for two pursuers with the maxmin capture point marked by the C. Optimal evasion dictates that the evader travels toward C along a straight-line path.

4.1.3 Pursuers that aren't involved in capture

As in SPSE games, E should travel to the optimal capture point in minimum time, and so should any pursuer, P_i, for which $C \in \mathcal{B}_{EP_i}$. However, there may be a number of pursuers,

P_j, that are not involved in the capture if E acts optimally. Hence, traveling to the optimal capture point in minimum time might not be the best pursuit behavior for P_j, because even along a time-optimal path, P_j can't reach C until after capture has been achieved by P_i. The best strategy for P_j is left as future work, but one possibility is for P_j to pursue in such a way as to maximize the penalty incurred by E for employing suboptimal evasive behavior.

4.1.4 Competing teams of pursuers

With more than one pursuer in the game, it is possible to formulate games where some pursuers compete against others. For example, consider the Prey, Protector, and Predator (P3) game [85], which is applicable to combat search and recovery scenarios.

4.1.4.1 Problem Statement

Consider the following games:

P4.1 **P3 Game of Kind:** Given the following teams of players:

- Red team:
  - m pursuers, P_j, $j = 1, ..., m$, known as predators;
- Blue team:
  - an evader, E, known as the prey;
  - q pursuers, R_k, $k = 1, ..., q$, known as protectors;

where the ratio of P_j's speed to E's is γ_{Pj}, and the ratio of R_k's speed to E's is γ_{Rk}; and given the following team goals:

- Red team: any P_j captures E before any R_k achieves rendezvous,
- Blue team: any R_k achieves rendezvous with E before any P_j achieves capture,

determine whether there exists a k such that for all j, R_k can rendezvous with E before capture by P_j, regardless of the actions of P_j.

P4.2 **P3 Game of Degree:** Given everything stated in the P3 game of kind, and also given as cost function the time, t_R, when the first R_k achieves rendezvous with E, find the optimal location for E to rendezvous with R_k such that t_R is minimized.

Note that the P3 game is similar to another multiplayer game known as the Lady, the Bandits and the Bodyguards [96], except that in that game the goal of the bodyguards is to intercept the bandit adversaries, and the bodyguards often (though not always) start from the location of the lady. Here the protector starts away from the prey, and the goal of the Blue team is to cooperate and rendezvous in order to rescue the prey.

4.1.4.2 Solution in the Absence of Obstacles

The solution of P4.1 in the case of perfect information is determined by constructing the pair-wise dominance regions.

Theorem 4.1.5 *The team of* $\{E, R_k : k = 1, .., q\}$ *dominates the team* $\{P_j : j = 1, .., m\}$ *if and only if:*

$$\exists k, \xi \; s.t. \, \forall \; j, \; \xi \in \{\mathcal{B}_{ER_k} \cap \mathcal{D}_{E/P_j}\}, \tag{4.3}$$

or equivalently,

$$\exists k, \xi \; s.t. \, \forall \; j, \; \xi \in \{\mathcal{B}_{ER_k} \cap \mathcal{D}_{R_k/P_j}\}. \tag{4.4}$$

Proof: To be able to guarantee rendezvous before capture, E and at least one R_k must be able to reach the rendezvous point before all P_j. Thus, the rendezvous point, ξ, must satisfy:

$$\forall \; j, \; \xi \in \{\mathcal{D}_{E/P_j} \cap \mathcal{D}_{R_k/P_j}\}. \tag{4.5}$$

Furthermore, dominance regions are defined using time-optimal paths, so the rendezvous must occur at a point where E and R_k can meet if both travel optimally. Thus, $\xi \in \mathcal{B}_{ER_k}$, which gives:

$$\forall\, j,\ \xi \in \{\mathcal{D}_{E/P_j} \cap \mathcal{D}_{R_k/P_j} \cap \mathcal{B}_{ER_k}\}. \tag{4.6}$$

Finally, by transitivity, if $\xi \in \mathcal{B}_{ER_k}$, then

$$\left(\xi \in \mathcal{D}_{E/P_j}\right) \Leftrightarrow \left(\xi \in \mathcal{D}_{R_k/P_j}\right), \tag{4.7}$$

which gives the two conditions stated in the theorem. □

Consider a P3 game with a single predator and a single protector. In the absence of obstacles, three Apollonius circles can be drawn using (3.10). Due to the transitivity of equality, any intersection between two of the circles must necessarily be an intersection of all three circles, and all of the dominance information can be obtained from any two of the Apollonius circles. Consider the protector/prey and predator/prey Apollonius circles. Place the origin at the prey and define the direction of zero azimuth as the line of sight from the prey to the protector. Then define the following four dimensionless parameters:

- γ_R: the ratio of speeds between protector and prey,
- γ_P: the ratio of speeds between predator and prey,
- α: the ratio of the initial distance between protector and prey to the initial distance between predator and prey,
- θ_P: the angle between the prey's lines of sight to the protector and the predator.

The solution to the game is as follows:

Theorem 4.1.6 *Given $\gamma_R > 1$, $\gamma_P > 1$, α, and θ_P, if $\exists\theta$ such that*

$$\alpha\left(\frac{\gamma_P^2 - 1}{\gamma_R^2 - 1}\right)\frac{-\cos(\theta) + \sqrt{\gamma_R^2 - \sin^2(\theta)}}{-\cos(\theta - \theta_P) + \sqrt{\gamma_P^2 - \sin^2(\theta - \theta_P)}} < 1, \tag{4.8}$$

then the Blue team dominates the game of kind. If no such θ exists, then the Red team dominates the game of kind. Furthermore, in the solution to the game of degree, (r^*, θ^*), θ^* must satisfy (4.8).

Proof: For a given angle θ, let the distance from the origin to the protector/prey Apollonius circle be r_R, and let the distance to the predator/prey Apollonius circle be r_P. These Apollonius circles can be expressed as:

$$r_R = \frac{-\cos(\theta) \pm \sqrt{\gamma_R^2 - \sin^2(\theta)}}{\gamma_R^2 - 1} d_R, \tag{4.9}$$

$$r_P = \frac{-\cos(\theta - \theta_P) \pm \sqrt{\gamma_P^2 - \sin^2(\theta - \theta_P)}}{\gamma_P^2 - 1} d_P, \tag{4.10}$$

where d_R is the initial distance between the prey and the protector, and d_P is the initial distance between the prey and the predator.

Equations (4.9) and (4.10) each provide two values of r for each θ. Since the prey is the slowest player, the dominance boundaries surround its initial location, so there are always one positive and one negative value of both r_R and r_P. Take the positive values, which correspond to the + sign in (4.9) and (4.10). Then the Blue team dominates if there exists a θ such that

$$r_R < r_P. \tag{4.11}$$

Since $r_P > 0$, this is equivalent to

$$\frac{r_R}{r_P} < 1. \tag{4.12}$$

Substitute (4.9) and (4.10) into (4.12), and substitute $\alpha = d_R/d_P$ to obtain (4.8). $\square$

Figure 4.2 shows a game with one predator, represented by the $*$, and one protector, represented by the $\triangle$. The parameters are:

- $\gamma_R = 2$,

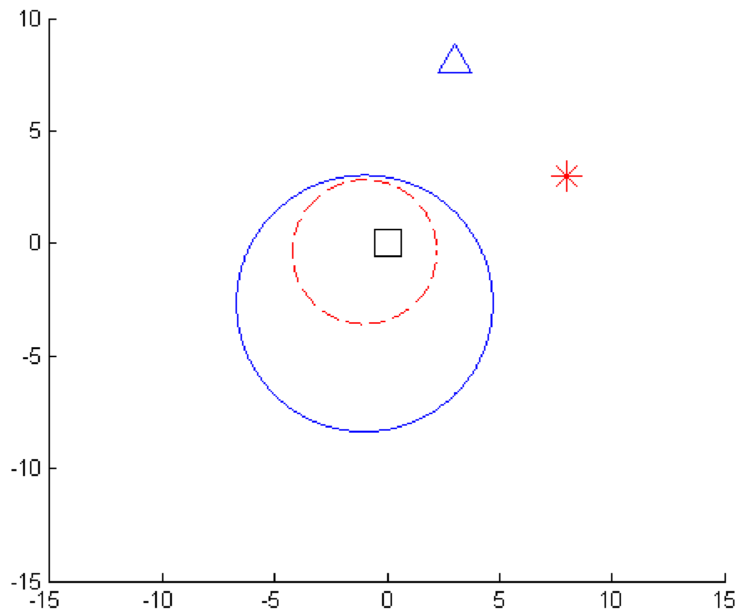

Figure 4.2: P3 game with faster predator.

- $\gamma_P = 3$,
- $\alpha = 1$,
- $\theta_P \approx 49°$.

Evaluating the left hand side of (4.8) yields a solution which is larger than 1 for all θ, and therefore the Red team dominates; that is, there is no location where the Blue team can rendezvous unless the predator acts suboptimally.

Theorem 4.1.6 follows from the Apollonius Circle Theorem, and indeed, Figure 4.2 shows the same result. In Figure 4.2, the predator/prey Apollonius circle is depicted with a dashed circle, and the protector/prey Apollonius circle is depicted with a solid circle. The protector/prey Apollonius circle lies entirely within the dominance region of the predator, and so there are no locations where the Blue team can rendezvous if the predator acts optimally.

This result easily generalizes for additional players. Suppose there are m predators and q protectors. Condition (4.8) is evaluated at most mq times. If any protector is found to

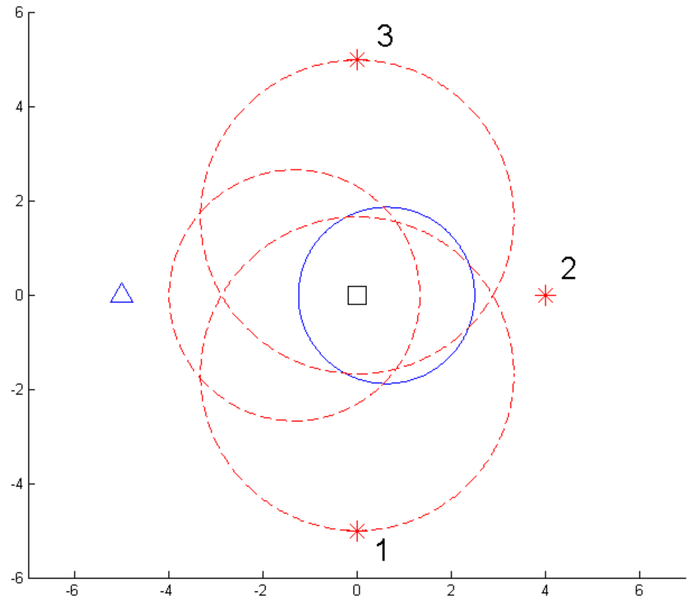

Figure 4.3: P3 game with three predators.

dominate all m predators, then the Blue team dominates the larger game, and the remaining protectors need not be evaluated. If all q protectors are dominated by at least one predator each, then the Red team dominates the larger game.

For example, consider the game in Figure 4.3 where the prey is represented by $\square$, the protector by $\triangle$, and the three predators by $*$, with the predators numbered as shown. The parameters of the game are:

- $m = 3$, $q = 1$,
- $\gamma_R = 3$,
- $\gamma_{P1} = \gamma_{P2} = \gamma_{P3} = 2$,
- $d_R = d_{P1} = d_{P3} = 5$, $d_{P2} = 4$,
- $\theta_R = 0$, $\theta_{P1} = 90°$, $\theta_{P2} = 180°$, $\theta_{P3} = 270°$.

In this game, the Blue team dominates because for angles near $\theta = 0$, i.e., to the left in the figure, the protector and prey can rendezvous at a location that lies within the prey's dominance region for all three of the predator/prey Apollonius circles. Indeed, evaluating condition (4.8) for $\theta = 0$ and for each of the games involving a single predator vs. the protector yields:

$$Predator\ 1: \quad \tfrac{\sqrt{3}}{4} < 1, \tag{4.13}$$

$$Predator\ 2: \quad \tfrac{5}{16} < 1, \tag{4.14}$$

$$Predator\ 3: \quad \tfrac{\sqrt{3}}{4} < 1. \tag{4.15}$$

Therefore, the protector dominates all individual predators, and the Blue team dominates the larger game.

4.1.4.3 Solution in the Presence of Obstacles

When obstacles are introduced, the solution is still given by Theorem 4.1.5 and the construction of pairwise dominance regions. The only difference is that the dominance regions are constructed using Theorem 3.2.5 and Remark 3.2.6 instead of Apollonius circles.

Figures 4.2 and 4.4 show the effect of an obstacle in the P3 game. The initial locations of the players are the same in both figures. The predator and the protector start at the same distance from the prey, but the predator is faster than the protector. In both figures, the dominance boundary for the predator/prey two player game is represented by the dashed line and the dominance boundary for the protector/prey game is represented by the solid line. In Figure 4.4, the thick line represents an obstacle. The singular surfaces are not shown to maintain clarity.

As stated previously, in Figure 4.2, when there is no obstacle present, the predator dominates the game because for all directions that the prey could choose to travel, the predator can capture it before the protector rescues it. However, in the presence of the obstacle, a portion of $\mathcal{B}_{ER}$ is contained within $\mathcal{D}_{E/P}$. The protector can therefore rescue the prey at any point along this section of $\mathcal{B}_{ER}$, and it is impossible for the predator to

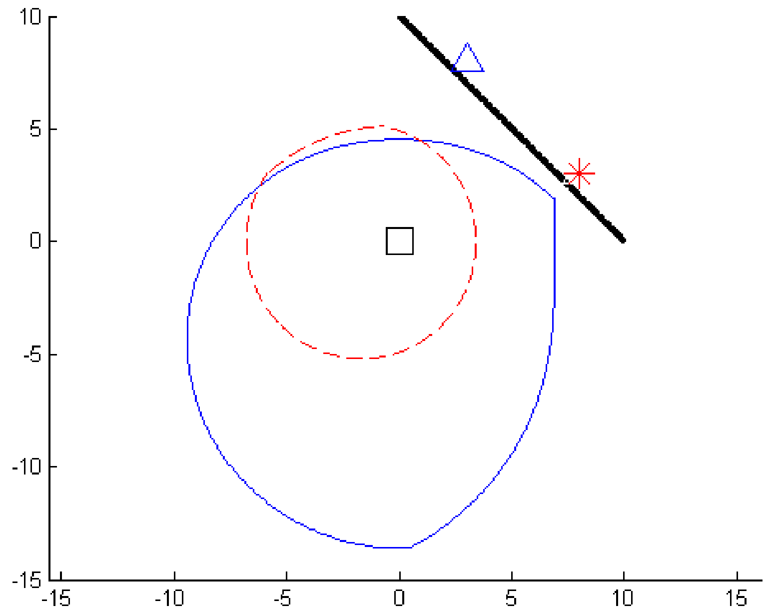

Figure 4.4: P3 game with a line segment obstacle.

achieve capture first.

4.1.4.4 P3 Game of Degree

Consider a simple P3 game with one prey, one predator, one protector, and no obstacles, as shown in Figure 4.5. The prey's initial location is shown by the $\square$. The predator's initial location is given by the $*$, and $\gamma_P = 2$. The protector's initial location is given by the $\triangle$, and $\gamma_R = 3$. $\mathcal{B}_{ER}$ is shown by the solid curve, and $\mathcal{B}_{EP}$ is shown by the dashed curve. In this game, the team $\{E, R\}$ dominates P, and E can rendezvous with R at any point on the solid curve that lies within the dotted curve.

The P3 game of degree can be formulated as a constrained minimization problem. Place the origin at E, and the angle of zero azimuth in the direction of R. Then the best rendezvous location is the minimizer of (4.9) subject to (4.8). Note that in some cases, no minimum exists since the set $\{\mathcal{B}_{ER} \cap \mathcal{D}_{E/P}\}$ is open. However, in these situations, if R_k and E wish to rendezvous quickly, they can rendezvous near the boundary of $\{\mathcal{B}_{ER} \cap \mathcal{D}_{E/P}\}$.

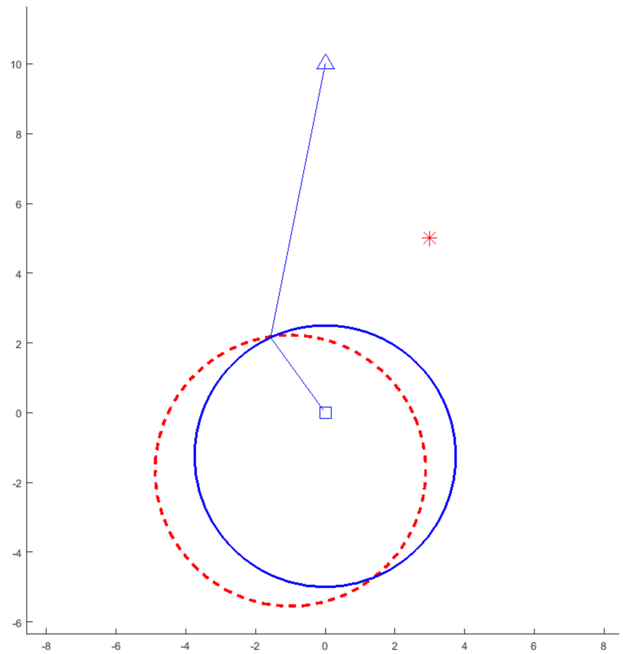

Figure 4.5: P3 Game With Perfect Information.

The solution, (r^*, θ^*), can be determined as follows:

$$\begin{aligned}
\theta^* &= \arg\inf_{\theta} \frac{-\cos(\theta) \pm \sqrt{\gamma_R^2 - \sin^2(\theta)}}{\gamma_R^2 - 1} d_R, \\
&\quad \text{subject to} \\
&\quad \alpha \left(\frac{\gamma_P^2 - 1}{\gamma_R^2 - 1} \right) \frac{-\cos(\theta) + \sqrt{\gamma_R^2 - \sin^2(\theta)}}{-\cos(\theta - \theta_P) + \sqrt{\gamma_P^2 - \sin^2(\theta - \theta_P)}} < 1, \qquad (4.16) \\
r^* &= \frac{-\cos(\theta^*) \pm \sqrt{\gamma_R^2 - \sin^2(\theta^*)}}{\gamma_R^2 - 1} d_R.
\end{aligned}$$

The straight lines in Figure 4.5 show trajectories for R and E that lead to a rendezvous location near (r^*, θ^*).

This example will be revisited in Section 5.2.3.1, which considers a P3 game where the location of the predator is not perfectly known.

4.2 Single Pursuer, Multiple Evaders

This section considers games with a single pursuer and multiple evaders where the payoff is the time to capture all evaders (i.e., the payoff is the final capture time).

4.2.1 Problem Statement

Two problems are of interest:

P4.3 **SPME game with specified capture order:** Given an evader, P, and n evaders, $E_i,\ i = 1, ..., n$, where the evaders are arranged in the order in which the pursuer must capture them; and given as payoff $t_{cf} = t_{cn}$, the capture time of the final evader, find $\vec{\psi}_E^*$, the heading for each evader that maximizes the minimum t_{cn}.

P4.4 **SPME game with free capture order:** Given an evader, P, and n evaders, $E_i,\ i = 1, ..., n$, where all evaders must be captured, but the choice of capture order is free, and given as payoff t_{cf}, the capture time of the final evader, find $\vec{\psi}_E^*$, the heading for each evader that maximizes the minimum t_{cf}, as well as the capture order which minimizes the maxmin t_{cf}.

Problem P4.3 has been considered in [62] using a method known as parallel-pursuit. This leads to the same trajectories as the method of dominance regions. However, this dissertation analyzes the game using (3.15), which yields a solution that requires only a maximization instead of the minmax calculation required by other methods. This occurs because the minimization is built into (3.15).

4.2.2 Two Evaders

To provide intuition, consider the case of two evaders. The general case is solved in the following section.

The minimum time required for the pursuer to capture the first evader can be determined from an Apollonius circle with the evader's choice of heading angle, ψ_{E1}:

$$t_{c1} = \frac{r_{E,1}(\psi_{E1})}{v_{E1}}. \tag{4.17}$$

If the evaders cooperate, then E_2 travels directly away from the capture point. The distance that E_2 travels before E_1 gets captured is:

$$d_{c1} = v_{E2} t_{c1}. \tag{4.18}$$

Consider Figure 4.6, and the triangles formed by the initial positions of P, E_1 and E_2, as well as the capture point of the first evader, C_1. Let the distance between P and E_1 be d_1, the distance between E_1 and E_2 be δ_2, and the distance between P and E_2 be a_2. Also, let the angle between the line from E_1 to P and the line from E_1 to E_2 be σ_2, which can be calculated from the law of cosines:

$$a_2^2 = d_1^2 + \delta_2^2 - 2d_1\delta_2 \cos\sigma_2, \tag{4.19}$$

$$\Rightarrow \sigma_2 = \cos^{-1}\left(\frac{a_2^2 - d_1^2 - \delta_2^2}{-2d_1\delta_2}\right). \tag{4.20}$$

The capture point C_1 lies on an Apollonius circle, and the distance from E_1 to C_1 is $r_{E,1}(\psi_{E1})$. Then from the law of cosines, the distance between C_1 and the starting point of the second evader, d_2, is given by:

$$[d_2(\psi_{E1})]^2 = [r_{E,1}(\psi_{E1})]^2 + \delta_2^2 - 2\delta_2 r_{E,1}(\psi_{E1})\cos(\psi_{E1} - \sigma_2). \tag{4.21}$$

Thus, the total distance between P and E_2 at t_{c1} is:

$$d_2' = d_{c1} + d_2, \tag{4.22}$$

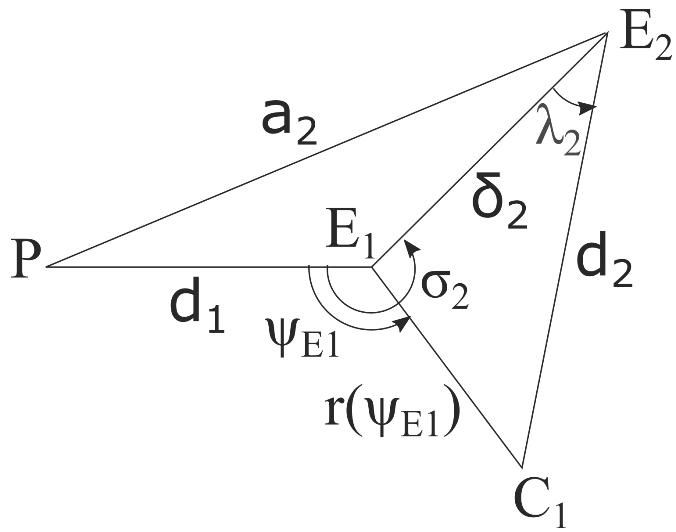

Figure 4.6: 2 Evader Scenario.

and the time that it takes for the pursuer to make up the distance lost while pursuing E_1 (d_{c1}), then overcome the initial separation (d_2) is:

$$\bar{t}_{c2} = \frac{d_{c1} + d_2}{v_P - v_{E2}} = \frac{v_{E2} r_{E,1}(\psi_{E1})}{v_{E_1}(v_P - v_{E2})} + \frac{d_2(\psi_{E1})}{v_P - v_{E2}}. \tag{4.23}$$

The total time to capture both evaders is then given by:

$$t_{c2}(\psi_{E1}) = t_{c1}(\psi_{E1}) + \bar{t}_{c2}(\psi_{E1}), \tag{4.24}$$

and the minmax capture time of the second evader (for a given capture order) is:

$$\begin{aligned} t'_{c2} &= \max_{\psi_{E1}} t_{c2}(\psi_{E1}) \\ &= \max_{\psi_{E1}} \left[\left(\frac{1}{v_{E1}} + \frac{v_{E2}}{v_{E1}(v_P - v_{E2})} \right) r_{E,1}(\psi_{E1}) + \frac{d_2(\psi_{E1})}{v_P - v_{E2}} \right]. \end{aligned} \tag{4.25}$$

This is the solution of P4.3 for $n = 2$. Then the solution to P4.4 is that the pursuer chooses the capture order with the lowest t'_{c2}; i.e., if ζ represents the set of all potential capture sequences, then

$$t^*_{c2} = \min_{\zeta} t'_{c2}(\zeta). \tag{4.26}$$

4.2.3 n-Evaders, specified order

To generalize the previous section, consider an alternative form of the arguments using the time delay, t_B, that is built into the generalized Apollonius circle. For the first evader, $t_{B1} = 0$, and d_1 is the distance between the pursuer's initial position and the first evader's initial position. With $t_{B1} = 0$, the generalized Apollonius circle reduces to the standard Apollonius circle, and thus (4.17) holds with no change.

Subsequent captures also occur on generalized Apollonius circles, where t_{Bi} is set to the total time required for the pursuer to achieve all prior captures in the sequence, and d_i is the distance between an evader's initial position and the capture location of the previous evader in the capture sequence. Returning to the two evader case, the first capture is on the curve described by (3.15) with $t_{B1} = 0$ and $d_1 = ||P - E_1||$. The second capture occurs along (3.15) with $t_{B2} = t_{c1}$, as given by (4.17), and $d = d_2$, as given by (4.21). The total time to capture all evaders is then given by:

$$t_{cf}(\psi_{E1}, \psi_{E2}) = t_{c2}(\psi_{E1}, \psi_{E2}) = \frac{r_{E,2}(\psi_{E1}, \psi_{E2})}{v_{E2}}, \tag{4.27}$$

and the minmax capture time is given by:

$$t'_{cf} = \max_{\psi_{E1}, \psi_{E2}} t_{cf}(\psi_{E1}, \psi_{E2}). \tag{4.28}$$

Note that with this formulation, calculating t_{c2} no longer requires separate calculations for d_{c1} and $\bar{t}_{c2}$, because the distance traveled by E_2 during the capture of E_1 is already included through the incorporation of t_{B2}. Furthermore, this formulation is recursive, and hence it generalizes to n evaders easily.

Theorem 4.2.1 *In a game with a single pursuer and n evaders, the i-th evader's capture time, $t_{c,i}$, and capture location, C_i, in the dominance boundary given by $(r_{E,i}, \psi_{E,i})$, satisfy* *the following:*

$$\left(\gamma_i^2-1\right)r_{E,i}^2+2\left(d_i\cos\psi_{E,i}-\gamma_i^2 v_P t_{c,i-1}\right)r_{E,i}+\left(\gamma_i^2 v_P^2 t_{c,i-1}^2-d_i^2\right)=0, \tag{4.29}$$

where

$$d_i(\psi_{E,i-1})=\sqrt{[r_{E,i-1}(\psi_{E,i-1})]^2+\delta_i^2-2\delta_i r_{E,i-1}(\psi_{E,i-1})\cos(\psi_{E,i-1}-\sigma_i)}, \tag{4.30}$$

$$t_{ci}=\frac{r_{E,i}(\psi_{Ei})}{v_{Ei}}, \tag{4.31}$$

δ_i is the distance between E_i and E_{i-1}, and σ_i is the angle formed by the line from E_{i-1} to E_{i-2} and the line from E_{i-1} to E_i, which can be calculated as follows:

$$\sigma_i=\cos^{-1}\left(\frac{a_i^2-d_{i-1}^2-\delta_i^2}{-2d_{i-1}\delta_i}\right), \tag{4.32}$$

where a_i is the distance between E_i and C_{i-2}.

Proof: Equations (4.30), (4.31), and (4.32) in Theorem 4.2.1 are simply the iterative application of (4.21), (4.17), and (4.20), respectively, which only require knowledge of E_{i-1}, C_{i-2}, and ψ_{E-1}. Equation (4.29) is the generalized Apollonius circle, where capture occurs if both players follow minimum-time paths. Note that to initialize this recursion, $E_0=C_0:=P$ and $r_{E,0}:=0$. □

The capture times and locations can then be determined with Algorithm 3, where λ_i is the angle between the line from E_i to E_{i-1} and the line from E_i to C_{i-1}, and θ_i^0 is the direction of zero azimuth for E_i. Line 12 calculates λ_i using the law of sines for the triangle $E_iE_{i-1}C_{i-1}$, as shown in Figure 4.6. The optimal evader headings can be calculated as follows:

$$\vec{\psi}_E^*=\arg\max_{\vec{\psi}_E}\text{n\_Capture}(P,\vec{E},\vec{\psi}_E). \tag{4.34}$$

Function *n_Capture* (P,$\vec{E}$,$\vec{\psi_E}$)

$E_0 = P$;

$C_0 = P$;

$r_{E,0} = 0$;

$d_0 = 0$;

$\psi_{E0} = 0$;

for $i = [1, n]$ **do**

$\delta_i = ||E_i - E_{i-1}||$;

$a_i = ||E_i - C_{i-2}||$;

$$\sigma_i = \cos^{-1}\left(\frac{a_i^2 - d_{i-1}^2 - \delta_i^2}{-2d_{i-1}\delta_i}\right);$$

$$d_i = \sqrt{[r_{E,i-1}(\psi_{E,i-1})]^2 + \delta_i^2 - 2\delta_i r_{E,i-1}(\psi_{E,i-1})\cos(\psi_{E,i-1} - \sigma_i - \theta_i^0)};$$

$$\lambda_i = \sin^{-1}\left(\frac{r_{E,i-1}\sin(\psi_{E,i-1} - \sigma_i - \theta_{i-1}^0)}{d_i}\right);$$

$$\theta_i^0 = \theta_{i-1}^0 + \sigma_i - \pi + \lambda_i;$$

$$r_{E,i} = \frac{1}{\gamma_i^2 - 1}\left[-d_i\cos(\psi_{Ei} - \theta_i^0) + \gamma_i^2 v_P t_{c,i-1} \pm \sqrt{\gamma_i^2(d_i\cos(\psi_{Ei} - \theta_i^0) - v_P t_{c,i-1})^2 + d_i^2(\gamma_i^2 - 1\sin^2(\psi_{Ei} - \theta_i^0)}\right] \tag{4.33}$$

$$C_i = E_i + \begin{bmatrix} r_{E,i}\cos\psi_{Ei} \\ r_{E,i}\sin\psi_{Ei} \end{bmatrix};$$

$t_{Ci} = \frac{r_{E,i}}{v_{Ei}}$;

end

return $\{C_i\}$, $\{t_{Ci}\}$;

Algorithm 3: Computation of capture locations and times for a particular capture order.

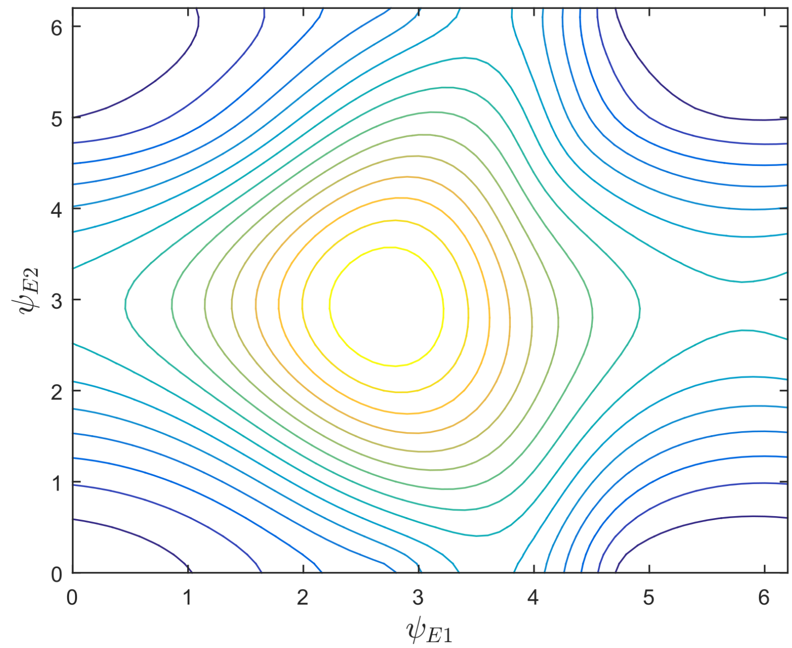

Figure 4.7: Contours of t_{C3} vs. (ψ_{E1}, ψ_{E2}).

Note that t_{cn} is always maximized for $\psi_{En} = \pi$. Thus, for a game with n evaders, the search space is $\mathbb{R}^{n-1}$. The optimal pursuit strategy requires calculating n_Capture(P,$\vec{E}$,$\vec{\psi}_E^*$) and traveling toward the capture points C_i in sequence.

For example, consider a game with three evaders where the pursuer is located at the origin and three evaders are located at $E_1 = (2, 0)$, $E_2 = (3, 3)$, and $E_3 = (0, 4)$, where $\gamma_1 = \gamma_2 = \gamma_3 = 2$. Figure 4.7 shows contours for the final capture time as a function of ψ_{E1} and ψ_{E2}. Notice that the maximum occurs at $(\psi_{E1}, \psi_{E2}) = (2.7303, 2.9189)$ and not at $(\psi_{E1}, \psi_{E2}) = (\pi, \pi)$. This can be seen in Figure 4.8, where solid lines represent the path of the pursuer, and dashed lines represent the paths of the evaders. The dominance boundaries $\mathcal{B}_{PE_1}$ and $\mathcal{B}_{PE_2}$ are plotted with dotted lines, but $\mathcal{B}_{EP_3}$ and the capture point C_3 are not shown in order to highlight P's interactions with E_1 and E_2. Note that E_1 and E_2 do not follow classical evasion with regard to points P and C_1, respectively. Instead, E_1 and E_2 sacrifice their own survival time in order to maximize the capture time of E_3.

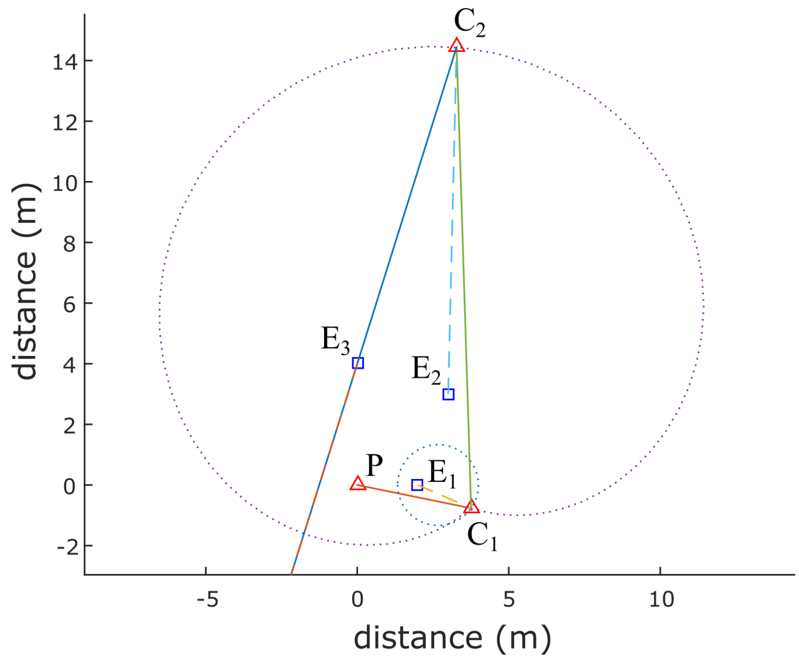

Figure 4.8: Trajectories for game with three evaders.

4.2.4 Capture Order

To calculate an upper bound on the minmax t_{cf}, the pursuer can evaluate the maximum capture time, t'_{cf}, for each capture order using Algorithm 3 and (4.34), then choose the order with the minimum t'_{cf}; i.e., if ζ represents the set of all potential capture sequences, then

$$t_{cf}^{ub} = \min_{\zeta} t'_{cf}(\zeta). \tag{4.35}$$

Figure 4.8 shows the best capture order using this method. However, if the capture order is not specified, then the evader headings calculated in (4.34) may not be optimal. The reason for this can be seen in Figure 4.8. The evasion heading for E_3 calculated with (4.34) for capture order $\{E_1, E_2, E_3\}$ causes E_3 to move toward the pursuer, and this leads to a change in the optimal capture order during the game. Figure 4.9 shows how the game plays out if all players iteratively compute their headings using Algorithm 3 and (4.34). This strategy will be referred to as the Iterative Static solution, because it considers only the current locations of the players, and not their locations at future times. As Figure 4.9 shows,

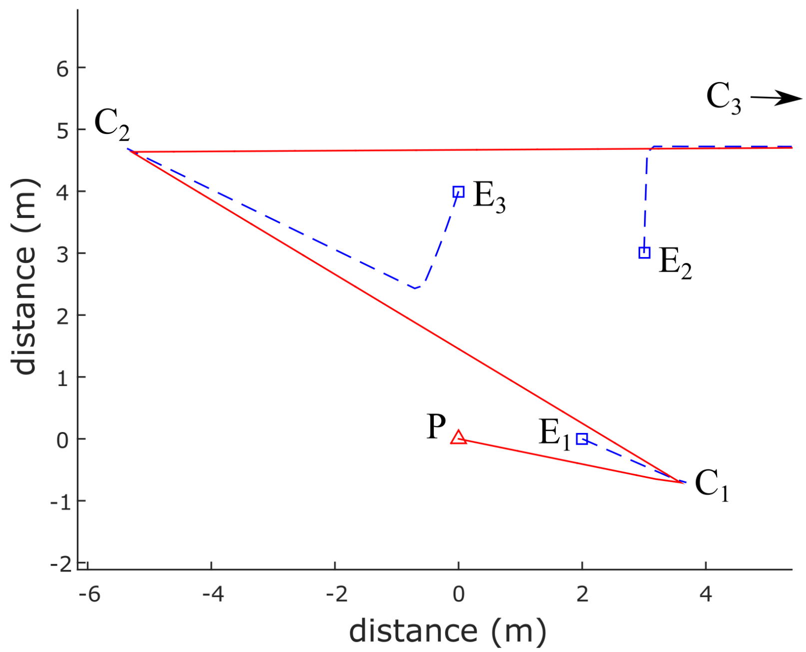

Figure 4.9: Trajectories for the iterative static solution.

the optimal capture order changes during the game, and this change occurs at the moment when E_2 and E_3 turn from their initial headings. Note that due to the non-infinitesimal step size in the numerical simulation, the moment when the two orders lead to equal capture times is passed over, and the capture order changes without the two alternatives ever being equal.

The Iterative Static strategy is suboptimal for the evaders because it leads to paths with turns. However, for P, following this strategy guarantees that no evasion strategy can lead to $t_{cf} > t_{cf}^{ub}$. As an example, consider the iterative static strategy shown in Figure 4.9 again. Figure 4.10 shows the progression of the upper bound as the players move. For comparison, it also shows how the upper bound changes if all the evaders follow a greedy strategy, where each follows a classical evasion strategy without regard for the other evaders. Even though the iterative static solution is not optimal for the evaders, cooperation still leads to better performance than the greedy strategy. The player trajectories for the greedy strategy are shown in Figure 4.11. Note that as expected, the remaining times to capture for both

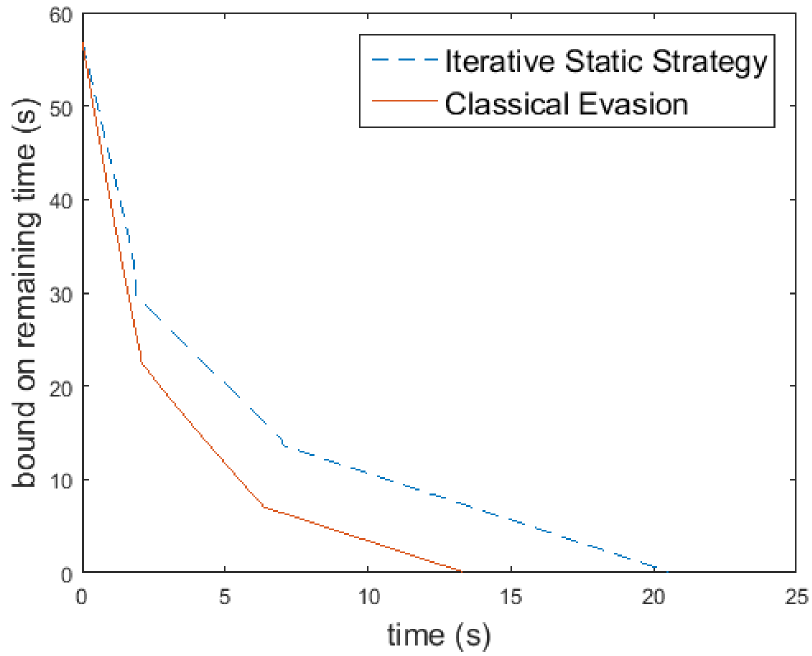

Figure 4.10: Bound on final capture time vs. time.

strategies are less than or equal to the bound throughout the game.

The optimal evasive headings must not be static solutions; i.e., they must consider future locations of the players. Furthermore, the optimal headings must avoid unnecessarily changing the optimal capture order (which can only benefit the pursuer).

Theorem 4.2.2 *For a SPME game with a free capture order, the singular surfaces consist of player locations where the maximization problem in* (4.34) *does not have a unique solution; i.e., they consist of points where two different capture orders give identical maximum values of t_{cf} for the same player locations. The optimal evasion strategy requires that the maximization in* (4.34) *be constrained such that the player trajectories do not cross these singular surfaces.*

Proof: Equation (4.35) selects the capture order that gives the minmax t_{cf}. Let this order be ζ^* with associated maxmin capture time t^*_{cf}, and let ζ_A be an arbitrary alternative capture order with maxmin capture time t^A_{cf}. If all evaders follow minimum time paths calculated

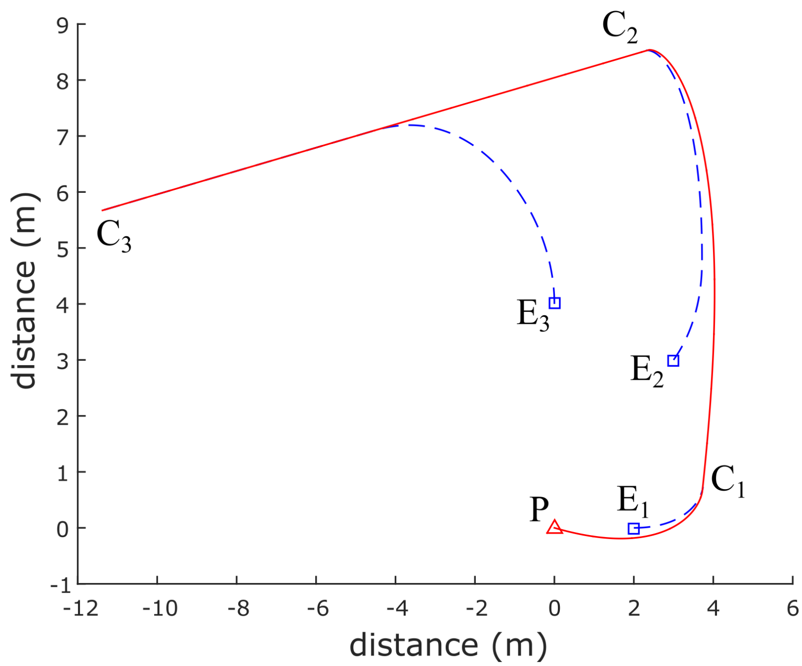

Figure 4.11: Trajectories using greedy classical evasion.

with (4.34) (i.e., no evaders purposely play suboptimally), then the only way for the pursuer's outcome to improve is for the minmax capture order to change. Since Algorithm 3 is a continuous function, by the intermediate value theorem, no $t_{cf}^{A} > t_{cf}^{*}$ can become less than t_{cf}^{*} without first being equal to it. $\square$

As an example, Figure 4.12 shows a configuration of three evaders where E_1 and E_2 are equidistant from the pursuer and E_3 is along the line that bisects the angle subtended by the radial lines from P to E_1 and E_2. In this configuration, if E_1 and E_2 have the same velocity, they can be exchanged in the capture order with no effect on t'_{cf}. Note that if E_3 is removed, in the two evader game, configurations with E_1 and E_2 equidistant from P and $v_{E1} = v_{E2}$ still lead to equivalent values of t'_{cf} for either capture order.

Figure 4.13 shows the scenario from Figure 4.9 with a circular arc centered at P at the moment when the capture order changes, which shows that at that time E_2 and E_3 are equidistant from P.

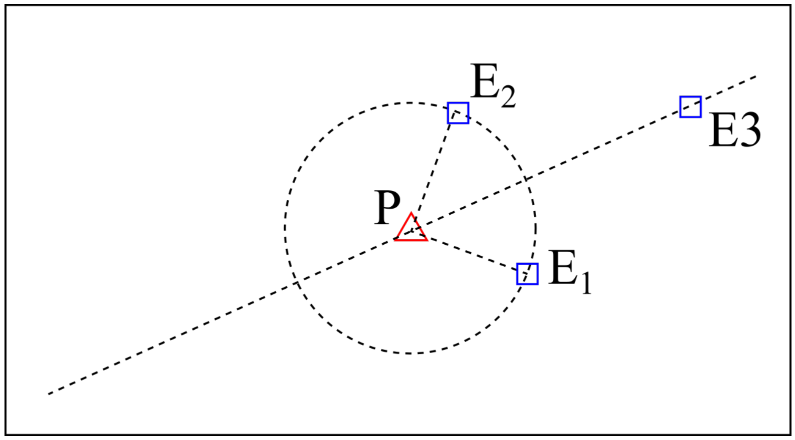

Figure 4.12: Singular arrangement in the SPME game.

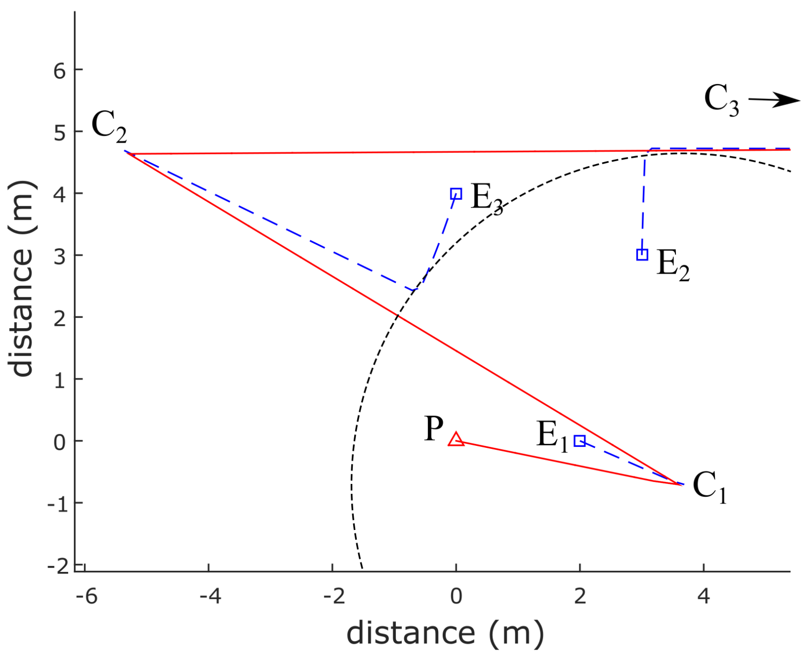

Figure 4.13: Iterative static solution with singular surface.

Further investigation of singular surfaces is left as future work. Once the singular surfaces are known, the determination of the evader headings for a particular capture order that maximize capture time while preserving capture order reduces to the maximization in (4.34), subject to the constraints imposed by singular surfaces.

The efficient determination of the optimal capture order is also left as future work. To address this problem, consider a fully connected directional graph where the nodes are:

$$\mathcal{N} = \{P, E_1, E_2, ..., E_n\}. \tag{4.36}$$

For simplicity of notation, let $E_0 = P$, and let each edge from $E_i,\ i \neq 0$ to E_0 have zero cost. Then the costs of the remaining edges from E_i to E_j are given by the times required for the pursuer to travel from C_i to C_j, which are dependent on the particular capture order selected. With this formulation, the problem of determining the optimal capture order is equivalent to the Sequence-Dependent Traveling Salesman Problem [76], which is a generalization of the standard Traveling Salesman Problem, and it is known to be NP-hard. Thus, efficient methods for determining capture order will likely be heuristic in nature.

4.3 Benefits and Future Work

There are a number of benefits to analyzing MPSE and SPME games through dominance. First, since MPSE and SPME games can be analyzed by decomposing the game into a set of SPSE games, all of the benefits from Chapter 3 apply as before. Namely, dominance regions can be used to analyze games with obstacles if the players move with simple motion. Second, it provides a method to analyze games with arbitrary numbers of players, and in some cases it is computationally simpler than other methods. For example, implementation of these methods does not require solving two-point boundary value problems. In the SPME game with specified capture order, where previous methods require the computation of maxmin saddle points, the proposed method only requires a maximization. Furthermore, an unspecified capture order can be incorporated by simply adding a constraint to the maximization. Finally, even though calculating the optimal capture order still scales poorly with the number of evaders, the method proposed in this dissertation is easily parallelizable, which increases the maximum number of evaders that can be considered in practice.

The final type of game that has not yet been considered in this chapter is the MPME game, which can be solved using the results of the MPSE and SPME games with one additional consideration. The analysis of the MPSE game provides the optimal capture point, C, for a group of pursuers against an evader. The analysis of the SPME game solves the scheduling problem, i.e., the problem of determining the order in which evaders should be pursued. The challenge of the MPME game is that in addition to solving optimal capture points and scheduling problems, the MPME game also requires an assignment problem, i.e., which pursuer or group of pursuers should pursue each evader or group of evaders. This is an interesting problem that is left as future work.

Including the MPME game, three key areas have been identified for future work in this chapter:

1 The study of singular surfaces in the SPME game. Figure 4.12 gives an example, but it is not exhaustive. As discussed in Theorem 4.2.2, once the singular surfaces are known, the determination of the evader headings that maximize capture time while perserving the capture order becomes a maximization problem subject to constraints.

2 The development of heuristics for determining the optimal capture order (which can be mapped to a sequence-dependent traveling salesman problem).

3 The MPME game, which can be analyzed using the same tools developed for the MPSE and SPME games. The primary challenge of the MPME game is that an additional assignment problem must be considered, i.e., which pursuer or group of pursuers should pursue each evader or group of evaders.

4.4 Summary

This chapter considers games with multiple pursuers and/or multiple evaders, and it provides solutions for the MPSE game, the P3 game, and the SPME game with time to final capture as the payoff. The complete solution is provided for SPME games with a specified capture order, and a solution is proposed for SPME games with free capture order. The solution with free capture order is based on the solution with specified capture order, but with the additional step of identifying singular surfaces which act as constraints during optimization. As in Chapter 3, the dominance regions provide all of the necessary information to solve these PE games.

CHAPTER 5

Games With Uncertainty

This chapter relaxes the assumption of full and perfect information that is imposed on the games in previous chapters. Specifically, it focuses on two types of uncertainty: uncertainty in the cost function and uncertainty in parameters and measurements.

This chapter builds upon the results of Chapters 3 and 4. Section 5.1 reconsiders the SPME game in the case where the cost function does not depend upon the final capture time, but instead upon the capture time of a particular, but unknown, evader. This evader is known as a Very Important Player (VIP), and the game is referred to as the VIP game. Then, Section 5.2 considers the sensitivity of the SPSE dominance regions to uncertainty in the parameters of the game. Section 5.2 also introduces the concept of probabilistic dominance, and it reconsiders the P3 game in the case where the predator's location is not perfectly known. Finally, Section 5.3 considers a limitation of the use of dominance regions, and it provides a scenario with very limited information where dominance regions are not able to solve the problem, but other methods are.

The primary contributions of this chapter are:

1 (5.3) and (5.4), which solve the VIP game;

2 (5.6), which gives the sensitivity of the dominance regions to perturbations in the game parameters;

3 (5.10) and (5.12), which give the probability of dominance for Gaussian uncertainty;

4 Section 5.3.4, which gives a pursuit law for scenarios with minimal information.

5.1 Uncertain Cost Functions

Consider a SPME game, where one of the evaders is a Very Important Player (VIP) that is more important than all others, and where the cost function depends only upon the capture time of the VIP. This game can be used to model scenarios where one vehicle in a fleet carries an important payload, and where the cost function depends only upon the fleet delivering the payload, not on the number of vehicles captured prior to delivery. One particular example of this game is in sports, like football, where one player carries the ball, and the cost function depends only upon the time when the ball carrier is tackled; tackling other players is irrelevant.

5.1.1 Problem Statement

Like the SPME game, the VIP game can be stated as the following two subproblems:

P5.1 **VIP game with specified capture order:** Given an evader, P, and n evaders, $E_i,\ i = 1, ..., n$, where the evaders are arranged in the order in which the pursuer must capture them; where a particular, but unknown, evader is the VIP and both teams share a known probability distribution, w, for the identity of the VIP; and given as payoff $t_{c,VIP}$, the capture time of the VIP; find $\vec{\psi}_E^*$, the heading for each evader that maximizes the minimum expected value of $t_{c,VIP}$.

P5.2 **VIP game with free capture order:** Given an evader, P, and n evaders, $E_i,\ i = 1, ..., n$; where a particular, but unknown, evader is the VIP and both teams share a known probability distribution, w, for the identity of the VIP; and given as payoff $t_{c,VIP}$, the capture time of the VIP; find $\vec{\psi}_E^*$, the heading for each evader that maximizes the minimum expected value of $t_{c,VIP}$, as well as the capture order, ζ^*, that minimizes the maxmin expected value of $t_{c,VIP}$.

The solution of P5.1 is similar to the SPME game. The true payoff function is:

$$J = t_{c,VIP}, \tag{5.1}$$

and the expectation of the value function is:

$$E[J] = \sum_{i=1}^{n} w_i t_{c,i}, \tag{5.2}$$

where w_i gives the probability that E_i is the VIP, and $\sum_{i=1}^{n} w_i = 1$. As in the SPME game from Section 4.2.3, the maxmin $E[J]$ for a particular capture order can be computed as an optimization of the function given in Algorithm 3:

$$\vec{\psi}_E^* = \arg\max_{\vec{\psi}_E} \sum_{i=1}^{n} w_i t_{c,i}, \tag{5.3}$$

where the capture times, $t_{c,i}$, are the outputs of Algorithm 3.

As in the SPME game with perfect information, if the capture order is free, then the $\vec{\psi}_E$ selected by (5.3) might lead to suboptimal evasion with a switch in the optimal capture order. However, as before, (5.3) still provides an upper bound for the minmax $E[J]$. One possible strategy for P is to utilize this bound, and choose the order with the smallest $\max\min E[J]$; i.e., if ζ represents the set of all potential capture sequences, then

$$E[J]^{ub} = \min_{\zeta} E[J(\zeta)]. \tag{5.4}$$

5.1.2 Example: Two evader VIP game

Figure 5.1 shows the capture times as a function of the probability that E_1 is the VIP for a two-evader game with $P = (0, 0)$, $E_1 = (3, 3)$, $E_2 = (0, 6)$, and $\gamma_1 = \gamma_2 = 2$. Figure 5.1a shows the capture times if E_1 is captured first, and Figure 5.1b shows the capture times if E_2 is captured first. In both subfigures, the capture time of E_1 is shown with a solid line, and the capture time of E_2 is shown with a dashed line. The evaders choose their headings using (5.3), and therefore as the probability that E_1 is the VIP increases to 1, the capture time of E_1 increases at the cost of an earlier capture for E_2. Similarly, as the probability that E_1 is the VIP decreases to 0, the capture time of E_2 increases at the cost of an earlier capture for E_1.

The payoff for each capture order as a function of w_1 is shown in Figure 5.2. Following (5.4), P should choose the order that minimizes the maxmin $E[J]$, and the expected values for the two capture orders intersect at approximately $w_1 = 0.37$. Therefore, for $0 \leq w_1 < 0.37$, the optimal capture order is $\{E_2, E_1\}$, and for $0.37 < w_1 \leq 1$, the optimal order is $\{E_1, E_2\}$.

The trajectories of the pursuer for this scenario can be seen in Figure 5.3, and trajectories are shown for four different values of w_1. The optimal capture of the first evader occurs at the sharp corner of each trajectory, but the capture locations of the second evader are not shown in order to emphasize the differences in the paths.

The solid lines represent the trajectories for $w_1 = 0$ and $w_1 = 1$, and as expected, if the VIP is known with certainty, then the optimal strategies are classical pursuit of the VIP and classical evasion without regard for the other evader. The dashed lines represent trajectories when w_1 is near the switching point $w_1 = 0.37$, and in both cases, the evaders choose to sacrifice the capture time of the first evader in order to increase the capture time of the second evader.

As in the SPME game, the calculation of this bound on the minmax $E[J]$ does not account for singular surfaces. Therefore, the solution is only valid if the maximization in (5.3) is subject to the constraint that the paths of the evaders never cross singular surfaces. Further investigation of these singular surfaces is again left as future work.

There are a number of interesting extensions to this problem that are also left as future work. For example, consider a game with incomplete information, where either the pursuer or the team of evaders knows the VIP with certainty, while the other team is only given a

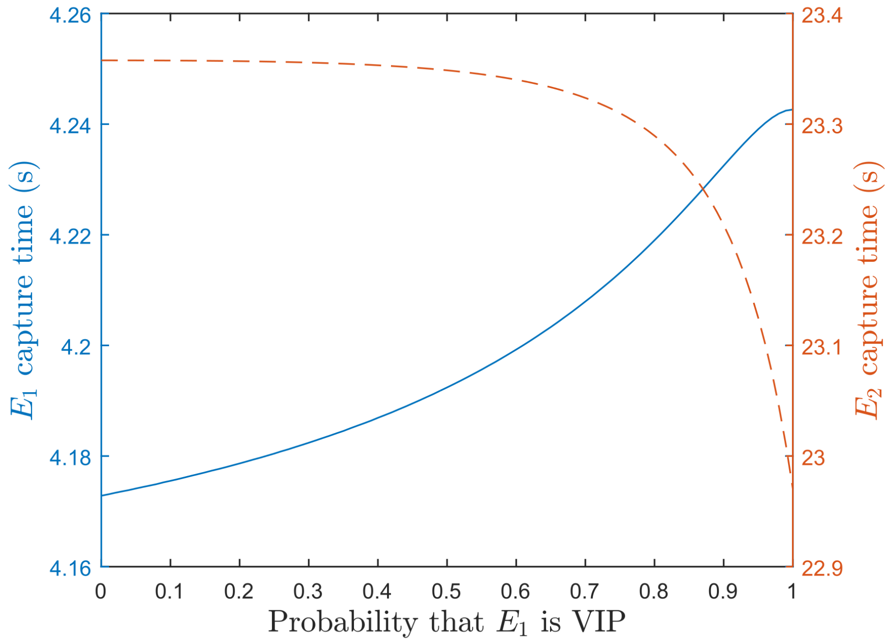

(a) Capture order: $\{E_1, E_2\}$

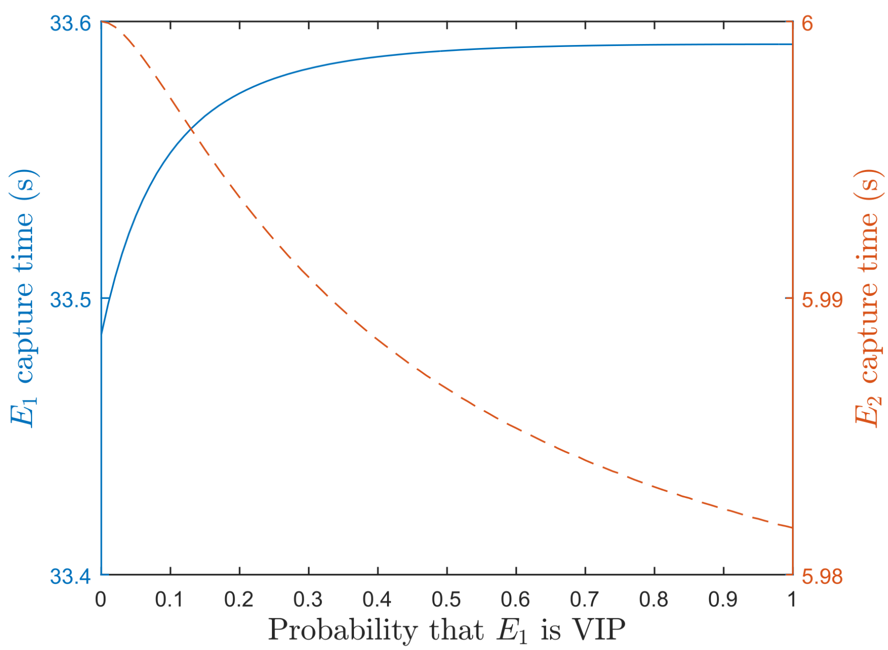

(b) Capture order: $\{E_2, E_1\}$

Figure 5.1: Capture times as a function of w_1.

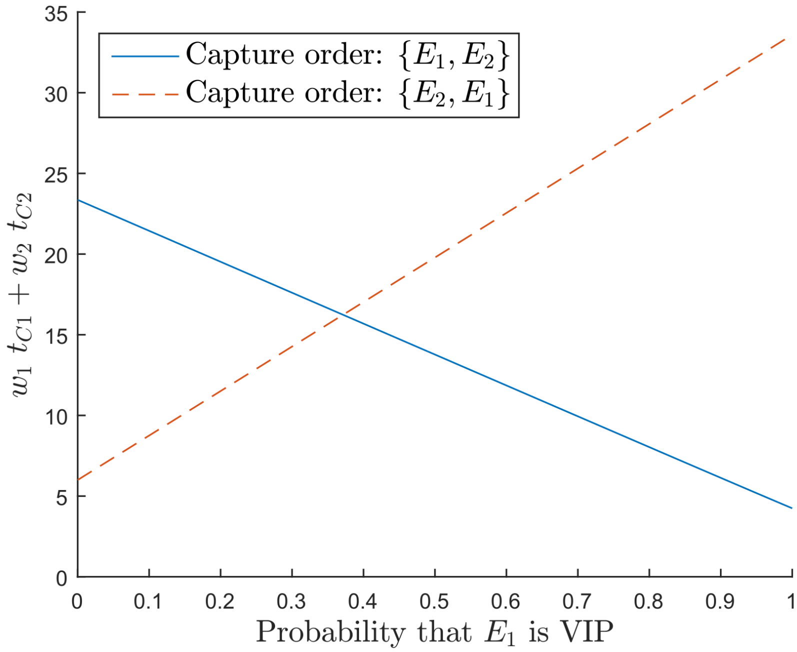

Figure 5.2: $E[J]$ as a function of w_1.

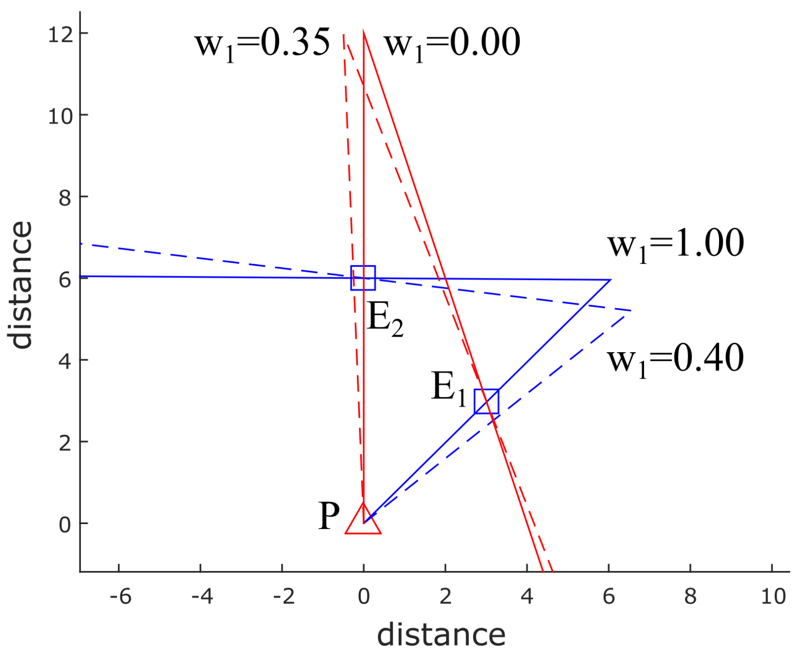

Figure 5.3: Trajectories for various values of w_1.

probability distribution that is known to both teams. Instead of the Nash equilibria considered in this work, the solution under incomplete information requires the identification of Bayes-Nash equilibria. Furthermore, a number of interesting questions are raised if both teams are given different probability distributions for the identity of the VIP, as well as a measure of confidence in their estimates. Namely, under what conditions do the following strategies give the best results?

1 Exploit known information; i.e., assume the given probability distribution is correct, and play optimally for that distribution.

2 Learn an opponent's probability distribution.

3 Influence an opponent's probability distribution (i.e., bluff).

4 Call an opponent's bluff and capitalize on their suboptimal play.

5.2 Uncertain Parameters & Measurements

This section considers PE games with uncertainty in parameters and measurements, including uncertainties in player speeds and locations as well as obstacle locations. Note that the results of this section extend the SPSE theory and result in probabilistic dominance regions, and since the other results in this dissertation are built upon SPSE games, the results of this section apply to the other games as well. As an example, this section considers a P3 game where the location of the predator is uncertain.

5.2.1 Problem Statement

P5.3 **Probabilistic dominance:** Given two players, A and B, with speeds v_A and v_B, respectively, and locations (x_A, y_A) and (x_B, y_B), where v_A, v_B, x_A, y_A, x_B and y_B are all random variables, and given an environment containing obstacles with parameters that are also random variables, determine a mapping $\mathcal{P}_{\mathcal{D}}$ which maps each point in the environment into the probability that player A dominates that point.

5.2.2 Probabilistic Dominance & Risk

As discussed in previous sections, dominance regions provide useful information about PE games, but in previous sections, they required perfect information about a player's opponent. However, with (3.15), the analysis of PE games through the construction of dominance regions allows for the application of existing techniques for handling uncertainty. As previously discussed, this is typically impractical with other PE solution methods, and it can therefore provide new insight into PE games.

This section discusses the sensitivity of the dominance boundary with respect to perturbations in the game parameters, and then it provides an expression for the probability of dominance in the presence of uncertainty. Finally, risk is introduced as a way to incorporate the probability of dominance into PE formulations.

5.2.2.1 Sensitivity of Dominance Regions to Parameters

The sensitivity of the dominance boundary with respect to perturbations in the game parameters is determined by solving (3.15) for r, and then calculating the partial derivatives with respect to each parameter. For simplicity of notation, let

$$c = \sqrt{\gamma^2 t_B^2 + d^2(\gamma^2 - \sin^2\theta) - 2d\gamma^2 t_b \cos\theta}. \tag{5.5}$$

Then the partial derivatives are as follows:

$$\frac{\partial r}{\partial \gamma} = \frac{-2\gamma}{(\gamma^2-1)^2}\left(\gamma^2 t_B - d\cos\theta \pm c\right) + \frac{\gamma}{\gamma^2-1}\left(2t_B \pm \frac{1}{c}\left(-2dt_B\cos\theta + d^2 + t_B^2\right)\right), \tag{5.6a}$$

$$\frac{\partial r}{\partial d} = \frac{1}{\gamma^2-1}\left(-\cos\theta \pm \frac{d(\gamma^2 - \sin^2\theta) - \gamma^2 t_B\cos\theta}{c}\right), \tag{5.6b}$$

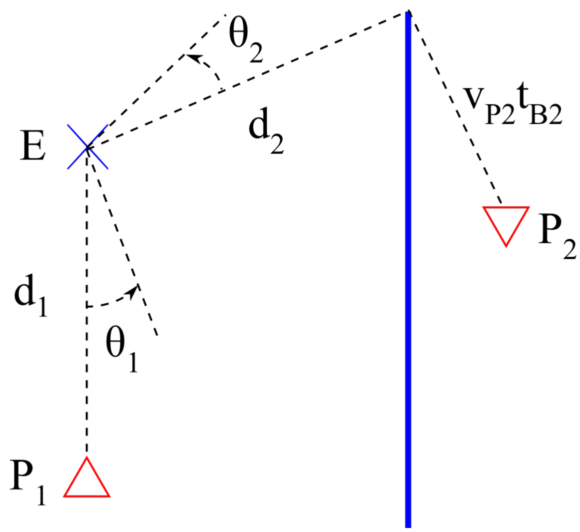

Figure 5.4: Dominance boundary variables.

$$\frac{\partial r}{\partial \theta} = \frac{d \sin\theta}{\gamma^2 - 1}\left(1 \pm \frac{\gamma^2 t_B - d\cos\theta}{c}\right), \tag{5.6c}$$

$$\frac{\partial r}{\partial t_B} = \frac{\gamma^2}{\gamma^2 - 1}\left(1 \pm \frac{t_B - d\cos\theta}{c}\right). \tag{5.6d}$$

Note that these sensitivities allow for the characterization of uncertainties in player parameters as well as the environment. Consider Figure 5.4, which shows two pursuers and their respective parameters in the presence of an obstacle. Sensitivity to d_1 and θ_1 characterize the sensitivity to perturbations in the location of P_1 relative to E. On the other hand, sensitivity to the location of P_2 is captured by the sensitivity to perturbations in t_{B2}, and perturbing P_2's location along a circle centered at the obstacle vertex produces no change in the dominance boundary. In this case, perturbations in d_2 and θ_2 characterize the sensitivity of the dominance boundary to perturbations in the measurements of the location of the obstacle vertex relative to E.

5.2.2.2 Dominance Regions Under Uncertainty

Equations (5.6a)-(5.6d) lead naturally to an analysis of the dominance boundary for PE games with uncertainty in the game parameters. Consider the vector, z, given by:

$$z = \begin{bmatrix} \gamma \\ d \\ \theta \\ t_B \end{bmatrix}. \tag{5.7}$$

Solving (3.15) for r and linearizing about the point z_0 gives

$$r(z) = r(z_0) + \left[\frac{\partial r}{\partial \gamma}\frac{\partial r}{\partial d}\frac{\partial r}{\partial \theta}\frac{\partial r}{\partial t_B}\right]\Bigg|_{z_0}(z - z_0). \tag{5.8}$$

Now assume that z is a Gaussian random vector with mean $\bar{z}$ as shown below and covariance Σ_z; that is,

$$\bar{z} = \begin{bmatrix} \bar{\gamma} \\ \bar{d} \\ \bar{\theta} \\ \bar{t}_B \end{bmatrix}, \tag{5.9}$$

where $\bar{\gamma}$, $\bar{d}$, $\bar{\theta}$, and $\bar{t}_B$ are the means of their respective random variables. The distance, r, of the dominance boundary from the origin is then a Gaussian random variable as well with mean and variance given by

$$\begin{aligned} \bar{r} &= r(\bar{z}), \\ \sigma_r^2 &= \left[\frac{\partial r}{\partial \gamma}\frac{\partial r}{\partial d}\frac{\partial r}{\partial \theta}\frac{\partial r}{\partial t_B}\right]\Bigg|_{\bar{z}} \Sigma_z \begin{bmatrix} \frac{\partial r}{\partial \gamma} \\ \frac{\partial r}{\partial d} \\ \frac{\partial r}{\partial \theta} \\ \frac{\partial r}{\partial t_B} \end{bmatrix}\Bigg|_{\bar{z}}. \end{aligned} \tag{5.10}$$

Figure 5.5 shows the probabilistic dominance boundary for the case when the covariance in z is given by

$$\Sigma_z = \begin{bmatrix} (0.05\gamma)^2 & 0 & 0 & 0 \\ 0 & (0.02d)^2 & 0 & 0 \\ 0 & 0 & (5^\circ)^2 & 0 \\ 0 & 0 & 0 & 0 \end{bmatrix}. \tag{5.11}$$

As before, the $\Box$ represents the evader, and the $\triangle$ represents the pursuer. The curve surrounding the pursuer represents the 3σ confidence interval of the distribution of the pursuer's initial location. As before, the dominance boundary mean is given by the Apollonius circle, and the dashed curves represent the 3σ confidence intervals of the distribution of the dominance boundary.

Finally, if $\bar{\gamma}, \bar{d}, \bar{t}_B$, and Σ_z are given, then the probability that the opponent dominates a point (r, θ) is given by the cumulative distribution function of a Gaussian and is easily computed:

$$\mathcal{P}_{\mathcal{D}}(r,\theta) = \frac{1}{\sigma_r\sqrt{2\pi}} \int_{-\infty}^{r} \exp\left[\frac{-(\omega-\bar{r})^2}{2\sigma_r^2}\right] \mathrm{d}\omega, \tag{5.12}$$

where $\bar{r} = \bar{r}(\theta)$ and $\sigma_r = \sigma_r(\theta)$.

Note that the dispersal surfaces and visibility surfaces must also be computed probabilistically, and the probabilistic dominance regions are then computed as the sum over all regions of the conditional probability of dominance given a particular region multiplied by the probability of being in that region:

$$\mathcal{P}_{\mathcal{D}} = \sum_i (\mathcal{P}_{\mathcal{D}}^i | \mathcal{R}^i) \Pr(\mathcal{R}^i). \tag{5.13}$$

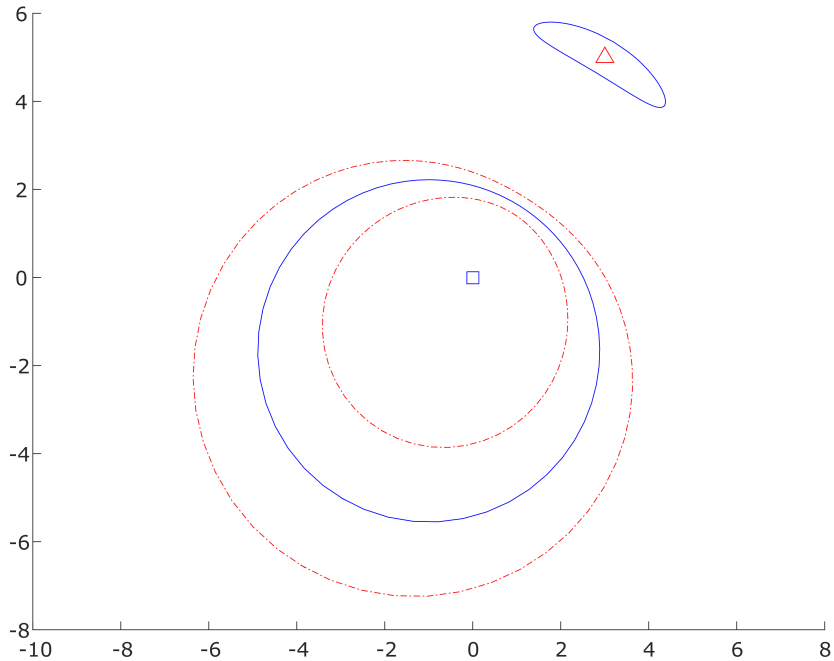

Figure 5.5: 3-σ dominance boundary.

5.2.2.3 Risk in PE Games

A typical PE game with two teams has a cost function of the form:

$$J = K(\vec{x}_f, t_f) + \int_0^{t_f} G(\vec{x}, u_B, u_R, t)\mathrm{d}t, \tag{5.14}$$

where $\vec{x} \in \mathbb{R}^{2\eta}$ contains the locations of all η players, t_f is the terminal time, and $\vec{x}_f = \vec{x}(t_f)$. One team controls the input vector u_B and attempts to maximize J, while the other team controls the input vector u_R and attempts to minimize J. The value of the game is

$$V(x) = \max_{u_B} \min_{u_R} J. \tag{5.15}$$

Consider a specific case of (5.14) where the cost function contains a risk function, with the risk f_r defined as follows:

$$f_r : \mathbb{R}^{2\eta} \to \mathbb{R}^+ : x \mapsto f_r(x). \tag{5.16}$$

The cost function then has the following form:

$$J = K(\vec{x}_f, t_f) + f_r(\vec{x}_f) + \int_0^{t_f} \Big(f_r(\vec{x}) + G(\vec{x}, u_B, u_R, t) \Big) \mathrm{d}t. \tag{5.17}$$

This risk could represent dangers or uncertainties in the environment, and in general it may not be known to all players. For example, consider the cooperative hunting of chimpanzees as described in [15]. Here, some chimpanzees are *drivers* and actively pursue the prey, some are *blockers* and take up positions to block the progression of the prey in a certain direction, and others are *ambushers* that hide and attempt to intercept the prey when it passes by. This can be modeled through an increased risk as the location of the evader approaches that of each chimpanzee, with the risk due to drivers and blockers being known to all players, but the risk due to ambushers being known only to the chimpanzees. Similarly, consider an anti-predator defense strategy where an adult prey attempts to draw a predator away from the prey's hidden offspring. Here, the risk increases as the predator gets closer to the offspring, and the prey attempts to minimize the risk, which is unknown to the predator.

In the following sections, risk at a point is proportional to the probability that an opponent dominates that point:

$$f_r \propto \mathcal{P}_{\mathcal{D}}. \tag{5.18}$$

5.2.3 Example PE Game with Risk

This section provides an example of a P3 game with probabilistic dominance as risk. This game was described in Section 4.1.4 along with the solution for the case with perfect information. Section 5.2.3.1 analyzes the game with uncertainty using the method developed in Section 5.2.2. Note that for simplicity, the environment does not contain obstacles in this example. However, as discussed in Section 5.2.2, (3.15) applies to the case with obstacles, and therefore this approach is applicable to games with obstacles as well.

5.2.3.1 P3 with Probabilistic Dominance as Terminal Risk

This section addresses the P3 game with uncertainty in the game parameters by using the probability that P dominates E at the rendezvous point as risk, and it solves an optimization problem to minimize the risk.

Consider the case with only a terminal cost. This gives

$$J = K(\vec{x}_f, t_f) + f_r(\vec{x}_f). \tag{5.19}$$

In Section 4.1.4.4, the components of the cost were:

$$K = t_f, \quad f_r \propto \begin{cases} 0 & \vec{x}_f \in \mathcal{D}_{E/P}, \\ 1 & otherwise. \end{cases} \tag{5.20}$$

In this section, let

$$f_r = \mathcal{P}_{\mathcal{D}}. \tag{5.21}$$

First, let $K = 0$; i.e., the only cost is risk at the rendezvous point. If P acts optimally, then R can only rescue E if they rendezvous at a point where they dominate P. Thus, they maximize their probability of winning the game regardless of P's actions if they minimize the probability that P dominates their rendezvous point. Therefore, the problem becomes:

$$\begin{gathered} \min_{r,\theta} \mathcal{P}_{\mathcal{D}}(r, \theta), \\ \text{subject to } \; Q(r, \theta + \theta_P) = 0, \end{gathered} \tag{5.22}$$

where $\mathcal{P}_{\mathcal{D}}(r, \theta)$ is calculated using (3.15), (5.10), and (5.12) with P's parameters; i.e., $\gamma = \gamma_P,\ d = d_P,\ t_{BP} = 0$, and $\theta = 0$ along the initial line of sight from E to P. The constraint, $Q(r, \theta + \theta_P)$, is the left-hand side of (3.15) with R's parameters; i.e., with $\gamma = \gamma_R,\ d = d_R,\ t_{BR} = 0$, and θ_P equal to the initial angle between E's lines of sight to R and P.

The KKT conditions [55] hold everywhere along $Q(r, \theta + \theta_P) = 0$, so the necessary condition for optimality is

$$\nabla \mathcal{P}_{\mathcal{D}} + \lambda \nabla Q = 0, \tag{5.23}$$

where λ is a Lagrange multiplier; i.e., the minimum risk occurs at a point where $\nabla \mathcal{P}_{\mathcal{D}}$ is parallel to the gradient of the constraint $\mathcal{B}_{ER}$. This can be seen in Figure 5.6b, which shows a P3 game where P has the same characteristics as those in Figure 5.5, and R has the same characteristics as the perfect information case in Figure 4.5, which is reproduced in Figure 5.6a for comparison. The dashed curves represent level curves of f_r. The solid circle represents $\mathcal{B}_{ER}$, and the straight line segments show the optimal paths to minimize the risk of P capturing E.

Finally, consider the tradeoff between minimizing the risk that P dominates and minimizing the time to rendezvous. This tradeoff is captured in the following weighted cost function where $K(\vec{x}_f, t_f) \propto t_f$ and $f_r(\vec{x}_f) \propto \mathcal{P}_{\mathcal{D}}(\vec{x}_f)$, and where w_t and w_r weigh the terminal time against the risk, respectively:

$$J = w_t t_f + w_r f_r(\vec{x}_f). \tag{5.24}$$

Varying the weights causes the optimal rendezvous point to move along $\mathcal{B}_{ER}$ between the solutions shown in Figures 5.6a and 5.6b.

5.3 Maximal Uncertainty: A Limitation of Dominance

Consider a SPSE game with even less information than in Section 5.2, where the position of the evader is only available as a uniform distribution over a half-space. This is the case if the only available measurement is $\mathrm{sgn}(\dot{\delta})$, the sign of the rate of change of the range between P and E, and these scenarios can occur for low cost autonomous vehicles. For example, consider a vehicle that measures only the strength of a received signal with an om-

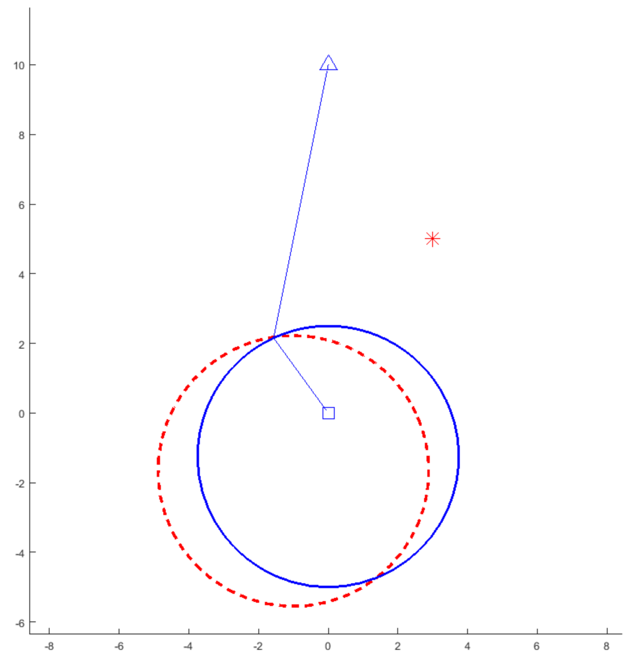

(a) P3 Game With Perfect Information

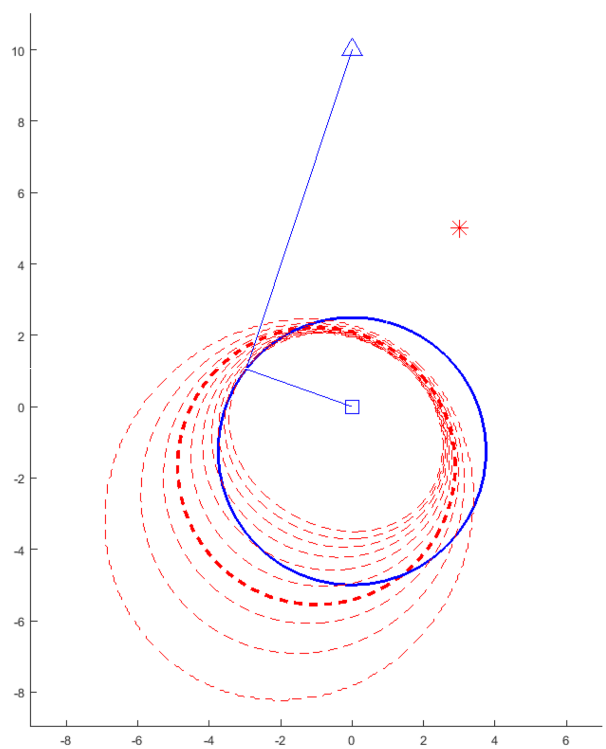

(b) P3 Game With Minimum Terminal Risk

Figure 5.6: P3 game: Effect of uncertainty in the predator's location.

nidirectional receiver, where the transmitted signal strength is unknown or the receiver is uncalibrated such that received signal strength does not map directly to range. In this case, range cannot be determined, but consecutive measurements can be compared to determine whether the range is increasing or decreasing. Here, due to the nature of the available information, dominance regions do not provide enough meaningful information to construct a pursuit strategy. However, [83] shows that this measurement is sufficient to asymptotically capture an evader. As [83] shows, the use of $\operatorname{sgn}(\dot{\delta})$ alone can lead to poor performance, but performance can be improved if P also measures ψ_P.

5.3.1 Problem Statement

The problem can be stated as follows:

P5.4 **Pursuit with minimal information:** Given a pursuer, P, with heading ψ_P, speed input v_P, and heading rate input u_ψ; and given a stationary target, E, where δ is the distance between P and E, and β is the line of sight angle from P to E; and also given, $\mu(t) = \operatorname{sgn}(\dot{\delta}(t))$; find a pursuit law $u_\psi(\psi_P, \mu)$ and $v_P(\psi_P, \mu)$ such that P asymptotically achieves point-capture of E.

5.3.2 System Model

Let P move with simple motion in the plane; i.e., do not account for inertia, and assume that $\dot{\psi}_P$ is unbounded. For simplicity, assume that the origin is fixed to P.

The polar form of the state and input vectors are

$$\vec{x}_\pi = \begin{pmatrix} \delta \\ \beta \\ \psi_P \end{pmatrix}, \quad \vec{u} = \begin{pmatrix} v_P \\ u_\psi \end{pmatrix}. \tag{5.25}$$

The dynamics are given by:

$$\begin{pmatrix} \dot{\delta} \\ \dot{\beta} \\ \dot{\psi}_v \end{pmatrix} = \begin{pmatrix} -v_P \cos(\beta - \psi_P) \\ \frac{v_P}{\delta} \sin(\beta - \psi_P) \\ u_\psi \end{pmatrix}, \tag{5.26}$$

and the system outputs are:

$$\vec{y}_\pi = \begin{pmatrix} \psi_v \\ \operatorname{sgn}(\dot{\delta}) \end{pmatrix}. \tag{5.27}$$

Additionally, some calculations utilize Cartesian coordinates. For this representation, the state of the system is:

$$\vec{x}_c = \begin{pmatrix} x_E \\ y_E \\ \psi_P \end{pmatrix}. \tag{5.28}$$

The system dynamics in the Cartesian model are given by:

$$\begin{pmatrix} \dot{x_E} \\ \dot{y_E} \\ \dot{\psi_P} \end{pmatrix} = \begin{pmatrix} -v_P \cos(\psi_P) \\ -v_P \sin(\psi_P) \\ u_\psi \end{pmatrix} = f_c(\vec{x}_c, \vec{u}, t). \tag{5.29}$$

Finally, the outputs are:

$$\vec{y}_c = \begin{pmatrix} \psi_P \\ \operatorname{sgn}\left(\frac{-v_P(x_E \cos(\psi_P) + y_E \sin(\psi_P))}{\sqrt{x_E^2 + y_E^2}} \right) \end{pmatrix}. \tag{5.30}$$

5.3.2.1 Nonlinear Separation Conditions

Reference [110] gives the following conditions that allow the use of an observer in nonlinear systems of the form

$$\begin{aligned} \dot{x}(t) &= f(t, x(t), u(t)), \\ y(t) &= g(t, x(t)). \end{aligned} \tag{5.31}$$

The following assumptions are made:

Assumption 1) f is continuously differentiable and vanishes when all of its arguments except t vanish. Additionally, there are constants a and c such that:

$$\begin{aligned} \|\nabla_x f(t, x, u)\| &\leq a, \\ \|\nabla_u f(t, x, u)\| &\leq a, \\ \forall t \geq 0, \forall x \in B_c, \forall u \in B_c, B_c &= w \in \Re : \|w\| \leq c. \end{aligned} \tag{5.32}$$

Assumption 2) g is continuous, and $g(0, 0) = 0$.

If the system satisfies the two assumptions, and if it is stabilizable and weakly detectable, then $x = 0,\ z = 0$ is a uniformly asymptotically stable equilibrium point of the following system:

$$\begin{aligned} \dot{x}(t) &= f(t, x(t), \eta(t, z(t))), \\ \dot{z}(t) &= \gamma(t, z(t), g(t, x(t)), \eta(t, z(t))). \end{aligned} \tag{5.33}$$

Another way of expressing this is to say that if the system is stabilized by the control law

$$u(t) = \eta(t, x(t)), \tag{5.34}$$

then it is also stabilized by the control law

$$u(t) = \eta(t, z(t)), \tag{5.35}$$

where $z(t)$ is the output of a weak detector for $x(t)$. The reader is referred to [110] for a definition and examples of weak detectability. This result requires no other assumptions such as linearity or time-invariance.

5.3.2.2 Modifications of Model

For the system dynamics in Cartesian form,

$$\nabla_{\vec{x}_c} f_c = \begin{pmatrix} 0 & 0 & v_P \sin(\psi_P) \\ 0 & 0 & -v_P \cos(\psi_P) \\ 0 & 0 & 0 \end{pmatrix}. \tag{5.36}$$

Therefore, if $\vec{x}_c$ and $\vec{u}$ are confined to a sphere of any finite size, $\|\nabla_{\vec{x}_c} f_c\|$ is bounded. Furthermore, $\|\nabla_{\vec{u}} f_c\|$ is also bounded because

$$\nabla_{\vec{u}} f_c = \begin{pmatrix} -\cos(\psi_P) & 0 \\ -\sin(\psi_P) & 0 \\ 0 & 1 \end{pmatrix}. \tag{5.37}$$

Since f_c is continuously differentiable and $f_c(0, 0, t) = 0$, all of the conditions given in the first assumption hold.

The system's first output, ψ_P, fulfills the requirements of the second assumption. The second output, μ, does not, but an alternative can be found that meets the assumption and is approximately equal to μ for all states except $x_E = y_E = 0$ where μ is undefined. Note that at $x_E = y_E = 0$, capture has been achieved.

From Eqn. (5.30):

$$\mu = \operatorname{sgn}\left(\frac{-v_P(x_E \cos(\psi_P) + y_E \sin(\psi_P))}{\sqrt{x_E^2 + y_E^2}} \right), \tag{5.38}$$

which is a function of both $\vec{x}_c(t)$ and $\vec{u}(t)$. The second assumption requires the function to be dependent on only the system state and time. If v_P is restricted to be non-negative, multiplying by its value does not affect the sign of the output, and it can therefore be dropped from the calculation without changing the system. Similarly, the denominator is non-negative, so it can also be dropped with the only loss of equality occurring at $x_E = y_E = 0$ when capture occurs.

$$\mu = \mathrm{sgn}(-x_E \cos(\psi_P) - y_E \sin(\psi_P)). \tag{5.39}$$

This function is equal to the original at all points except $x_E = y_E = 0$, and it vanishes when all of its arguments vanish, as required by the second assumption. The only remaining stipulation is that the function must be continuous. To accomplish this, a small ϵ is chosen, and μ is approximated by the following function:

$$\mu \approx \frac{-x_E \cos(\psi_P) - y_E \sin(\psi_P)}{\sqrt{(-x_E \cos(\psi_P) - y_E \sin(\psi_P))^2 + \epsilon^2}}. \tag{5.40}$$

This approximation is equal to the original function for $\epsilon = 0$ and $x_E,\ y_E$ not both zero. It represents a smoothing of the function with increasingly sharper corners as ϵ shrinks to zero. Its value is equal to zero for $x_E = y_E = 0$.

This approximation gives an output dependent only upon the system state and time that is continuous for all states, $\vec{x}_c$, and equal to zero for $\vec{x}_c = 0$ at $t = 0$. This fulfills all requirements of the second assumption, which implies that uniform asymptotic stability of the equilibrium is achieved if the output of a weak detector is used in place of the actual state as an input to a stabilizing controller.

5.3.3 Separated Problem Statement

Problem P5.4 can therefore be divided into the following subproblems:

P5.5 **Controller:** Given a pursuer with a known heading angle ψ_P, and a target with a known location (δ, β), find a guidance law, i.e., a velocity function $v_P(t)$ and a turn-rate function $u_\psi(t)$ such that P reaches E.

P5.6 **Detector:** Given μ, the sign of the P's range-rate to the target, and ψ_P, the pursuer's heading, find an estimate of the location of E, $(\hat{\delta}, \hat{\beta})$, such that the controller found in P5.5 is able to stabilize the system.

5.3.3.1 Controller

First, a stabilizing controller is designed as if complete state information was available. Then, this stabilizing control law is applied to an estimate of the state which is produced by an observer that is discussed in Section 5.3.3.2. A solution with a constant forward velocity v_P is assumed in order to simplify the problem.

The controller is developed with the polar form of the system dynamics, and the control strategy is based on two sliding surfaces. The first control surface is chosen to be the difference between the current and desired values of δ,

$$S_1 = \delta - \delta_{des}, \tag{5.41}$$

with the following desired dynamics:

$$\dot{S}_1 = -\lambda_{S1} S_1. \tag{5.42}$$

These dynamics guarantee that S_1 decays to zero exponentially, at a rate given by $\lambda_{S1} > 0$, which is a design parameter.

Substituting (5.41) into (5.42) and taking the derivative of (5.41) gives:

$$\dot{\delta} - \dot{\delta}_{des} = -\lambda_{S1}(\delta - \delta_{des}). \tag{5.43}$$

Substituting the system dynamics for $\dot{\delta}$ from (5.26) into (5.43) gives:

$$-v_P \cos(\beta - \psi_P) - \dot{\delta}_{des} = -\lambda_{S1}(\delta - \delta_{des}).$$

If a desired ψ_P could be chosen, it would be selected such that:

$$\beta - \psi_{P,des} = \arccos\left(\frac{\lambda_{S1}(\delta - \delta_{des}) - \dot{\delta}_{des}}{v_P}\right). \tag{5.44}$$

For simplicity of calculations, define:

$$\alpha_\psi = \beta - \psi_P, \qquad \alpha_{\psi,des} = \beta - \psi_{P,des}.$$

Then, the second sliding surface is:

$$S_2 = \alpha_\psi - \alpha_{\psi,des}, \tag{5.45}$$

with the following desired dynamics:

$$\dot{S}_2 = -\lambda_{S2} S_2, \quad \lambda_{S2} > 0. \tag{5.46}$$

Again, substituting (5.45) into (5.46) and taking the derivative of (5.45) gives:

$$\dot{\alpha}_\psi - \dot{\alpha}_{\psi,des} = -\lambda_{S2}(\alpha_\psi - \alpha_{\psi,des}).$$

Substituting the system dynamics for $\dot{\beta}$ and $\dot{\psi_P}$ from (5.26) into $\dot{\alpha}_\psi$ gives:

$$\frac{v_P}{\delta} \sin(\beta - \psi_P) - u_\psi - \dot{\alpha}_{\psi,des} = -\lambda_{S2}(\alpha_\psi - \alpha_{\psi,des}).$$

The control input, u_ψ, is therefore

$$u_\psi = \lambda_{S2}(\alpha_\psi - \alpha_{\psi,des}) + \frac{v_P}{\delta}\sin(\beta - \psi_P) - \dot{\alpha}_{\psi,des}. \tag{5.47}$$

5.3.3.2 Observer

The model assumes perfect knowledge of the heading angle, ψ_P, so the next goal is to develop an observer that estimates x_E and y_E, the Cartesian coordinates of E. An estimate of the sensor output is calculated from (5.40):

$$\hat{\mu} = \frac{-\hat{x}_E\cos(\psi_P) - \hat{y}_E\sin(\psi_P)}{\sqrt{(-\hat{x}_E\cos(\psi_P) - \hat{y}_E\sin(\psi_P))^2 + \epsilon^2}}. \tag{5.48}$$

The error in the estimate of μ is

$$\tilde{\mu} = \mu - \hat{\mu}. \tag{5.49}$$

The observer is constructed with the following form:

$$\dot{\hat{x}}_c = \begin{pmatrix} \dot{\hat{x}}_E \\ \dot{\hat{y}}_E \\ \dot{\psi}_P \end{pmatrix} = \begin{pmatrix} -v_P\cos(\psi_P)(k_1\mu + k_2\tilde{\mu}) \\ -v_P\sin(\psi_P)(k_3\mu + k_4\tilde{\mu}) \\ u_\psi \end{pmatrix}, \tag{5.50}$$
$$k_1,\ k_2,\ k_3,\ k_4 > 0.$$

The estimation error is:

$$\tilde{x}_c = \vec{x}_c - \hat{x}_c = \begin{pmatrix} \tilde{x}_E \\ \tilde{y}_E \\ 0 \end{pmatrix} = \begin{pmatrix} x_E - \hat{x}_E \\ y_E - \hat{y}_E \\ 0 \end{pmatrix}.$$

Finally, the dynamics of the error are:

$$\dot{\tilde{x}}_c = \dot{\vec{x}}_c - \dot{\hat{x}}_c = \begin{pmatrix} -v_P \cos(\psi_P)(1 - k_1\mu - k_2\tilde{\mu}) \\ -v_P \sin(\psi_P)(1 - k_3\mu - k_4\tilde{\mu}) \\ 0 \end{pmatrix}. \tag{5.51}$$

The result in Section 5.3.2.1 only requires weak detectability, and [83] provides gains such that the error dynamics given by (5.51) fulfill this requirement.

5.3.4 Pursuit Law Summary

The pursuit law consists of the following, where the controller gains, $\lambda_{S1}, \lambda_{S2} > 0$, and the observer gain, $k_2 > 0$, are design parameters:

1 Known pursuer heading angle, ψ_P, and measurement of $\mu = \text{sgn}(\dot{\delta})$;

2 Constant velocity input, v_P;

3 Estimated coordinates of E, $(\hat{x}_E, \hat{y}_E)$, with dynamics given by (5.50) and with $k_1 = k_3 = 1$ and $k_4 = k_2$:

$$\begin{pmatrix} \dot{\hat{x}}_E \\ \dot{\hat{y}}_E \end{pmatrix} = \begin{pmatrix} -v_P \cos(\psi_P)(\mu + k_2\tilde{\mu}) \\ -v_P \sin(\psi_P)(\mu + k_2\tilde{\mu}) \end{pmatrix},$$

where $\tilde{\mu}$ is given by (5.48) and (5.49);

4 Turn-rate given by (5.47), but using the estimate of E's location, $(\hat{\delta}, \hat{\beta})$:

$$u_\psi = \lambda_{S2}(\hat{\beta} - \psi_P - \hat{\alpha}_{\psi,des}) + \frac{v_P}{\hat{\delta}} \sin(\hat{\beta} - \psi_P) - \dot{\hat{\alpha}}_{\psi,des}.$$

From (5.44):

$$\hat{\alpha}_{\psi,des} = \arccos\left(\frac{\lambda_{S1}(\hat{\delta} - \hat{\delta}_{des}) - \dot{\hat{\delta}}_{des}}{v_P}\right).$$

Ideally, P moves directly toward E, but choose $\dot{\delta}_{des} = -v_P(1 - \epsilon_2)$ to avoid singularities when taking the derivative of $\hat{\alpha}_{des}$. Finally, $\hat{\delta}_{des}$ is calculated from (5.43) with the estimated range:

$$\hat{\delta}_{des} = \hat{\delta} + \frac{\dot{\hat{\delta}} - \dot{\delta}_{des}}{\lambda_{S1}}.$$

5.3.5 Simulation Results

This section provides simulation results for the pursuit law described in Section 5.3.4. Results are presented for both stationary and moving targets.

References [81] and [83] discuss the pursuit law's response to measurement corruption and observer gains, and they provide guidelines for selecting these quantities that lead to more desirable trajectories. Reference [83] also discusses the response to initial estimates, and certain estimates are shown to produce undesirable behavior. To overcome this, [83] provides an exploration method that improves the initial estimate without incurring significant performance costs.

Stationary targets Figure 5.7a shows an overhead view of P's trajectory for a variety of starting locations and initial estimates. Each $\triangle$ with its corresponding trajectory represents a separate simulation, and the "X" to the right of each $\triangle$ represents its initial estimate of E's location. The $\square$ at the center of the figure represents E. As the figure shows, P is able to successfully reach E in all simulations.

Figure 5.7b shows the errors in the estimates $\hat{x}_E$ and $\hat{y}_E$ over time for each of the simulations depicted in Figure 5.7a.

Moving targets This pursuit law is also successful when E moves. Figure 5.8 shows an overhead view of the trajectory of P when it is pursuing a moving target. As before, $\triangle$ represents P's starting location, and the "X" represents the initial estimate of E's location. The actual locations of E at different points in time are shown by the circles. E moves

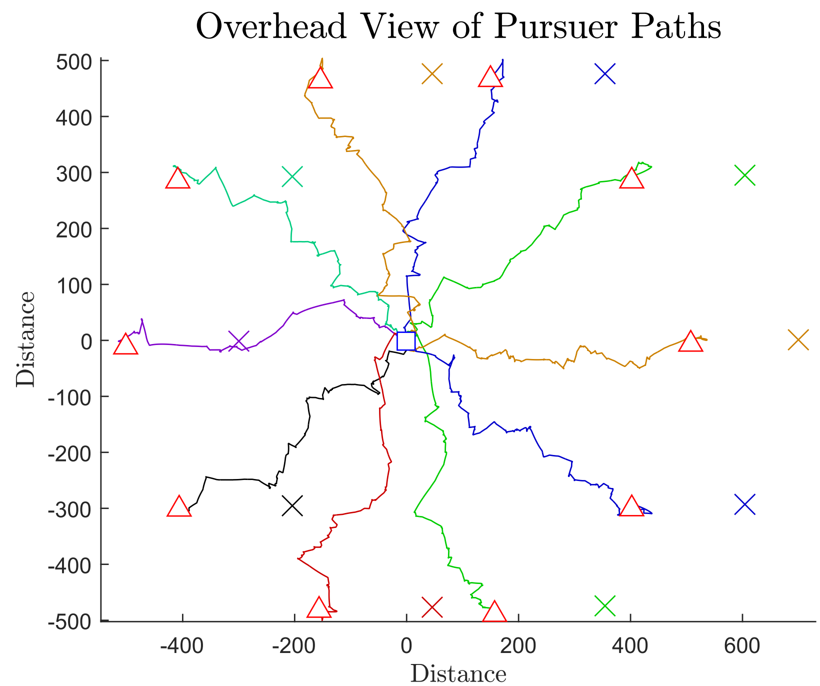

(a) Trajectories

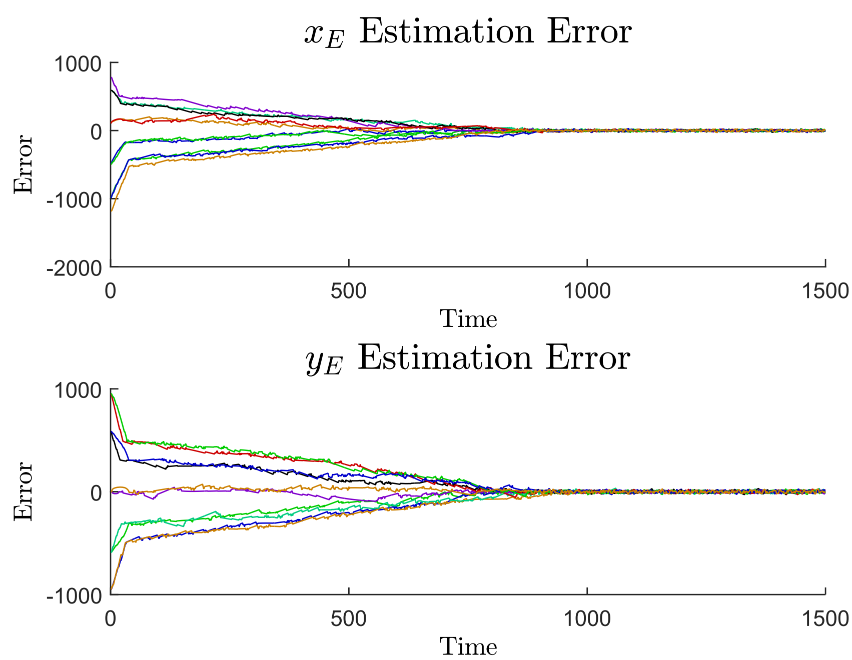

(b) Estimation Error

Figure 5.7: Stationary target.

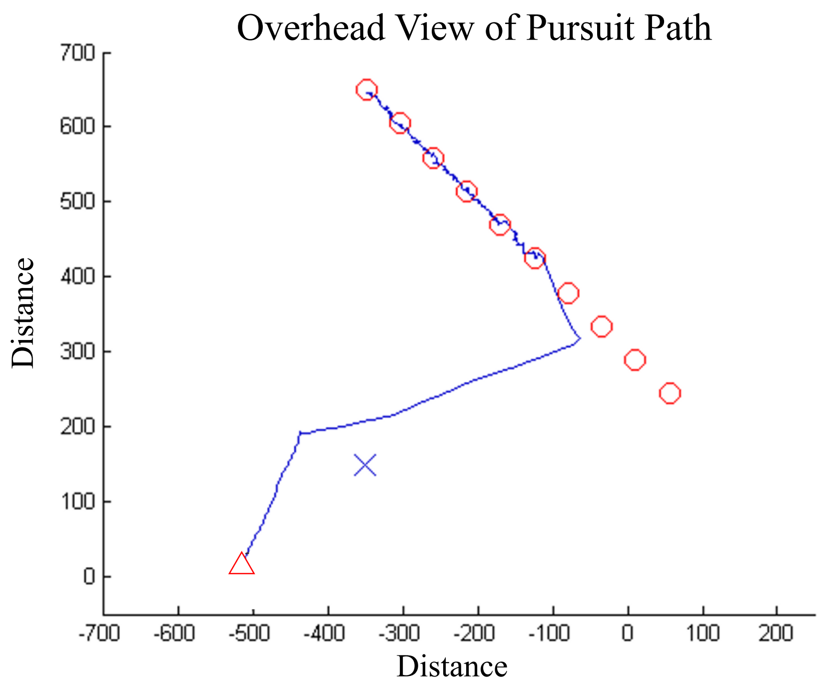

Figure 5.8: Moving target.

linearly with constant speed from lower right to upper left.

5.3.6 Further Restrictions On Available Information

Reference [83] provides additional analysis of problem P5.4, and it shows that of the two measurements, $\operatorname{sgn}(\dot{\delta})$ and ψ_P, the fundamental measurement is $\operatorname{sgn}(\dot{\delta})$. That is, measurements of $\operatorname{sgn}(\dot{\delta})$ alone are sufficient to asymptotically capture an evader, even when ψ_P is unknown; $\operatorname{sgn}(\dot{\delta})$ is also necessary, and pursuit with ψ_P alone fails. Reference [83] provides a pursuit law utilizing only measurements of $\operatorname{sgn}(\dot{\delta})$ that successfully achieves asymptotic capture, and this result holds not only for evaders moving with constant heading, as in Section 5.3.5, but against an adversarial E utilizing classical evasion as well.

Finally, [6] shows that the pursuit law provided in Section 5.3.4 is not only applicable when $\operatorname{sgn}(\dot{\delta})$ is received continuously, but that it can also be modified for scenarios where P only receives measurements when located at certain quantized distances from E. This makes the pursuit law implementable on a number of low cost autonomous vehicles through the use of their communication radios with no additional hardware requirements.

5.4 Summary

This chapter solves PE games in the presence of uncertainty, and it considers the effect of information on optimal behaviors in PE games through three scenarios. The first involves a SPME game where the cost function is the capture time of a particular, but unknown, evader. The second involves a SPSE game where the game parameters and measurements are uncertain, and it introduces the concept of probabilistic dominance. Through the results of Chapter 4, this result is not only applicable to SPSE games, but MPSE and SPME games as well, and an example is provided of a P3 game with uncertainty in the location of the predator. Finally, the third scenario involves very limited information, and it highlights a limitation of dominance regions.

CHAPTER 6

Conclusions

As autonomous and semi-autonomous vehicles become more widespread, it is important that their designers relax *a priori* assumptions of strictly benign environments. Real environments are sometimes hostile and often unpredictable, and adversarial games provide a way to increase safety and effectiveness when operating in these environments. This dissertation studies a particular class of adversarial games involving pursuit and evasion, and it expands the method of dominance regions to provide solutions for games with obstacles, uncertainty, and cooperation among heterogeneous teams.

6.1 Summary

This dissertation treats a number of pursuit-evasion games, including games between a single pursuer and a single evader, games with additional pursuers and evaders, and games with uncertainty. In Chapter 1, the work is motivated and a general problem statement is provided. Chapter 2 surveys the existing literature and introduces the classical techniques used to solve pursuit-evasion games. The main body of the dissertation is divided into three chapters which build upon each other to solve increasingly complex games.

Chapter 3 analyzes games between a single pursuer and a single evader for two cases: where the players both move with simple motion and where one player moves with simple motion while the other has a constrained minimum turn radius. The dominance regions are determined for both scenarios, and these dominance regions are shown to be generalizations of the Apollonius circle. This method is shown to agree with existing solutions, and then it is utilized to solve games in the presence of polygonal obstacles.

Chapter 4 builds upon the results provided in Chapter 3 by showing that both the multiple pursuer, single evader game and the single pursuer, multiple evader game can be decomposed into a set of single pursuer, single evader games. It also introduces the Prey, Protector, and Predator game which features competing teams of pursuers.

Chapters 3 and 4 both assume the availability of full and perfect information. Chapter 5 relaxes this assumption and studies pursuit-evasion games with uncertainty in the game parameters, the measurements of the positions of players and obstacles, and the cost function. The sensitivity of solutions to changes in the available information is studied, and probabilistic dominance regions are introduced. In addition, two games from Chapter 4 are reconsidered in the presence of uncertain information, and the effect of the reduction in information is studied. Finally, Chapter 5 considers a scenario with very limited information in order to highlight a limitation of the method of dominance regions.

6.2 Concluding Remarks

Pursuit-evasion games occur in a number of scenarios of interest, and they therefore have a rich history in the literature. However, even simple formulations can lead to surprisingly complex solutions. Because of this, the implementation of PE theory has been limited in practice. This dissertation investigates a solution method based on the idea of dominance. This method simplifies some PE formulations that are very challenging with other methods, and from a seemingly straightforward construction, it is capable of producing complex interactions.

This dissertation only considers constraints on minimum turn radius, because the isochrones for players with simple motion and Dubins cars are known in closed form in the literature. However, the approach is not limited to these dynamics, and indeed, it can be used any time the isochrones can be computed or approximated. This differentiates it from other PE solution methods, because it is able to handle non-convex state constraints, such as a collection of polygonal obstacles. By using this method, the challenge of solving a PE game is primarily linked to the problem of computing reachable sets for a single player, without considering adversaries. For complex problems, approximate PE solutions may be obtainable if these reachable sets can be approximated.

While this dissertation does not treat every known pursuit-evasion game, it does provide a general framework that can be used for a broad class of problems, and it opens up a number of interesting directions for continued study.

6.3 Future Directions

- **Methods for computing reachable sets:** Investigate methods for the exact or approximate determination of reachable sets for higher fidelity vehicle models. Since isochrones form the boundary of the reachable sets, and since dominance regions are simply the intersections of isochrones, reachable set computations also solve pursuit-evasion games. For complex dynamics, this might take a form similar to probabilistic path planners. With the results of this dissertation, PE games involving Dubins cars in the presence of obstacles would be solved by an investigation of the singular surfaces; i.e., the surfaces that correspond to visibility and dispersal surfaces for an agent moving with simple motion.

- **Singular surfaces and capture order heuristics in the SPME game:** Identify the surfaces in the SPME game where the maxmin payoff is identical for different capture orders. Once these surfaces are known, the problem of optimizing evasive headings reduces to an optimization problem with the singular surfaces as constraints. The primary remaining barrier to implementing a complete SPME solution would then be an investigation of fast heuristics for determining the optimal capture order (which can be mapped to a sequence-dependent traveling salesman problem).

- **Pursuer assignment in the MPME game:** The MPME game can be analyzed using the same tools developed for the MPSE and SPME games once the additional assignment problem has been considered, i.e., which pursuer or group of pursuers should pursue each evader or group of evaders.

- **Information structures:** Investigate the effects of varying information structures on PE games. For example, Section 5.1 considers a game where both teams share a probability distribution for the identity of the VIP; how does the solution change if one team knows with certainty while the other knows only a probability distribution? As another example, how does the solution of the SPME game change if the pursuer has to explore the environment in order to gain information about the locations of the evaders?

BIBLIOGRAPHY

[1] B. Alspach. Searching and sweeping graphs: a brief survey. *Le Matematiche*, 59(1,2), 2006.

[2] E. Bakolas and P. Tsiotras. The zermelovoronoi diagram: A dynamic partition problem. *Automatica*, 46(12):2059–2067, 2010.

[3] E. Bakolas and P. Tsiotras. Relay pursuit of a maneuvering target using dynamic voronoi diagrams. *Automatica*, 48(9):2213 – 2220, 2012.

[4] E.N Barron, L.C Evans, and R. Jensen. Viscosity solutions of isaacs' equations and differential games with lipschitz controls. *Journal of Differential Equations*, 53(2):213–233, 1984.

[5] T. Basar and G.J. Olsder. *Dynamic Noncooperative Game Theory*. Society for Industrial and Applied Mathematics, 2nd edition, 1998.

[6] R. Bencatel, D.W. Oyler, L. Liu, D. Sun, and A.R. Girard. Homing guidance using spatially quantized signals. *under review*.

[7] D. Bhadauria and V. Isler. Capturing an evader in a polygonal environment with obstacles. In *Proceedings of the 22nd International Joint Conference on Artificial Intelligence*, pages 2054–2059, Barcelona, Spain, July 2011.

[8] D. Bhadauria, K. Klein, V. Isler, and S. Suri. Capturing an evader in polygonal environments with obstacles: The full visibility case. *The International Journal of Robotics Research*, 31(10):1176–1189, 2012.

[9] S. Bhattacharya, T. Basar, and M. Falcone. Surveillance for security as a pursuit-evasion game. In R. Poovendran and W. Saad, editors, *Decision and Game Theory for Security*, volume 8840 of *Lecture Notes in Computer Science*, pages 370–379. Springer International Publishing, 2014.

[10] S. Bhattacharya, T. Basar, and N. Hovakimyan. Game-theoretic analysis of a visibility based pursuit-evasion game in the presence of a circular obstacle. *AIP Conference Proceedings*, 1479(1):1222–1225, 2012.

[11] S. Bhattacharya, T. Basar, and N. Hovakimyan. On the construction of barrier in a visibility based pursuit evasion game. In *European Control Conference*, pages 1894–1901, June 2014.

[12] S. Bhattacharya and S. Hutchinson. On the existence of nash equilibrium for a two player pursuit-evasion game with visibility constraints. In G.S. Chirikjian, H. Choset, M. Morales, and T. Murphey, editors, *Algorithmic Foundation of Robotics VIII*, volume 57 of *Springer Tracts in Advanced Robotics*, pages 251–265. Springer Berlin Heidelberg, 2010.

[13] S. Bhattacharya, S. Hutchinson, and T. Basar. Game-theoretic analysis of a visibility based pursuit-evasion game in the presence of obstacles. In *American Control Conference*, pages 373–378, June 2009.

[14] C. Boesch. Cooperative hunting in wild chimpanzees. *Animal Behaviour*, 48(3):653–667, 1994.

[15] C. Boesch. Cooperative hunting roles among tai chimpanzees. *Human Nature*, 13(1):27–46, 2002.

[16] S.D. Bopardikar, F. Bullo, and J.P. Hespanha. On discrete-time pursuit-evasion games with sensing limitations. *IEEE Transactions on Robotics*, 24(6):1429–1439, Dec 2008.

[17] R.L. Boyell. Defending a moving target against missile or torpedo attack. *Aerospace and Electronic Systems, IEEE Transactions on*, AES-12(4):522–526, July 1976.

[18] J.V. Breakwell and P. Hagedorn. Point capture of two evaders in succession. *Journal of Optimization Theory and Applications*, 27(1):89–97, 1979.

[19] G.H. Burgin and L.B. Sidor. Rule-based air combat simulation. Technical Report 4160, NASA Contractor Report, September 1988.

[20] AA Chikrij. Methods of group pursuit. In *Stochastic Optimization*, pages 632–640. Springer, 1986.

[21] T.H. Chung, G.A. Hollinger, and V. Isler. Search and pursuit-evasion in mobile robotics. *Autonomous Robots*, 31(4):299–316, November 2011.

[22] E.J. Cockayne and G.W.C. Hall. Plane motion of a particle subject to curvature constraints. *SIAM Journal on Control*, 13(1):197–220, 1975.

[23] S. Cowen, S. Briest, and J. Dombrowski. Underwater docking of autonomous undersea vehicles using optical terminal guidance. In *OCEANS '97. MTS/IEEE Conference Proceedings*, volume 2, pages 1143–1147, Oct 1997.

[24] M.G. Crandall, L.C. Evans, and P.L. Lions. Some properties of viscosity solutions of hamilton-jacobi equations. *Transactions of the American Mathematical Society*, 282(2):487–502, 1984.

[25] M.G. Crandall and P.L. Lions. Viscosity solutions of hamilton-jacobi equations. *Transactions of the American Mathematical Society*, 277(1):1–42, 1983.

[26] H. Ehtamo and T. Raivio. On applied nonlinear and bilevel programming or pursuit-evasion games. *Journal of Optimization Theory and Applications*, 108(1):65–96, 2001.

[27] J.M. Eklund, J. Sprinkle, and S.S. Sastry. Switched and symmetric pursuit/evasion games using online model predictive control with application to autonomous aircraft. *Control Systems Technology, IEEE Transactions on*, 20(3):604–620, May 2012.

[28] J. Las Fargeas, P.T. Kabamba, and A.R. Girard. Cooperative surveillance and pursuit using unmanned aerial vehicles and unattended ground sensors. *Sensors*, 15(1):1365–1388, 2015.

[29] M.D. Feezor, F.Yates Sorrell, P.R. Blankinship, and J.G. Bellingham. Autonomous underwater vehicle homing/docking via electromagnetic guidance. *IEEE Journal of Oceanic Engineering*, 26(4):515–521, Oct 2001.

[30] J. Flynn. Lion and man: A bounded pursuit game. Technical Report 161, Stanford University Department of Statistics, Oct 1970.

[31] M. Foley and W. Schmitendorf. A class of differential games with two pursuers versus one evader. *Automatic Control, IEEE Transactions on*, 19(3):239–243, Jun 1974.

[32] F.V. Fomin and D.M. Thilikos. An annotated bibliography on guaranteed graph searching. *Theoretical Computer Science*, 399(3):236–245, 2008. Graph Searching.

[33] A. Friedman. *Differential Games*. Wiley, 1971.

[34] E. Garcia, D.W. Casbeer, and M. Pachter. Active target defense differential game with a fast defender. In *American Control Conference (ACC), 2015*, pages 3752–3757, July 2015.

[35] E. Garcia, D.W. Casbeer, and M. Pachter. Escape regions of the active target defense differential game. In *ASME 2015 Dynamic Systems and Control Conference*, pages V001T03A001–V001T03A001. American Society of Mechanical Engineers, 2015.

[36] E. Garcia, D.W. Casbeer, K.D. Pham, and M. Pachter. Cooperative aircraft defense from an attacking missile. In *53rd IEEE Conference on Decision and Control*, December 2014.

[37] W.M. Getz and M. Pachter. Two-target pursuit-evasion differential games in the plane. *Journal of Optimization Theory and Applications*, 34(3):383–403, July 1981.

[38] C. Giovannangeli, M. Heymann, and E. Rivlin. Pursiut-evasion games in presence of obstacles in unknown environments: Towards an optimal pursuit strategy. In V. Kordic, editor, *Cutting Edge Robotics 2010*, chapter 4. InTech, 2010.

[39] A.R. Girard and P.T. Kabamba. Proportional navigation: Optimal homing and optimal evasion. *SIAM Review*, 2015.

[40] M.A. Goodrich, B.S. Morse, D. Gerhardt, J.L. Cooper, M. Quigley, J.A. Adams, and C. Humphrey. Supporting wilderness search and rescue using a camera-equipped mini uav. *Journal of Field Robotics*, 25(1-2):89–110, 2008.

[41] N. Greenwood. A differential game in three dimensions: The aerial dogfight scenario. *Dynamics and Control*, 2(2):161–200, 1992.

[42] W. Grimm, U.R. Prasad, and K.H. Well. Open-loop guidance for pre-launch maneuvering in medium-range air combat. In *Proceedings of the 27th IEEE Conference on Decision and Control*, volume 2, pages 1442–1447, Dec 1988.

[43] W. Grimm and K.H. Well. Modelling air combat as differential game recent approaches and future requirements. In R.P. Hamalainen and H.K. Ehtamo, editors, *Differential Games Developments in Modelling and Computation*, volume 156 of *Lecture Notes in Control and Information Sciences*, pages 1–13. Springer Berlin Heidelberg, 1991.

[44] O. Hajek. *Pursuit Games: An Introduction to the Theory and Applications of Differential Games of Pursuit and Evasion*. Dover Books on Mathematics Series. Dover Publications, 2008.

[45] J. Hershberger and S. Suri. An optimal algorithm for euclidean shortest paths in the plane. *SIAM J. Comput.*, 28(6):2215–2256, Aug 1999.

[46] I. Hwang, D.M. Stipanovic, and C.J. Tomlin. Polytopic approximations of reachable sets applied to linear dynamic games and a class of nonlinear systems. In E.H. Abed, editor, *Advances in Control, Communication Networks, and Transportation Systems*, Systems and Control: Foundations & Applications, pages 3–19. Birkhuser Boston, 2005.

[47] F. Imado. Some aspects of a realistic three-dimensional pursuit-evasion game. *Journal of Guidance, Control, and Dynamics*, 16(2):289–293, March 1993.

[48] R. Isaacs. *Differential Games: A Mathematical Theory with Applications to Warfare and Pursuit, Control and Optimization*. Wiley, 1965.

[49] J.R. Isbell. Pursuit around a hole. *Naval Research Logistics Quarterly*, 14(4):569–571, 1967.

[50] S. Jin and Z. Qu. Pursuit-evasion games with multi-pursuer vs. one fast evader. In *Intelligent Control and Automation (WCICA), 2010 8th World Congress on*, pages 3184–3189, July 2010.

[51] P.T. Kabamba and A.R. Girard. *Fundamentals of Aerospace Navigation and Guidance*. Cambridge University Press, 2014.

[52] S. Karaman and E. Frazzoli. Incremental sampling-based algorithms for a class of pursuit-evasion games. In D. Hsu, V. Isler, J.C. Latombe, and M.C. Lin, editors, *Algorithmic Foundations of Robotics IX*, volume 68 of *Springer Tracts in Advanced Robotics*, pages 71–87. Springer Berlin Heidelberg, 2011.

[53] N. Karnad and V. Isler. Lion and man game in the presence of a circular obstacle. In *IEEE/RSJ International Conference on Intelligent Robots and Systems*, pages 5045–5050, Oct 2009.

[54] S. Kopparty and C.V. Ravishankar. A framework for pursuit evasion games in $\mathbb{R}^n$. *Information Processing Letters*, 96(3):114–122, 2005.

[55] H. W. Kuhn and A. W. Tucker. Nonlinear programming. In *Proceedings of the Second Berkeley Symposium on Mathematical Statistics and Probability*, pages 481–492, Berkeley, Calif., 1951. University of California Press.

[56] M.F. Land. Chasing and pursuit in the dolichopodid fly poecilobothrus nobilitatus. *Journal of Comparative Physiology A*, 173(5):605–613, 1993.

[57] N.M. Le. On determining optimal strategies in pursuit games in the plane. *Theoretical Computer Science*, 197(12):203–234, 1998.

[58] J.J. Leonard, A.A. Bennett, C.M. Smith, and H. Feder. Autonomous underwater vehicle navigation. In *IEEE ICRA Workshop on Navigation of Outdoor Autonomous Vehicles*, Leuven, Belgium, May 1998. Citeseer.

[59] J. Lewin. *Differential games: theory and methods for solving game problems with singular surfaces*. Springer-Verlag New York, 1994.

[60] P.L. Lions. Generalized solutions of hamilton-jacobi equations. *Research Notes in Mathematics Series*, 69, 1982.

[61] S.Y. Liu, Z. Zhou, C. Tomlin, and J.K. Hedrick. Evasion of a team of dubins vehicles from a hidden pursuer. In *IEEE International Conference on Robotics and Automation (ICRA)*, pages 6771–6776, May 2014.

[62] S.Y. Liu, Z. Zhou, C. Tomlin, and K. Hedrick. Evasion as a team against a faster pursuer. In *American Control Conference (ACC), 2013*, pages 5368–5373, June 2013.

[63] L.D. Mech. *Handbook of Animal Radio-Tracking*. University of Minnesota Press, Minneapolis, MN, 1983.

[64] L.D. Mech and S.M. Barber. A critique of wildlife radio-tracking and its use in national parks. Technical report, Biological Resources Management Division, U.S. National Park Service, 2002.

[65] A.A. Melikyan and N.V. Ovakimyan. Singular trajectory in the problem of simple pursuit on a manifold. *Journal of Applied Mathematics and Mechanics*, 55(1):48–55, 1991.

[66] A.A. Melikyan, N.V. Ovakimyan, and L.L. Harutiunian. Games of simple pursuit and approach on a two-dimensional cone. *Journal of Optimization Theory and Applications*, 98(3):515–543, 1998.

[67] S. Le Menec. Differential games and symbolic programming to calculate a guaranteed aircraft evasion in modern aerial duels. In *Proceedings of the 33rd IEEE Conference on Decision and Control*, volume 4, pages 3868–3870, Dec 1994.

[68] S. Le Menec. Linear differential game with two pursuers and one evader. In M. Breton and K. Szajowski, editors, *Advances in Dynamic Games*, volume 11 of *Annals of the International Society of Dynamic Games*, pages 209–226. Birkhauser Boston, 2011.

[69] A.W. Merz. The game of two identical cars. *Journal of Optimization Theory and Applications*, 9(5):324–343, 1972.

[70] A.W. Merz. To pursue or to evade - that is the question. *Journal of Guidance*, 8(2):161–166, March-April 1985.

[71] A.W. Merz. Implementing air combat guidance laws. *Journal of Dynamic Systems, Measurement, and Control*, 111(4):605–608, December 1989.

[72] A.W. Merz and D.S. Hague. Coplanar tail-chase aerial combat as a differential game. *AIAA Journal*, 15(10):1419–1423, October 1977.

[73] J.S.B. Mitchell. Shortest paths among obstacles in the plane. In *Proceedings of the Ninth Annual Symposium on Computational Geometry*, SCG '93, pages 308–317, New York, NY, USA, 1993. ACM.

[74] E. Mueller, S.Z. Yong, M. Zhu, and E. Frazzoli. Anytime computation algorithms for stochastically parametric approach-evasion differential games. In *IEEE RSJ International Conference on Intelligent Robots and Systems (IROS)*, pages 3816–3821, Nov 2013.

[75] B.K. Nielsen and B. Mohl. Hull-mounted hydrophones for passive acoustic detection and tracking of sperm whales (physeter macrocephalus). *Applied Acoustics*, 67(1112):1175–1186, 2006.

[76] M. Niendorf, P.T. Kabamba, and A.R. Girard. Stability of solutions to classes of traveling salesman problems. *IEEE Transactions on Cybernetics*, PP(99), 2015.

[77] Nils J Nilsson. Shakey the robot. Technical Report 323, S.R.I. International, Menlo Park, CA, 1984.

[78] D.J. Nowak. Exploitation of self organization in uac swarms for optimization in combat environments. Master's thesis, Air Force Institute of Technology, 2008.

[79] D.W. Oyler and A.R. Girard. Survey of pursuit-evasion games and solution techniques. *under review*.

[80] D.W. Oyler and A.R. Girard. Dominance regions in the homicidal chauffeur problem. In *American Control Conference*, 2016.

[81] D.W. Oyler, P.T. Kabamba, and A.R. Girard. A homing guidance law for binary range-rate measurements. In *52nd IEEE Conference on Decision and Control*, pages 1295–1300, Florence, Italy, Dec 2013.

[82] D.W. Oyler, P.T. Kabamba, and A.R. Girard. Pursuit-evasion games in the presence of a line segment obstacle. In *53rd IEEE Conference on Decision and Control*, pages 1149–1154, Dec 2014.

[83] D.W. Oyler, P.T. Kabamba, and A.R. Girard. Binary range-rate measurements and homing guidance. *Journal of Dynamic Systems, Measurement, and Control*, 137(4), April 2015.

[84] D.W. Oyler, P.T. Kabamba, and A.R. Girard. Dominance in pursuit-evasion games with uncertainty. In *54th IEEE Conference on Decision and Control*, pages 5859–5864, Dec 2015.

[85] D.W. Oyler, P.T. Kabamba, and A.R. Girard. Pursuit-evasion games in the presence of obstacles. *Automatica*, 65(C):1–11, March 2016.

[86] D.W. Oyler, Y. Yildiz, A.R. Girard, and I.V. Kolmanovsky. A game theoretical model of traffic with multiple interacting drivers for use in autonomous vehicle development. In *American Control Conference*, 2016.

[87] N.F. Palumbo, R.A. Blauwkamp, and J.M. Lloyd. Modern homing missile guidance theory and techniques. *Johns Hopkins APL Technical Digest*, 29(1):42–59, 2010.

[88] V.S. Patsko and V.L. Turova. Level sets of the value function in differential games with the homicidal chauffeur dynamics. *International Game Theory Review*, 03(01):67–112, 2001.

[89] V.S. Patsko and V.L. Turova. Families of semipermeable curves in differential games with the homicidal chauffeur dynamics. *Automatica*, 40(12):2059–2068, 2004.

[90] A. Perelman, T. Shima, and I. Rusnak. Cooperative differential games strategies for active aircraft protection from a homing missile. *Journal of Guidance, Control, and Dynamics*, 34(3):761–773, May 2011.

[91] L S Pontryagin. On the theory of differential games. *Russian Mathematical Surveys*, 21(4):193, 1966.

[92] L.S. Pontryagin. Linear differential games. *SIAM Journal on Control*, 12(2):262–267, 1974.

[93] L.S. Pontryagin. Linear differential games of pursuit. *Mathematics of the USSR-Sbornik*, 40(3):285, 1981.

[94] L.S. Pontryagin. *Mathematical theory of optimal processes*. CRC Press, 1987.

[95] R. Rountree, F. Juanes, and J.E. Blue. Potential for the use of remotely operated vehicles (rovs) as a platform for passive acoustics. *Listening to Fish: Proceedings of the International Workshop on the Applications of Passive Acoustics in Fisheries*, pages 138–146, 2002.

[96] I. Rusnak. The lady, the bandits, and the bodyguards-a two team dynamic game. In *Proceedings of the 16th World IFAC Congress*, pages 934–939, 2005.

[97] B.F. Schaudt. *Multiplicatively Weighted Crystal Growth Voronoi Diagrams*. PhD thesis, Dartmouth College, July 1991.

[98] L. Schenato, S. Oh, S. Sastry, and P. Bose. Swarm coordination for pursuit evasion games using sensor networks. In *Proceedings of the International Conference on Robotics and Automation*, 2005.

[99] W. Scott and N.E. Leonard. Dynamics of pursuit and evasion in a heterogeneous herd. In *53rd IEEE Conference on Decision and Control*, December 2014.

[100] S. Shankaran, D.M. Stipanovic, and C.J. Tomlin. Collision avoidance strategies for a three-player game. In M. Breton and K. Szajowski, editors, *Advances in Dynamic Games*, volume 11 of *Annals of the International Society of Dynamic Games*, pages 253–271. Birkhuser Boston, 2011.

[101] R.L. Shaw. *Fighter Combat: Tactics and Maneuvering*. Naval Institute Press, 1985.

[102] I.I. Shevchenko. Guaranteed strategies with memory for alternative pursuit. *Automation and Remote Control*, 75(10):1861–1868, 2014.

[103] T. Shima. Optimal cooperative pursuit and evasion strategies against a homing missile. *Journal of Guidance, Control, and Dynamics*, 34(2):414–425, March 2011.

[104] J. Shinar and G. Silberman. A discrete dynamic game modelling anti-missile defense scenarios. *Dynamics and Control*, 5(1):55–67, 1995.

[105] R.E Smith, B.A Dike, R.K Mehra, B Ravichandran, and A El-Fallah. Classifier systems in combat: Two-sided learning of maneuvers for advanced fighter aircraft. *Computer Methods in Applied Mechanics and Engineering*, 186(24):421–437, 2000.

[106] P. Soravia. Pursuitevasion problems and viscosity solutions of isaacs equations. *SIAM Journal on Control and Optimization*, 31(3):604–623, 1993.

[107] L. Stutters, Honghai Liu, C. Tiltman, and D.J. Brown. Navigation technologies for autonomous underwater vehicles. *IEEE Transactions on Systems, Man, and Cybernetics, Part C: Applications and Reviews*, 38(4):581–589, July 2008.

[108] G. Vachtsevanos, L. Tang, and J. Reimann. An intelligent approach to coordinated control of multiple unmanned aerial vehicles. In *American Helicopter Society 60th Annual Forum*, 2004.

[109] J. Vaganay, P. Baccou, and B. Jouvencel. Homing by acoustic ranging to a single beacon. In *OCEANS 2000 MTS/IEEE Conference and Exhibition*, volume 2, pages 1457–1462, Providence, RI, 2000.

[110] M. Vidyasagar. On the stabilization of nonlinear systems using state detection. *IEEE Transactions on Automatic Control*, 25(3):504–509, Jun 1980.

[111] T.L. Vincent and R.B. Cline. Differential game analysis using projections of the playable set. In *Proceedings of the 27th IEEE Conference on Decision and Control*, volume 2, pages 1430–1435, Dec 1988.

[112] D.M. Wojcik. Passive localization of underwater acoustic beacons. Master's thesis, Massachusetts Institute of Technology and Woods Hole Oceanographic Institution, Cambridge, MA, 1993.

[113] Y. Yavin. Stochastic two-target pursuit-evasion differential games in the plane. *Journal of Optimization Theory and Applications*, 56(3):325–343, March 1988.

[114] Y. Yavin and M. Pachter. *Pursuit-evasion differential games*. Oxford, Pergamon Press, 1987.

[115] Y. Yavin and R. De Villiers. Stochastic pursuit-evasion differential games in 3d. *Journal of Optimization Theory and Applications*, 56(3):345–357, 1988.

[116] S.W. Zhang, W. Xiang, L. Zili, and M.V. Srinivasan. Visual tracking of moving targets by freely flying honeybees. *Visual Neuroscience*, 4:379–386, 4 1990.